MOLECULARLY IMPRINTED POLYMERS: RATIONAL DESIGN, CONTROLLED SYNTHESIS AND NOVEL APPLICATIONS

A thesis submitted to the Department of Pure and Applied Chemistry, University of Strathclyde, in partial of the regulations for the Degree of Doctor in Philosophy in Chemistry

FAIZATUL SHIMAL BINTI MEHAMOD

JULY 2011

ACKNOWLEDGEMENTS

It is a pleasure to thank all those people who made this thesis possible and an enjoyable experience for me.

First of all, I would like to express my deepest sense of gratitude to my supervisor, Professor Peter Cormack, for his untiring effort, commitment, encouragement, guidance, support and understanding in the production of the thesis.

I would like to express my gratitude to the Ministry of Higher Education and Universiti Malaysia Terengganu (UMT) for financing my study, and thank you to the University of Strathclyde for providing me a place to do my PhD research.

My sincere gratitude is also extended to all lab technicians in the Department of Pure & Applied Chemistry. In particular, I am thankful to Gavin Bain and Dr Abed Khalaf for their generous assistance during this time. Also, special thanks to all members past and present in lab TG619 for sharing knowledge and invaluable assistance.

It would be difficult to list all of my friends one by one here, but I would like to show my appreciation to all of them for the love, laughter, emotional support and caring they provided, either from near or afar. There are no words that can thank them enough for lending me their shoulders through the difficult times and making my life ever so colourful over the past four years.

Finally, I wish to thank my family for their continuous love and encouragement, for always believing in me and for never failing to provide all the support. My beloved husband, Adil Abdul Ghani, and my lovely daughter, Dania Natasha, thank you very much.

ABSTRACT

Molecular imprinting, a technique for the preparation of polymeric materials that are capable of molecular recognition in various applications, is developing rapidly. In this study, work was directed towards the synthesis of novel molecularly imprinted polymers (MIPs) that enable high performance separations in analytical science and other fields. Furthermore, a new method of MIP synthesis, using controlled radical polymerisation, was explored, and a computational modelling method evaluated which enables the prediction of binding isotherms of MIPs in a qualitative manner prior to synthesis.

The synthesis of ketamine imprinted polymers *via* a conventional approach is described. The overall aim of this study was to develop a new analytical method, Molecularly Imprinted Liquid Chromatography-Tandem Mass Spectrometry (MILC-MS/MS) for the detection of ketamine in hair. A key requirement was the production of ketamine imprinted polymer particulates in an appropriate physical format for the direct packing of the imprinted materials into chromatography columns, which were then hyphenated to a mass spectrometer. Several polymers were synthesised and their molecular recognition properties characterised using liquid chromatography techniques. A new analytical method for ketamine was set in place.

The utility of controlled radical polymerisation in the preparation of MIPs was explored. The controlled radical polymerisation method of choice was reversible addition-fragmentation chain transfer (RAFT). The synthesis and use of a RAFT agent (CPDB) in MIP syntheses is described. It was discovered that polymers prepared *via* RAFT polymerisations enhanced the chromatographic performance of MIPs.

Through a collaborative research study, an aim was to develop and evaluate a computational model for MIPs which predicted, in silico, the qualitative binding isotherms of a MIP. Real imprinted polymers were synthesised and their binding isotherms measured in order to test the validity of the predictive model. Pyridine imprinted and non-imprinted polymers were synthesised in monolithic form. There was good agreement between the predicted and experimental binding data.

LIST OF ABBREVIATIONS

(±)-Ket	(±)-Ketamine Column
(S)-Ket	(S)-Ketamine Column
AGET	Activators Generated by Electron Transfer
AIBN	2,2'-Azobisisobutyronitrile
ARGET	Activators Regenerated by Electron Transfer
ATRP	Atom-Transfer Radical Polymerisation
BET	Brunauer, Emmett and Teller
CEC	Capillary Electrochromatography
CPDB	Cyanoisopropyl Dithiobenzoate
CRP	Controlled Radical Polymerisation
CSIRO	Commonwealth Scientific and Industrial Research Organisation
CSPs	Chiral Stationary Phases
DCM	Dichloromethane
DEVPA	*N,N'*-diethyl(4-vinyl phenyl)amidine
DVB-80	Divinylbenzene-80
EGDMA	Ethylene Glycol Dimethacrylate
EIA	Enzyme Immunoassay
ESI	Electrospray Interface
FPIA	Fluorescence Polarization Immunoassay
FRP	Free Radical Polymerisation
GC-MS/MS	Gas Chromatography-Tandem Mass Spectrometry
GEMC	Gibbs Ensemble Monte Carlo
HEMA	2-Hydroxyethyl methacrylate

HPLC	High-Performance Liquid Chromatography
ICAR	Initiators for Continuous Activator Regeneration
IF	Imprinting factor
IS	Internal Standard
ITO	Indium Tin Oxide
LC	Liquid Chromatography
LINCS	Linear Constraint Solver
LLE	Liquid-Liquid Extraction
LLOQ	Lower Limit of Quantification
LOD	Limit of Detection
LPME	Liquid Phase Microextraction
LSD	Lysergic Acid Diethylamide
M	Monomer
MAA	Methacrylic Acid
MILC-MS/MS	Molecularly Imprinted Liquid Chromatography-Tandem Mass Spectrometry
MIP	Molecular Imprinted Polymer
MISPE	Molecularly Imprinted Solid-Phase Extraction
MS	Mass Spectrometry
NAB	Anabasine
NAT	Anatabine
NIP	Non-Imprinted Polymer
NMR	Nuclear Magnetic Resonance
NMRP	Nitroxide-Mediated Radical Polymerisation
NNK	Nicotine
NNN	Nornicotine
NVT	Number-Volume-Temperature

PCMCs	Protein Coated Micro-Crystals
PCP	Phencyclidine
PETRA	Pentaerythritol Triacrylate
PME	Particle Mesh Ewald
RAFT	Reversible Addition-Fragmentation Chain-Transfer Polymerisation
RIA	Radio-Immunoassay
SAW	Surface Acoustic Wave
SIM	Selected Ion Monitoring
SOFT	Society of Forensic Toxicologists
SOHT	Society of Hair Testing
SPE	Solid-Phase Extraction
SPME	Solid-Phase Microextraction
SR & NI	Simultaneous Reverse and Normal Initiation
SRM	Selected Reaction Monitoring
T	Template
THF	Tetrahydrofuran
TLC	Thin Layer Chromatography
TraPPE	Transferable Potential for Phase Equilibria
TRIM	Trimethylolpropane Trimethacrylate
TSA	Transition State Analogue
TSNA	Tobacco-Specific Nitrosamines
UPLC	Ultra-Performance Liquid Chromatography
UV	Ultra-Violet
VAc	Vinylacetate
VLE	Vapour-Liquid Equilibrium
VMD	Visual Molecular Dynamic

VMD	Visual Molecular Dynamic
VOCs	Volatile Organic Compounds
X	Crosslinker

CONTENTS

CHAPTER 1

INTRODUCTION TO MOLECULARLY IMPRINTED POLYMERS (MIPs)

1.1 Molecular Imprinting

Molecularly imprinted polymers (MIPs) have drawn extensive attention for the production of polymeric artificial receptors for specific molecular recognition and highly useful synthetic mimics of antibodies or enzymes. Due to their molecular recognition capability, MIPs have captured the imagination of many and encouraged their use in numerous application areas, including analytical chemistry,[1],[2],[3] forensic science,[4],[5],[6] chemical sensing[7] and catalysis.[8]

Cormack *et al.*[9] reported that the synthesis of molecularly imprinted polymers is a chemically complex pursuit and demands a good understanding of chemical equilibria, molecular recognition theory, thermodynamics and polymer chemistry in order to ensure a high level of molecular recognition. Furthermore, Wulff and coworkers[10] stated that 'The polymers should normally be rather rigid to preserve the structure of the cavity after splitting off of the template. On the other hand, a high flexibility of the polymers should be present to facilitate a fast equilibrium between release and re-uptake of the template in the cavity. These two properties are contradictory to each other, and a careful optimisation can be necessary'.

However, the synthesis of MIPs is a relatively straightforward procedure. Figure 1.1 shows a typical molecular imprinting process. Initially, the template directs the organisation of vinyl monomers into a template-monomer assembly that is stabilised by covalent or non-covalent chemical bonds. Following the polymerisation, the template-monomer assembly is copolymerised with an excess of a crosslinking agent in a solvent that acts to solubilise the template-monomer assembly, crosslinking agent, and free radical initiator and, if appropriate, stabilise the assembly. Once the polymerisation is complete, removal of the template molecule from the porous, polymer network reveals binding sites which are complementary in size, shape and chemical functionality to the analyte. In this way, a molecular memory is introduced into the polymer, which is now capable of rebinding the analyte with a very high molecular selectivity. This is the basis for essentially all known applications.

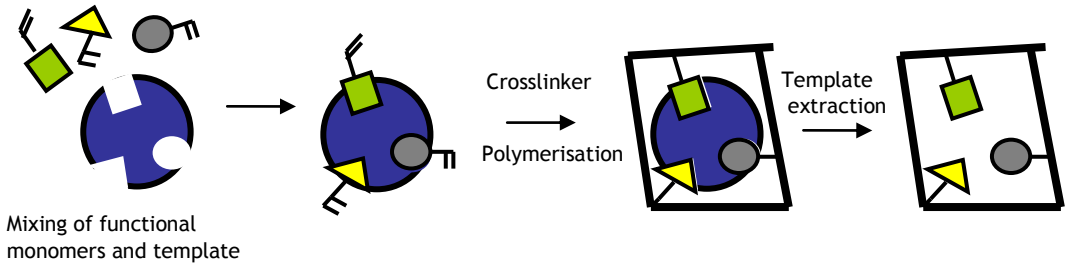

Figure 1.1 Schematic representation of a typical molecular imprinting process[11]

The resulting imprinted polymers are stable, robust and resistant to a wide range of pH, temperature and solvents. Therefore, the behaviour of MIPs emulates the interactions established by natural receptors to selectively retain a target molecule (*i.e.*, antibody–antigen) but without the associated stability limitations.[12] In addition, it is important to point out that MIP synthesis is also

relatively cheap and easy to perform, making MIPs an attractive alternative to the use of natural receptors.

Due to the sheer number of experimental variables involved, such as the nature and levels of template, functional monomer(s), crosslinker(s), solvent(s) and initiator, the method of initiation and the duration of polymerisation, it gives a great challenge to researchers in designing and synthesising MIPs. Moreover, optimisation of the imprinted products can be more difficult because there are many variables to consider, some or all of which can potentially impact upon the chemical, morphological and molecular recognition properties of the imprinted materials.[13]

1.2 A Brief History of Imprinting

Molecular imprinting techniques evolved from the antibody formation mechanisms with pre-determined molecular recognition properties. In 1894, Emil Fischer proposed a model for how a substrate fits into the active site of an enzyme, known as the 'lock-and-key' model.[14] The unique geometric structure of the enzyme's active binding site is particularly suitable for a substrate. Only recognised substrate with a corresponding shape will bind selectively to the enzyme, while an incorrectly shaped molecule will not be recognised as it does not fit the binding site (Figure 1.2).

As a crucial step in catalysing biological reactions, this model is rather constructive to visualise the formation of the enzyme-substrate complex. Despite the fact that the shapes of the active sites of many enzymes do not match exactly the shapes of their substrates, they change shape when the substrate binds to the

enzyme. This creates a shape into which the substrate fits. It is known as the induced-fit model and was described by Daniel E. Koshland, Jr. in 1958.[15] Today, the concept is normally used to describe substrate-binding behaviour of various enzymes.

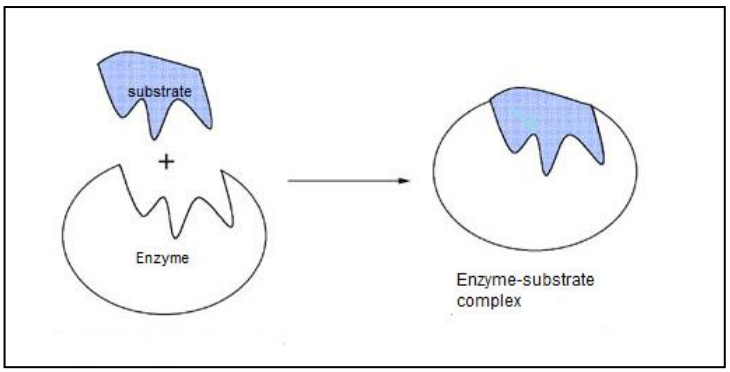

Figure 1.2 Fischer's Lock-and-Key concept in an enzyme-substrate complex (adapted from *Biochemistry*, Third Ed., 1988)[16]

In a similar way, molecular imprinting was used as early as the 1930s by M.V. Polyakov to selectively capture various additives in a silica matrix.[17] In the 1940s, Linus Pauling hypothesised that a process similar to molecular imprinting could be responsible for the selectivity of antibodies to their respective antigens.[18],[19] The theory was supported by experiments performed by his graduate student, Frank Dickey, who demonstrated imprinting and specific adsorption of several different dyes in silica.[20]

We now know that antibodies are produced by clonal-selection, but the idea of a pliable antibody taking shape in response to a foreign antigen was intriguing. Imprinting in silica gained some popularity over the next 15 years, but did not really catch on due to the instability of the silica matrix and limitations in the diversity of compatible template molecules.

The concept of molecular imprinting was revived in the 1970s when Günter Wulff discovered that highly crosslinked organic polymers could be used to make molecular imprints with high specificity.[21] Wulff used what is now termed the 'covalent approach'. Subsequently, throughout the 1970s and 1980s, the Wulff group published extensively on their works using this approach. In this approach, the template and functional monomer are covalently bound together and incorporated as a unit into the polymer. The approach is only useful if the covalent bond is reversible; it must form rapidly but it must also be weak enough to allow easy extraction of the template to leave behind a polymer with imprinted cavities.

The second major breakthrough in organic polymer imprinting occurred in 1981 when Mosbach and Arshady described non-covalent molecular interactions as the driving force for molecular imprinting.[22] The non-covalent approach is based on the formation of relatively weak non-covalent interactions (*e.g.*, hydrogen bonding) between selected monomers and template molecules before polymerisation. It is a more versatile approach than the covalent approach. The template and functional monomers form a complex through non-covalent intermolecular interactions which can be rapidly formed and easily disrupted. The drawback to the non-covalent approach is that complex formation tends to be incomplete such that an excess of functional monomer is normally employed, leading to imprinted products with a non-uniform population of binding sites.

An intermediate option is the semi-covalent approach attributed to Sellergren and Andersson,[23] and Whitcombe *et al.*[24] In this case, the semi-covalent approach offers an intermediate alternative in which the template is covalently bound to a

functional monomer during polymerisation, as in the covalent approach, but the template rebinding is based only on non-covalent interactions.

1.3 Molecular Imprinting Approaches

1.3.1 Covalent Approach

In the covalent approach pioneered by Wulff and co-workers, reversible chemical bonds are maintained between the template and the functional monomers during the polymerisation, and these are re-established during rebinding. Wulff and co-workers first produced MIPs by synthesising specific sugar derivatives which contained a polymerisable function such as vinylphenyl boronate.[25] After polymerisation, they hydrolysed off the sugar moiety and used the polymer for selective binding (Figure 1.3). For this covalent molecular imprinting, they found that the selectivity of the MIP increased with an increase in the degree of crosslinking.[26] The success of this approach led to the development of many other imprinted polymers, having different reversible covalent bonds for a variety of template molecules and new methods to produce them.

However, the range of templates which can be covalently imprinted is limited by the type of chemical functional groups in the template. In a typical covalent imprinting system, a template-monomer complex is formed through reversible covalent binding such as boronic acid esters, Schiff bases, acetals and ester bonds.

The boronate ester bond is well known for the covalent imprinting of templates which are either mono-alcohols or which show diol motifs (such as carbohydrates).[27] These form the strongest reversible functional group interactions and are most readily used to create synthetic molecular receptors.[28]

Acetals have also been used to form covalent MIPs but these bonds are formed slowly and therefore have not been used widely.[29]

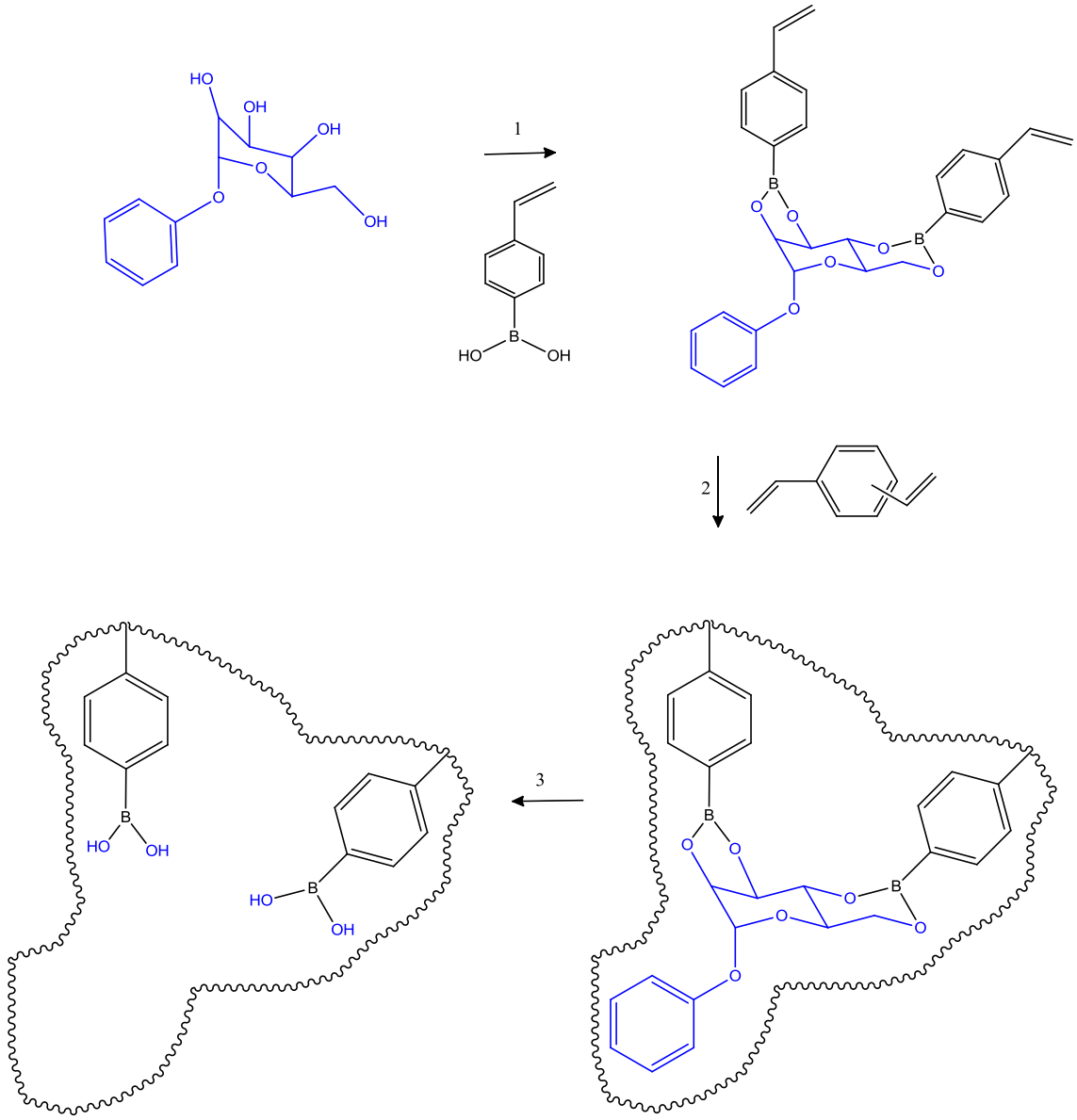

Figure 1.3 Covalent imprinting of phenyl-α-*D*-mannopyranoside with 4-vinylphenyl-boronic acid as the functional monomer.

(1) Chemical derivatisation of the template; (2) Polymerisation; (3) Template extraction.[25]

Imprinting with Schiff bases has been used to functionalise copolymers of styrene/diisopropenylbenzene and methacrylamide.[30] However, this bond does not equilibrate fast enough to be used for rapid chromatography.[29] Meanwhile, ester bonds do not readily hydrolyse, which would create a low number of binding sites in a MIP; this work was discussed by Wulff 1995.[31]

Figure 1.4 shows a general schematic representation of the covalent approach. The covalent approach involves the formation of reversible covalent bonds between the template and monomers before polymerisation. Following polymerisation of the functionalised template with a crosslinker, the template is removed from the polymer by cleavage of the corresponding covalent bonds, which are re-formed upon rebinding of the analyte. The high stability of template-monomer interaction provided by the covalent bonds during polymerisation will lead to a rather homogenous population of binding sites, minimising the existence of non-specific binding sites.

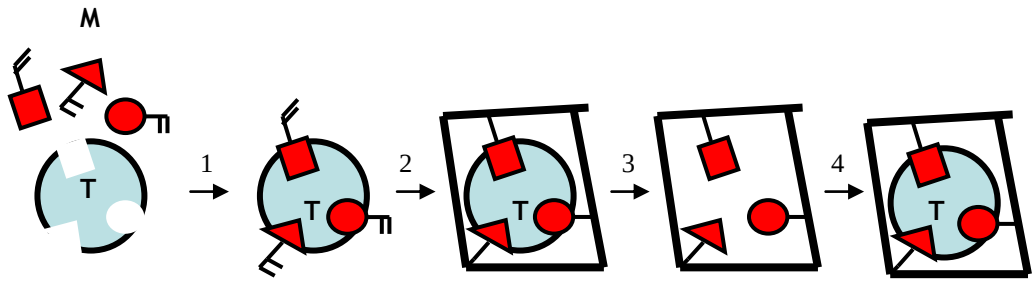

Figure 1.4 Schematic representation of a covalent imprinting process (M= functional monomers and T= template; 1= Synthesis of polymerisable template; 2= Copolymerisation of the polymerisable template; 3= Extraction of template from the imprinted polymer network; 4= Rebinding)[31]

This approach is rather restrictive since it is not easy to design an appropriate template–monomer complex in which covalent bond formation and cleavage are readily reversible under mild conditions. However, the spatial arrangement of the monomer residues within the binding site ought to be optimal for efficient template binding, leading to highly selective materials.

1.3.2 Non-Covalent Approach

The non-covalent approach to molecular imprinting, pioneered by Mosbach and coworkers,[32] is the most commonly used approach for scientists preparing imprinted materials on a routine basis. This approach is very attractive since it is simple, the products show high affinity for their targets and it is broadly applicable.[33],[34] The non-covalent imprinting approach utilises the concept of self-assembly in the MIP pre-polymerisation mixture which contains template, monomers and initiator in a porogen prior to the initiation of polymerisation.

Generally speaking, the template is mixed directly with one or several functional monomers and copolymerised with crosslinking agent. The self-assembly takes place through the formation of non-covalent interactions between the template and the functional monomer, such as hydrogen bonding, electrostatic, Van der Waals and π-π interactions. Following polymerisation, the functional monomers are fixed in position by the highly crosslinked polymeric structure. Once polymerisation is complete, removal of the template molecules from the porous, polymer network reveals binding sites which are complementary in size, shape and chemical functionality to the analyte. In this way, a molecular memory is introduced into the polymer, which is now capable of rebinding the analyte with a

very high specificity. Figure 1.5 shows a schematic representation of the non-covalent imprinting process.

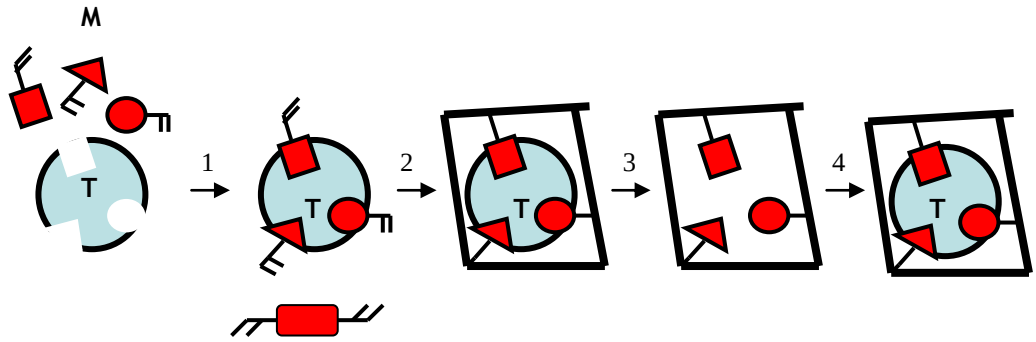

Figure 1.5 Schematic representation of a non-covalent imprinting process (M= functional monomers and T= template; 1= Self-assembly in solution of the template with the functional monomers; 2= Copolymerisation of the template-monomer complex with an excess of a crosslinking agent; 3= Solvent extraction of template from the imprinted polymer network, thus revealing the imprinted binding site; 4= Rebinding)[35]

Care must be taken when choosing the monomers, crosslinkers, and porogens in order to achieve efficient imprinting. Typically, the functional monomers are added in excess relative to the amount of template in order to complete the template-monomer complexation and to maintain stability under polymerisation conditions, but also to ensure that all the template molecules form imprinted cavities. However, the excess of free monomers is incorporated randomly into the polymeric matrix leading to the formation of non-selective binding sites. The most commonly used monomers are acidic vinyl monomers, such as methacrylic acid, (MAA)[36] and heteroaromatic basic monomers, such as vinylpyridine. MAA can be used to create good binding sites for a large variety of template structures containing hydrogen bond -donating or -accepting functional groups.[37] Commonly,

these binding sites are capable of discriminating subtle structural differences in the template, similar in essence to the selectivity displayed by antibodies.

Due to its simplicity and versatility, this technique has been widely exploited. For example, Philip *et al.*[38] used monomers from cashew nut shell to develop a molecularly imprinted polymer *via* the non-covalent approach, Yang *et al.*[39] successfully prepared a non-covalent molecularly imprinted solid-phase extraction (MISPE) cartridge for the extraction of cotinine from human urine, Zurutuza *et al.*[40] used MISPE for the extraction of cocaine metabolites from aqueous samples, and Vallano *et al.*[41] prepared a highly selective MIP column for capillary electrochromatography, to name but a few. Other highlights include work from Kempe *et al.*,[42] Sellergren *et al.*[43] and Bereczki *et al.*[44]

1.3.3 Semi-Covalent Approach

The semi-covalent approach merges features of the covalent and non-covalent approaches. It was developed by Michael Whitcombe and coworkers at the Institute of Food Research in Reading, UK.[24],[45] This approach employs covalent template-monomer constructs in the imprinting step but entirely non-covalent interactions for rebinding.[46] Just like covalent imprinting, the template-functional monomer construct has to be synthesised and characterised prior to use in the polymerisation. There is no excess of functional monomer, the mole ratio between the template and the functional monomer is stoichiometric, therefore the amount of non-specific binding is minimised. Furthermore, the binding sites are more uniform, template bleeding is less likely and template rebinding is not subject to kinetic restrictions of covalent bond formation except for diffusion, which remains as a limiting factor in the rebinding process.[35]

There have been two main methodologies in the semi-covalent approach. The first is direct connection of template and monomer by an ester or amide linkage, and the second exploits a sacrificial spacer between the template and polymerisable element in the imprinting step.

In the first approach, the target molecule and the polymerisable groups are directly connected *via* an ester or amide linkage. Once the polymerisation is complete, hydrolysis of the ester or amide group releases the template and reveals the imprinted cavities in the binding sites. The functional group moiety in the cavities can then rebind the template or its analogue *via* non-covalent interactions. This can best be illustrated by an example such as that shown in Figure 1.6, which shows the schematic representation of this approach using testosterone methacrylate as the template monomer, as reported by Cheong *et al.*[47]

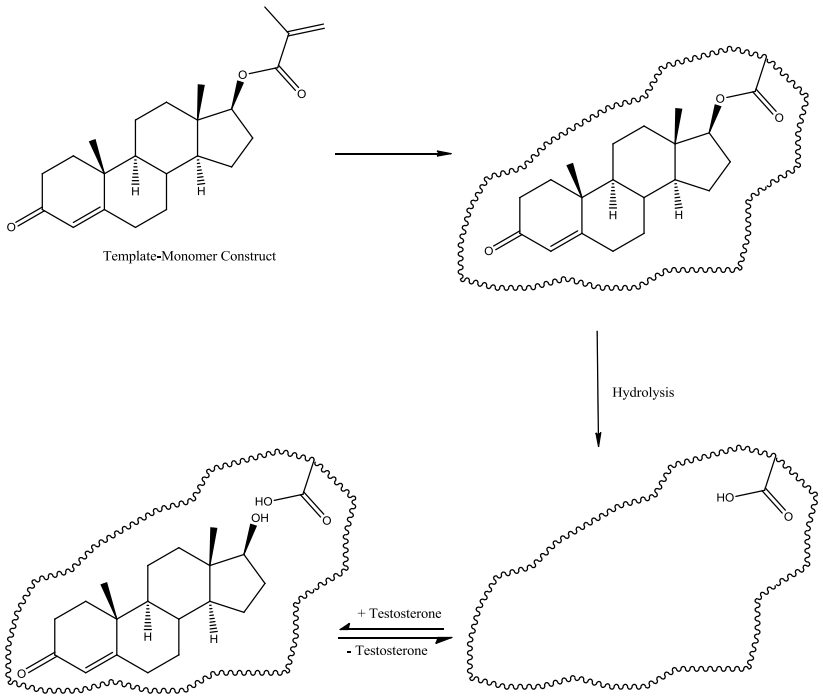

Figure 1.6 Schematic of semi-covalent molecular imprinting using an ester bond[47]

The second method of semi-covalent molecular imprinting is the use of a sacrificial spacer functional group. It needs to be introduced between the template and functional group precursor, such that the rebound target molecule can both fit the 'hole' left by the template and form a hydrogen bond with the functionality in the imprinted site. The main point to this approach is the development of suitable geometry between the template and functional group precursors. At the template cleavage stage, the spacer will be lost. Thus, it is known as the sacrificial spacer method.

This approach has been used for a variety of different templates such as cholesterol,[48] dioxin analogues[49] (environmental toxins) and nortriptyline.[50] The carbonyl group is a commonly used sacrificial spacer group and can be introduced in the form of a carbonate ester group, carbamate (urethane) group[50] and urea linkages.[49] Other examples of spacers are salicylamide,[51] which is used in the imprinting of amine templates, and silicone-based spacers[52] for the imprinting of pyridine after template removal. Figure 1.7 shows an example of a sacrificial spacer approach for the imprinting of cholesterol.

The decision of which of the three main imprinting approaches to be used depends on the nature of the template, the monomers chosen and also the requirements of the final intended application. These three methods each have their own advantages and disadvantages, but the trend at the moment leans towards using the non-covalent and semi-covalent approaches due to the versatility in imprinting of a large number of template types.

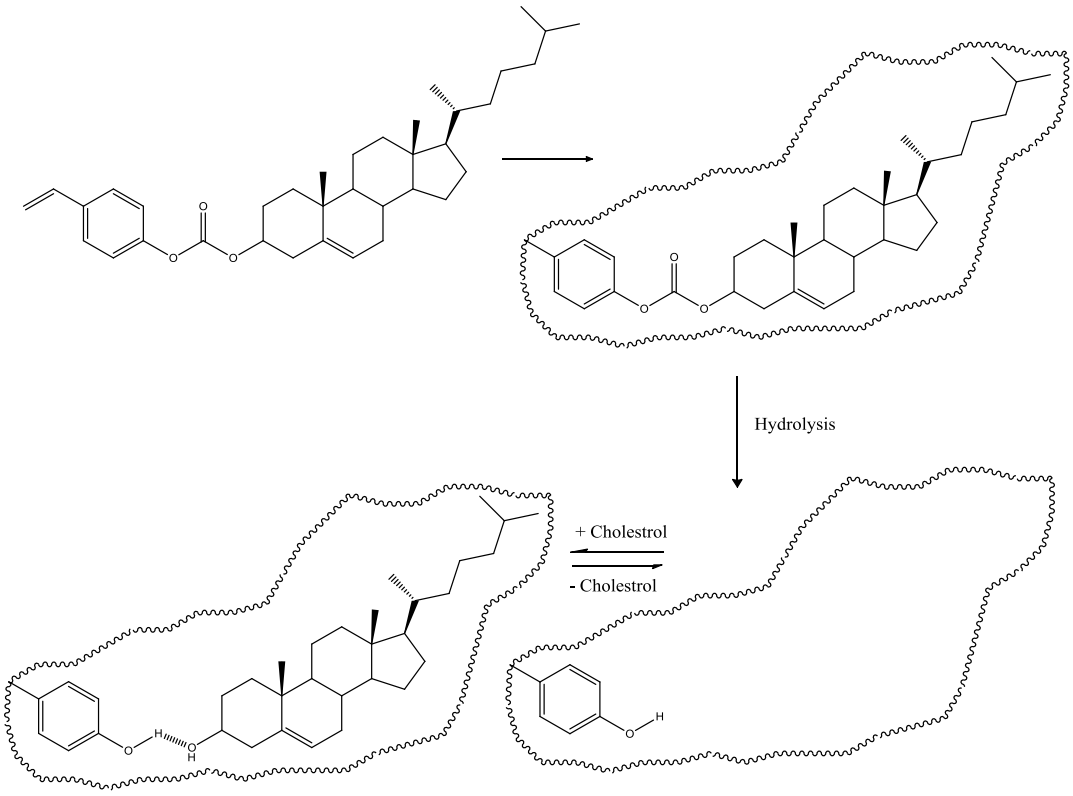

Figure 1.7 Sacrificial spacer method (semi-covalent approach) for the imprinting of cholesterol[24]

1.4 MIP Syntheses

The polymerisable formulation for an imprinted polymer comprises a template (the target molecule), functional monomer, crosslinker, solvent and initiator. In the following, the details of the template molecule and the selection of suitable functional monomers, crosslinkers, solvent, initiators and general polymerisation procedures are discussed.

1.4.1 Template

The template molecule plays a key role in all molecular imprinting processes as it directs the organisation of the functional groups pendent to the functional monomers.[9] The template chosen must be chemically inert and stable under the

polymerisation conditions; virtually all polymerisations are based on free radical polymerisations. It must not participate in the radical reaction and must be stable upon exposure to UV radiation or high polymerisation temperatures.

Most MIPs are prepared using small organic molecules as templates. The imprinting of small, organic molecules (*e.g.,* pharmaceuticals, pesticides, amino acids and peptides, nucleotide bases, steroids, and sugars) is now well established and considered almost routine.[53] Although specially adapted protocols have been proposed for larger templates, *e.g.,* proteins and cells, the imprinting of much larger structures is still a challenge.[54] The primary reason for this is the fact that larger templates are often less rigid, and thus do not facilitate the creation of well-defined binding cavities during the imprinting process, or are labile.

A close structural analogue to the targeted analyte is sometimes chosen as a template molecule. This is to avoid a 'template bleeding' problem from arising during analysis, especially for a quantitative analysis at trace level, which occurs as a result of template molecules remaining in the imprinted polymer even after extensive washing.[55] Chiral templates have been used often during screening processes. In these cases the quality of the imprint (the cavity with binding sites) can be measured by its ability to resolve a racemate, which can be tested either in a batch procedure or by using the polymeric materials as chromatographic supports.

1.4.2 Functional Monomer

The careful choice of functional monomer is an important consideration to provide complementary interactions with the template. For covalent molecular

imprinting, there is no need to consider the optimisation of the template to functional monomer ratio because the template dictates the number of functional monomers that can be covalently attached; furthermore, the functional monomers are attached in a stoichiometric manner. However, for non-covalent molecular imprinting, the optimal template/monomer ratio is normally established empirically by evaluating several polymers made with different formulations with increasing functional monomers contents.[56] Ratios of template to functional monomer of 1:4 and upwards are rather common.[9]

From the general mechanism for the formation of MIP binding sites, functional monomers are responsible for the binding interactions in the imprinted binding sites. For non-covalent molecular imprinting protocols, functional monomers are normally used in excess relative to the number of moles of template to favour the formation of template-functional monomer assemblies. To maximise complex formation and the imprinting effect, the most important consideration is to match the functionality of the template with the functionality of the functional monomer in a complementary fashion.[9] Indeed, it may be necessary to employ more than one functional monomer to achieve the desired effect.

Commonly used functional monomers can be classified into three main categories as shown in Figure 1.8. Acidic functional monomers are useful for templates that can accept a proton; alternatively, basic functional monomers will form better interactions with templates that can donate protons. For uncharged templates, a neutral functional monomer may help to increase their interactions.[57]

Acidic (A)

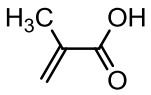

A1

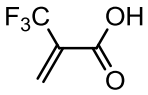

A2

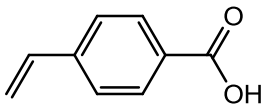

A3

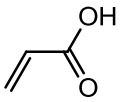

A4

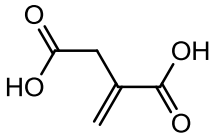

A5

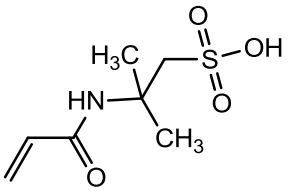

A6

Basic (B)

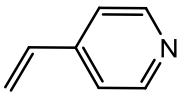

B1

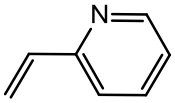

B2

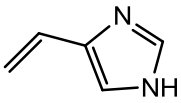

B3

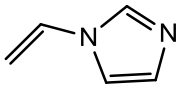

B4

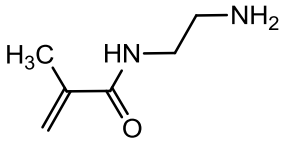

B5

Neutral (N)

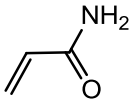

N1

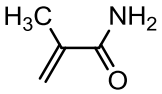

N2

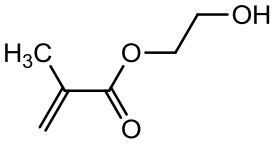

N3

Figure 1.8 Selection of functional monomers used in non-covalent molecular imprinting

Acidic; **A1**: methacrylic acid (MAA); **A2**: 2-(trifluoromethyl)acrylic acid (TFMAA); **A3**: *p*-vinylbenzoic acid; **A4**: acrylic acid; **A5**: itaconic acid; **A6**: acrylamido-(2-methyl)-propane sulfonic acid (AMPSA). **Basic**; **B1**: 4-vinylpyridine (4-VP); **B2**: 2-vinylpyridine (2-VP); **B3**: 4-(5)-vinylimidazole; **B4**:1-vinyl imidazole; **B5**: N-(2-aminethyl)-methacrylamide. **Neutral**; **N1**: acrylamide; **N2**: methacrylamide; **N3:** 2-hydroxyethyl methacrylate (2-HEMA)

The selection of functional monomers useful for covalent and semi-covalent imprinting is more restricted because of the antagonistic requirements of polymerisation and template extraction. The functional monomer must form a covalent bond with the template that is stable under the polymerisation conditions. However, the extraction of the template requires that the bond is readily cleaved once the polymer has been formed.

1.4.3 Crosslinkers

The selectivity of MIPs with respect to molecular recognition is greatly influenced by the amount and nature of the crosslinking agent used in the synthesis of the imprinted polymer. Careful selection of crosslinker which also act as a functional monomer is another important choice to provide complementary interactions with the template and substrates.

In an imprinted polymer, the crosslinker is added to fulfil three major functions. The fundamental role of the crosslinker is to control the morphology of the polymer matrix which will determine the type of polymer product obtained. Besides, it serves to stabilise the imprinted binding sites. It also makes the imprinted polymer insoluble in solvents and imparts mechanical stability to the polymer matrix.[9]

The imprinting efficiency is dependent upon the molar ratios between the template, functional monomer and crosslinker. The high degree of crosslinking enables the binding sites to maintain a three-dimensional structure which is complementary in both shape and chemical functionality to that of the template after removal of the template, and thus the functional groups are held in an

optimal orientation for rebinding the template, allowing the synthetic receptor to 'recognise' the original template.[47] However, it has recently been shown that it is possible to use a crosslinker content as low as 22 mol %,[58] or even around 19 mol % in some cases, yet still retain the selectivity.[59]

The chemical structure of the crosslinker also contributes to the imprinting efficiency. For example, ethylene glycol dimethacrylate (EGDMA) has been used extensively in non-covalent molecular imprinting, normally at levels greater than 75 mol % relative to the functional monomer. Where crosslinkers containing three vinyl groups (*e.g.*, pentaerythritol triacrylate, PETRA **5** or trimethylolpropane trimethacrylate, TRIM **6**) have been reported, only 50 mol % was sufficient to yield highly crosslinked polymer networks with the desired molecular recognition properties.[60],[61] In addition, MIPs prepared with TRIM as crosslinker showed good capability in terms of load capacity and selectivity when compared with EGDMA-based materials. The factors listed below might have given rise to the higher load capacity and selectivity. Firstly, the mass of template imprinted per unit mass of polymer was greater for the TRIM-based MIPs than for the EGDMA-based MIPs, although the molar ratio of the template to the functional monomer was maintained constant. This could conceivably cause more recognition sites per unit mass for the TRIM-based MIPs than for the EGDMA-based MIPs. Secondly, TRIM-based MIPs have some macropores that may be beneficial for improved mass transfer of the analyte during the recognition process. Furthermore, having three vinyl groups in the crosslinker possibly leads to imprinted sites with higher integrity and selectivity than imprinted sites in EGDMA-based MIPs.

There are only a few examples of water-soluble crosslinkers such as *N,N'*-diacryloyl piperazine (DAP) **2** and *N,N'*-methylene bisacrylamide (MDAA) **4** being employed for molecular imprinting polymerisation in aqueous medium.[62],[63] It is believed that more applications are expected in the future for these water-soluble crosslinkers. The chemical structures of several crosslinkers are shown in Figure 1.9.

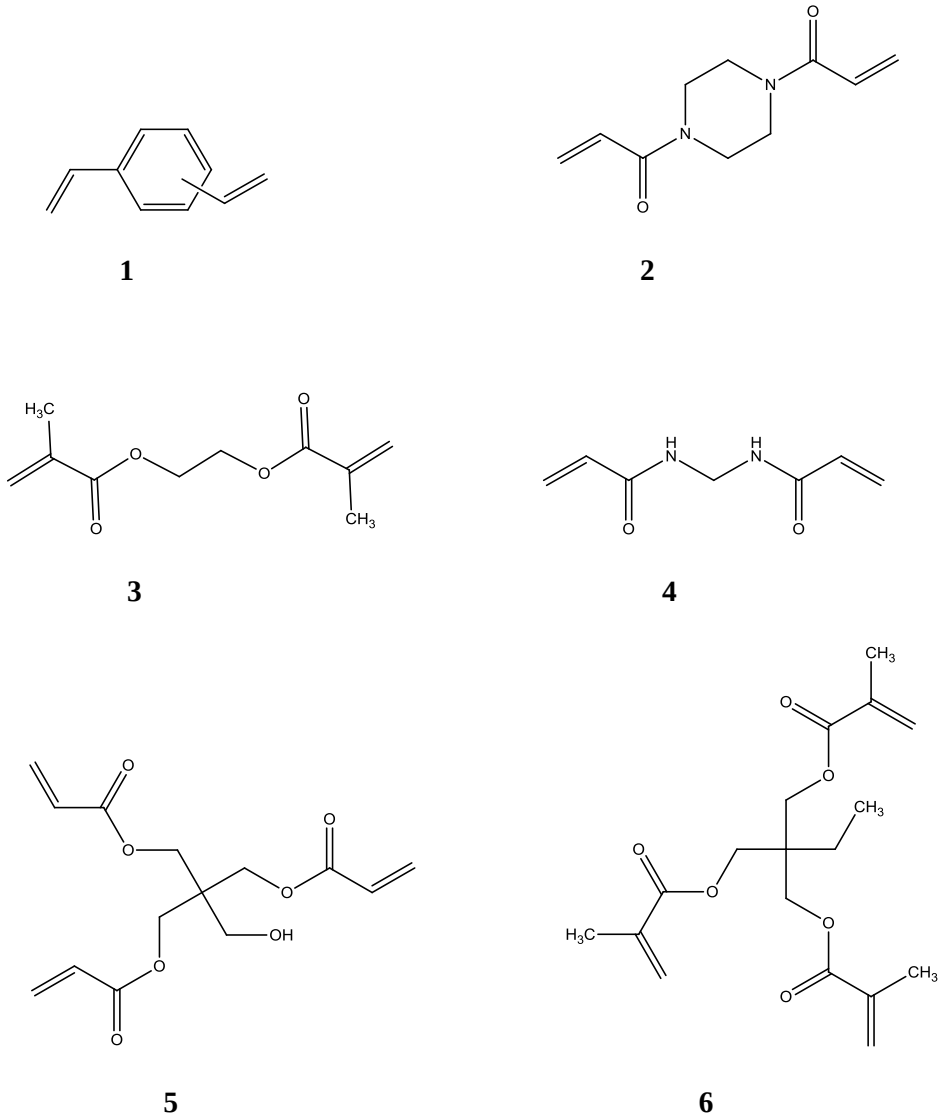

Figure 1.9 Chemical structures of a selection of crosslinkers.

1: *p*-divinylbenzene; **2**: 1,4-diacryloyl piperazine (DAP); **3**: ethylene glycol dimethacrylate (EGDMA); **4**: *N,N'*-methylene bisacrylamide (MDAA); **5**: pentaerythritol triacrylate (PETRA); **6**: trimethylolpropane trimethacrylate (TRIM)

1.4.4 Solvents (Porogens)

The main function of solvent in a polymerisation is to solubilise the constituents, and facilitate the complex formation between template and monomer(s) in the case of non-covalent molecular imprinting. In addition, it is also responsible for creating the pores in macroporous polymers. Therefore, it is commonly referred to as the 'porogen'.

When macroporous polymers are being prepared, the nature and the level of the porogen added will determine the morphology and the total pore volume. Thermodynamically good solvents tend to lead to polymers with well developed pore structures and high specific surface areas, whereas thermodynamically poor solvents lead to polymers with poorly developed pore structures and low specific surface areas. Increasing the volume of porogen increases the pore volume.[9]

Selection of the porogen is dependent on the type of imprinting. For covalent imprinting, many different solvents can be employed as long as they are able to dissolve all components into one phase and give porous products. However, in non-covalent imprinting, the solvents employed are generally apolar and aprotic in nature, such as toluene, dichloromethane and chloroform.

In some cases, when the template is very polar and not well dissolved in apolar solvents (*e.g.*, chloroform, toluene or acetonitrile), then dimethyl sulfoxide (DMSO)[64],[65] and even water/methanol mixtures[66] have been used as an alternative. It is interesting to note that the solubility problem can be overcome in some instances *via* precipitation polymerisation under dilute conditions.

It is very desirable to develop water-based imprinting protocols, as this resembles the environment of biochemical processes and might lead to MIPs that approach antibody-like binding abilities.[67] There are a few examples of molecular imprinting in aqueous media which have been reported,[66],[68],[69] but it is still a great challenge to imprint and rebind the template effectively in such polar environment *via* non-covalent imprinting methods.

1.4.5 Initiators

Many chemical initiators with different chemical properties can be used as the radical source in free radical polymerisation.[70] Normally, they are used at low levels compared to the monomer, *e.g.*, 1 wt. %, or 1 mol % with respect to the total number of moles of polymerisable double bonds. The rate and mode of decomposition of an initiator to radicals can be triggered and controlled in a number of ways, including heat, light and by chemical/electrochemical means, depending upon the chemical nature of the initiator.

For example, the azo initiator azobisisobutyronitrile (AIBN) **I1** can be conveniently decomposed by photolysis (UV) or thermolysis to give stabilised carbon-centred radicals which are capable of initiating the growth of a number of vinyl monomers which then leads to propagation. However, the presence of oxygen retards free radical polymerisations. Thus, in order to maximise the rates of monomer propagation and ensure good batch-to-batch reproducibility of polymerisations, removal of the dissolved oxygen from monomer solutions immediately prior to polymerisation is advisable. Removal of dissolved oxygen can be achieved simply by ultrasonication or by sparging of the monomer solution by an inert gas, *e.g.*, nitrogen or argon.

The chemical structures of selected polymerisation initiators are shown in Figure 1.10.

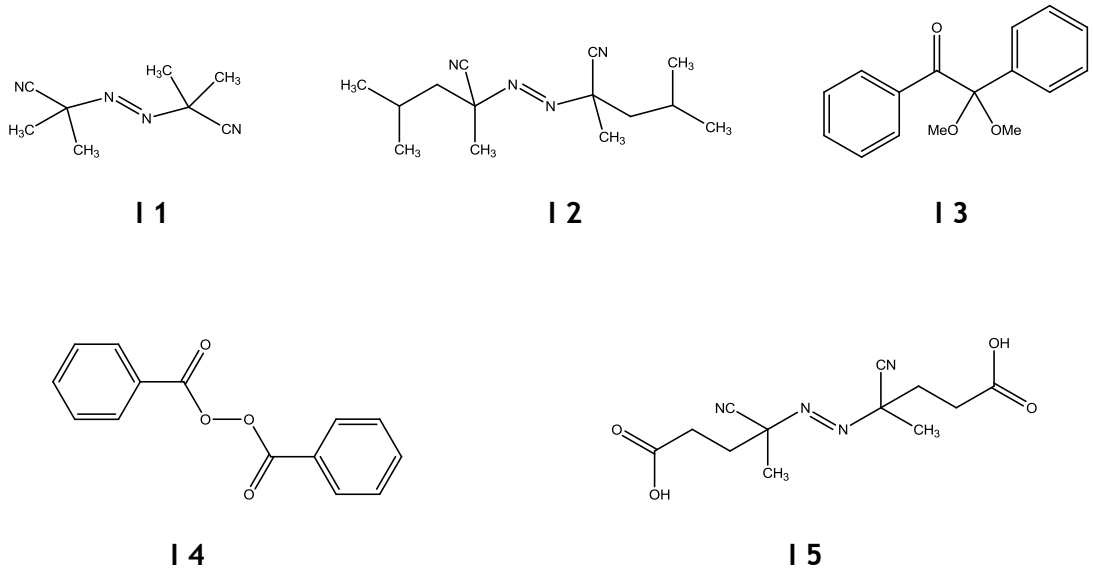

Figure 1.10 Chemical structures of selected initiators:

I1: azobisisobutyronitrile (AIBN); **I2**: azobisdimethylvaleronitrile (ABDV); **I3**: dimethylacetal of benzil; **I4**: benzoylperoxide (BPO); **I5**: 4,4'-azo(4-cyanovaleric acid).

1.5 Polymerisation Methods in Molecular Imprinting

A variety of polymerisation methods have been investigated to prepare MIPs according to their intended applications. For example, spherical particles with narrow size distributions are preferable for solid-phase extraction (SPE) and chromatographic applications, whereas films/membranes may be most appropriate for sensor applications. An increasing number of polymerisation methods to synthesise MIPs has been developed including bulk polymerisation,[71],[72] suspension polymerisation,[73],[74] two-step swelling polymerisation,[75],[76],[77],[78] core-shell polymerisation[79] and precipitation polymerisation.[80],[81],[82] A recent study has compared many types of

polymerisation and highlighted the advantages and disadvantages for each in terms of imprinting effects and ease of application.[83] A few of the newer methods are outlined below.

1.5.1 Solution Polymerisation

Solution polymerisation is the most widely used method to synthesise MIPs due to its simplicity and versatility.[84],[85],[86] Basically, the template molecule, functional monomer, crosslinker, initiator and porogen are mixed well and proceed to polymerise under heating or ultra-violet (UV) radiation. As a result, the polymer obtained is a monolithic polymeric block that normally needs to be crushed, mechanically ground and wet-sieved to deliver particles of a desired size range. The diameters of the particles are usually in the micrometer range and have a broad particle size distribution.[87],[88] Mean particle sizes of around 25 μm are usually used in chromatographic studies,[89] especially when the MIPs are used in High Performance Liquid Chromatography (HPLC) columns, immobilised on Thin Layer Chromatography (TLC) plates or entrapped in capillary columns using acrylamide gels or silicate matrices.[90]

Although the synthesis of the polymer is fast and simple, the process is time consuming (*i.e.*, grinding and size fractionation) and wasteful, since it leads to a substantial loss of useful polymer. Besides, the particles produced are highly irregular in size and shape and generally give less efficient column packing for chromatography. Thus it may lead to reduced chromatographic performance. Moreover, lack of control during the polymerisation process, may lead to heterogeneity in the pores network.

1.5.2 Suspension Polymerisation

Suspension polymerisation is a rather simple method for the preparation of imprinted polymers that do not requiring mechanical grinding and which are in the form of spherical particles. In principle, this approach offers an attractive alternative to solution polymers since it should produce a higher yield of particles with better chromatographic characteristics. The large beads obtained *via* this method are generally polydisperse spheres of micron size.[91] There are two types of suspension polymerisation that have been developed, namely 'oil-in-water'[45],[92],[93] and 'oil-in-oil' suspensions, depending on the nature of the continuous and discontinuous (dispersed) phases used.

An 'oil-in-water' suspension technique has been studied for the imprinting of certain compounds.[94],[95] In this technique, an organic-based imprinting mixture was mixed with water containing a polymer such as poly(vinyl alcohol) or poly(vinylpyrrolidone) as the stabiliser. The two phases are mixed to produce a suspension of small organic droplets in the aqueous dispersant. The polymer beads formed must be washed to remove all stabilisers. Aqueous suspension polymerisation is only feasible for template and functional monomer interactions which are strong, such as covalent bonds because the presence of water in non-covalent imprinting protocols can disrupt the interactions between functional monomer and templates, leading to a poorer imprinting effect.

To enhance the performance of the above method, an 'oil-in-oil' approach was introduced. Instead of using water, perfluorocarbon liquids are used as the suspension medium.[96] Perfluorocarbons are immiscible with most organic compounds and are also non-toxic and chemically inert and thus do not disrupt the

interactions used in non-covalent imprinting.[97] However, these solvents are expensive and it is difficult to stabilise the suspension of an imprinting mixture in fluorocarbon liquids due to the density mis-match between the two phases.

1.5.3 Two-Step Swelling Polymerisation

This method was developed by Hosoya *et al.*[98] and Haginaka *et al.*[99] It has been used to prepare MIPs for a wide range of templates.[66],[98],[100],[101] The technique requires several swelling steps on the initial particles with the imprinting mixture before polymerisation proceeds. Generally, monodisperse polymer beads with controlled diameters can be obtained *via* this method.[75],[76],[98] A polymer seed, often a polystyrene latex, is swollen with initiator and an activating solvent. Sodium dodecyl sulfate is used to stabilise the swollen seed in water as it absorbs the emulsion. In the second step, the swollen seed is added to a dispersion of polymerisation components in water, stabilised using a polymer such as poly(vinyl alcohol). After the monomer has been absorbed into the seeds, polymerisation is carried out to yield high quality spherical beads with improved chromatographic performance.[102] However, the presence of water during the swelling step is a problem which could interfere with the imprinting and thus lead to a decrease in selectivity of molecular recognition.

1.5.4 Core-Shell Polymerisation

This method, which produces core-shell particles having the imprinted sites at the surfaces of the polymer, may be of particular use for the binding of larger molecules such as protein or in drug delivery applications.[103] Molecularly imprinted core-shell particles can be prepared in water using uniform colloid particles as the support.[104]

The particles are typically synthesised in a two-step procedure. At first, an insoluble seed (core) is synthesised using conventional emulsion polymerisation. This is then followed by incubation with a second emulsion containing the monomers and initiators that will synthesise the shell. By a process of droplet fusion and monomer migration, the second emulsion coats the seed particles and it grows to form the shell.[85],[105] As an example, Carter and Rimmer[106] used a two-stage emulsion polymerisation method to prepare caffeine-imprinted core-shell nanobeads in an aqueous medium. Similarly, Pérez *et al*.[79] utilised a covalent imprinting approach to prepare cholesterol-imprinted core-shell nanoparticles in a two-stage polymerisation process. Barahona and coworkers,[107] synthesised core-shell MIP microspheres by precipitation polymerisation for the in-line MISPE extraction of thiabendazole from citrus fruits and orange juice samples.

1.5.5 Precipitation Polymerisation

Precipitation polymerisation is a method to produce imprinted polymer microsphere particles of uniform size in the range 0.1-10 μm[108] that are free from stabiliser or surfactant. The basic method was evolved by Stöver and his coworkers[80] and adapted later by Ye e*t al*.[109] and Wang *et al*.[110] for imprinting purposes. The polymerisations are carried out in a solvent (often acetonitrile) in which both the monomers and initiator are soluble. As the polymer forms, it precipitates from the solution. The monomer loading is very low, generally 1-4 % w/v relative to the solvent, and a high amount of the monomer mixture is a crosslinker.[111] The polymer beads produced *via* this method are protected from aggregation during polymerisation by their crosslinked surfaces. In addition, the solvent plays a crucial role in the formation of polymer particles. This technique is

discussed in more detail in a later chapter. A schematic representation of precipitation polymerisation mechanism is shown in Figure 1.11.

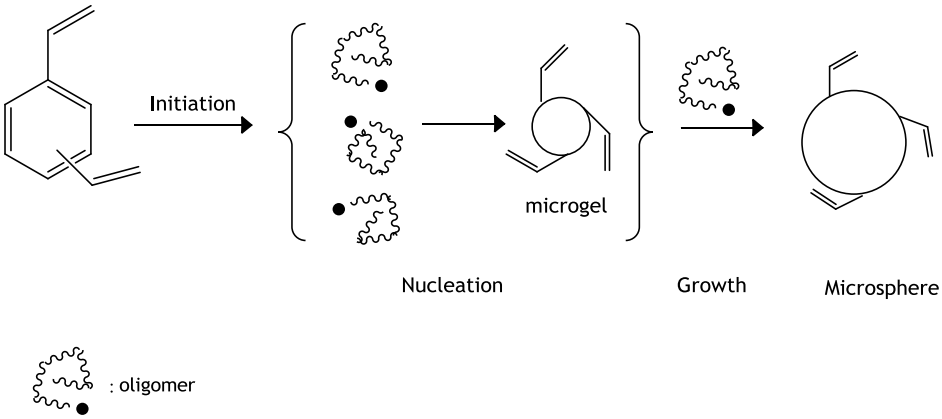

Figure 1.11 The mechanism of precipitation polymerisation[82]

1.6 Applications of Molecularly Imprinted Polymers (MIPs)

MIPs have a broad range of potential applications in areas such as chromatography, solid-phase extraction (SPE), biomimetic sensors, catalysis and drug delivery and, in principle, in any application where molecular recognition is of importance.

1.6.1 Enantioseparation

Historically, chromatographic separation is the most prominent application in the molecular imprinting area.[21] The experimental application of modern liquid chromatographic techniques is of fundamental significance to characterise the properties of imprinted materials such as selectivity, affinity towards the template molecule, number of binding sites or binding kinetics. In addition, it is also the basis of the most significant applications such as racemic mixture resolution and solid-phase extraction (SPE).[35]

Chiral separation of racemic mixtures has attracted strong interest because of the increasing demand for enantiomerically pure compounds.[60],[112],[113] Additionally, polymers imprinted with chiral templates offer a new generation of tailor-made separation materials. A characteristic feature of MIP chiral stationary phases (CSPs) is that the elution order of the enantiomers can be predicted easily.[114] For instance, when the (*S)*-enantiomer is used as the template, the (*R)*-enantiomer will be eluted first, and *vice versa* if the (*R)*-enantiomer is used as the template.

Since the time when the first racemic separation of amino acid derivatives by non-covalent molecular imprinting approach was reported by Andersson *et al.*,[115] significant advances in this field have been made. Highly efficient chirally discriminating MIPs have been prepared under favourable polymerisation conditions, such as by use of trifunctional crosslinkers[61] and acrylamide as functional monomer.[116] In addition, there are numerous reports on the use of capillary electrochromatography (CEC) for the separation of amino acids used in pharmaceuticals, drugs and nucleic acids.[117],[118]

Separation of enantiomers is one of the key issues in the pharmaceutical industry, where often the final product must be in a single pure enantiomer form. Many chiral pharmaceutical compounds, such as timolol,[119] *(S)*-propranolol,[120],[121] naproxen,[42],[100] ephedrine[122],[123] and benzylbenzodiazepine[124] have been separated by the use of MIPs. Most of the works reported were based on applications including controlled released, drug monitoring devices and biological receptor mimetics. In addition, recent progress in this area has been discussed extensively by Maier *et al.*[125] and Sparnacci *et al.*[126]

1.6.2 The Imprinting of Proteins

The considerable biological and technological importance of proteins has attracted interest in developing MIPs capable of selective binding proteins.[127],[128],[129] However, due to the complexity of protein structures, it is a challenge to obtain protein-specific MIPs. In addition, proteins are usually large such that they readily become entrapped inside the imprinted polymer networks and are difficult to extract, especially when conventional imprinting methods are used. To overcome this problem, a surface imprinting approach has been developed to imprint proteins.[60],[130] For example, the first protein imprinted was imprinted on the surface of porous silica particles using a silane-boronate monomer and glycoprotein transferrin as the template.[127]

Besides that, other promising approaches for the imprinting of protein have been developed by other researchers, such as imprinting within hydrogels[131],[132],[133] and the epitope approach.[134] A recent approach developed is based on immobilising biomolecules on the surface of dry microcrystals with full retention of bioactivity known as Protein Coated Micro-Crystals (PCMCs). PCMCs are nanostructures particles made by a one step process developed by Moore *et al*.[135],[136] The use of the PCMC strategy in molecular imprinting has allowed the retention of selected protein native conformation in organic media and the creation of access pores lined with nanocavities which facilitate protein extraction and re-introduction into the imprinted polymer.[137] For example, Brown *et al*.[138] prepared PCMCs with haemoglobin and myoglobin to produce highly selective binding sites in synthetic polymers.

1.6.3 Solid-Phase Extraction (SPE)

Solid-phase extraction (SPE) is used routinely in many different areas of analytical chemistry, especially in environmental and pharmaceutical analysis. The development of SPE has largely been at the expense of liquid-liquid extraction (LLE).[139] Conventionally, the stationary phases of SPE include reversed-phase sorbents (*e.g.,* C_{18}), normal phase sorbents (*e.g.,* silica gel) and ion-exchange sorbents (*e.g.,* SCX and SAX). For a sorbent to be useful, it must enable selective extractions to be achieved. MIPs potentially offer high specificity and stability, as well as compatibility with both organic solvents and aqueous media. They are thus very attractive SPE materials and this has led to the development of the molecularly imprinted solid-phase extraction (MISPE) method.

MISPE is similar to conventional SPE protocols in that it requires conditioning, loading, clean-up and elution steps.[140] A schematic illustration of these steps is shown in Figure 1.12. MISPE can be performed in off-line mode (MIP is packed in polyethylene cartridges) and on-line mode (MIP is packed in LC pre-column), with the system normally being coupled to a chromatographic technique.[141], [142],[143], [144] Furthermore, this method offers cleaner extracts, reduced interferences during the analysis and increased sensitivity.

The study of MIPs as SPE sorbents was first described by Sellergren in 1994, for the extraction of pentamidine from urine samples.[145] A urine sample was spiked with pentamidine and the MIP-based extraction resulted in a clean extract and enrichment of the sample to a level where direct injection of the extract could be applied. This was followed by the development of a propranolol-derived MIP from aqueous samples[146].

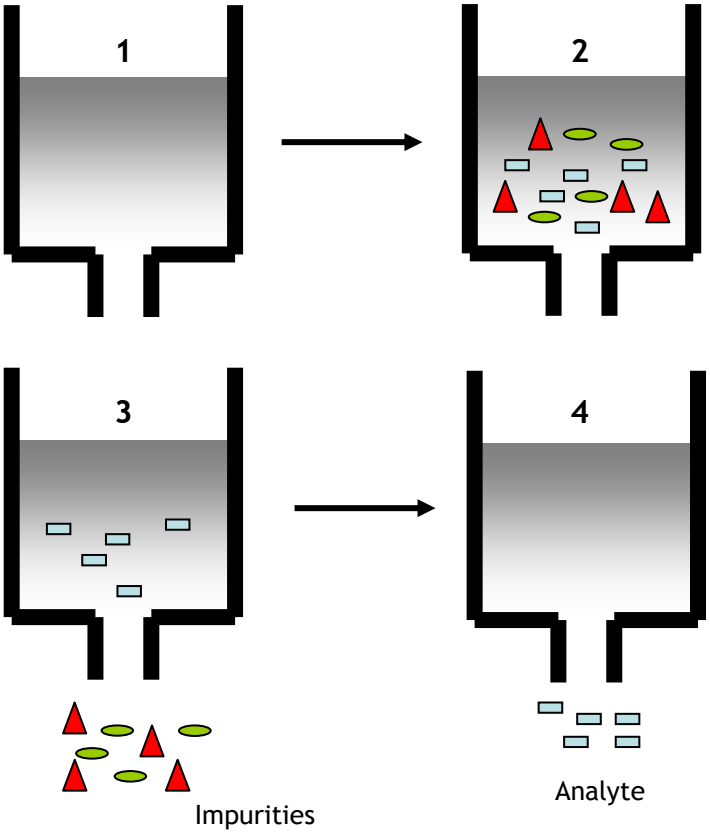

Figure 1.12 Schematic illustration of sample preparation using MISPE

1: The MIP sorbent is conditioned; 2: The complex sample containing the template is loaded; 3: The sorbent is washed with an appropriate solvent(s) to remove the impurities; 4: The enriched and cleaned template/analyte is eluted and collected ready for analysis.

Thereafter, research on utilising MISPE has been growing rapidly in the past years and there are now a large number of publications concerning different types of analytes in the environmental and pharmaceutical analysis fields. Muldoon and coworkers[147] reported on the MIP approach in bioanalysis by using an atrazine-derived MIP to extract the herbicide from organic extracts from beef liver. Another example of the use of atrazine-MISPE was reported by Matsui *et al.*[148] for environmental analysis. A further example of MISPE was reported by Zander

et al.,[141] who evaluated the application of nicotine-MISPE for analysis of nicotine and its oxidation products in a nicotine containing chewing gum. Nicotine-MISPE work has also been carried out by other researchers.[149],[150]

More recently, Ariffin *et al.*[4],[151] developed a method for MISPE prior to analysis using LC-MS for the detection of benzodiazepines. Interestingly, this work opened the door to the application of MISPE in forensic toxicology. The method was found to be simpler and cleaner compared to conventional SPE. A second example of the use of MISPE in forensic toxicology was presented by Harun *et al.*,[152] who evaluated the application of MIPSE for the extraction of ketamine and its metabolites from forensic hair samples.

MIP Technologies AB (Lund, Sweden) was a leading company in the development of MIPs. Today, the company is owned by another company called Biotage. Biotage manufactures a range of sample preparation tools for bioanalytical, clinical, environmental, food and forensic applications. Currently, the company offers a new SPE product, namely AFFINILUTE™ MIP. The products are a range of highly selective SPE phases based on molecularly imprinted polymers. For example, AFFINILUTE™ MIP-TSNAs (tobacco-specific nitrosamines), a class selective SPE sorbent for multi-residue extraction of four different TSNAs (*e.g.*, nicotine (NNK), nornicotine (NNN), anabasine (NAB) and anatabine (NAT)) which can be selectively extracted from biological samples with high recoveries. The method is claimed as robust, recoveries achieved are higher than 90 % and the clean extracts allow low detection levels with minimised matrix effect.[117]

However, this area of application is still not well established even although many examples of MISPE for a range of different compounds have been reported. The main limitation of MISPE is template *'bleeding'* (template leaching out from the polymer), a problem which may interfere with trace analysis. This problem could be overcome by using a structural analogue of the analyte as template for the preparation of the polymer.[153] However, if there is no suitable analogue molecule available, then thermal annihilation, microwave-assisted extraction and desorption with supercritical fluids techniques may be applicable as reported by Ellwanger *et al.*.[154] Therefore, several techniques have been investigated for preparing homogenous MIP particles such as precipitation, dispersion and suspension polymerisation.[83],[110],[155]

1.6.4 Biomimetic sensors

Molecular imprinting has become a universal tool for the preparation of artificial and robust recognition materials mimicking natural systems. One of the most fascinating applications in the area of molecular imprinting is the used of MIPs as recognition elements in biosensor-like devices.[11] In a conventional biosensor, the recognition element could be an enzyme, antibody or receptor, which is normally immobilised at the interface between the sensor and the sample to be analysed. MIPs are easily obtained by copolymerisation of suitable functional monomers and crosslinkers in the presence of the target molecule. These polymers exhibit excellent thermal, chemical and mechanical stability besides having selectivity similar to that of natural systems. This makes them promising materials for sensing applications.

Many applications of MIPs as biomimetic sensors have been reported. MIPs can be conveniently immobilised on an electrode surface or in a membrane configuration. In this mode, they may find broad applications for *in situ* analysis and environmental monitoring.[11] For example, the detection of morphine with a Pt electrode,[156] the detection of theophylline with an ITO (indium tin oxide) electrode,[157] the detection of caffeine with molecularly imprinted quantum dot photoluminescence,[158] and food analysis.[159],[160] Recently, several MIPs have been proposed for TNT (trinitrotoluene) sensing and other related molecules from the gas phase.[161] Reviews of this technology were reported by Hillberg in 2005[162] and Ye and Haupt in 2004.[163]

1.6.5 Catalysis

Another particularly appealing field for the application of MIPs is as enzyme-mimetic catalysts.[164],[165],[166] Catalytically active sites can be designed in MIP networks by employing a transition state analogue (TSA) as a template molecule, similar to catalytic antibodies which are raised against an analogue of the transition state of a catalytic reaction.

For an example, research conducted by Wulff and coworkers,[167],[86] used a functional monomer having an amidine moiety (*i.e., N,N'*-diethyl(4-vinyl phenyl) amidine, DEVPA) to prepare a MIP catalyst. They found that strong ionic interactions between the amidine residues and the TSA enabled DEVPA to form a stable complex with the TSA. In addition, Wen *et al.*[168] studied MIPs having two functional groups (*i.e.*, amidine and imidazole) as opposed to MIPs having only one single functional group. The results showed an enhancement in hydrolytic activities with a co-operative effect induced by the amidine and imidazole

functionalities. For further insight and examples of catalysis in MIPs, a review in this field is reported by Wulff.[166]

1.6.6 Drug delivery

Imprinted polymers have shown a good potential in several areas of drug development but are relatively new in the area of drug delivery. They have been applied usefully as excipients in controlled release delivery systems.[169],[170] Drug delivery systems are required when the therapeutic agent needs to be protected against metabolic attack or when there are absorption barriers or dosage limitations.[171] The ideal delivery vehicle will ensure that the drug is released at the right dose, at the right site and for the required time. In addition, it also must be biocompatible or biodegradable so that it will not be transformed into toxic fragments within the body.

Controlled drug release research in the MIP field has been focusing mainly on slowing the rate at which the drug is released into an organism. This makes it possible to maintain the therapeutic concentration of the drug over an extended period of time. The first report of imprinted polymers that afforded a sustained release mechanism was by Norell *et al.*[172] Polymers imprinted with theophylline, a methyl xanthine used in the treatment of asthma, were evaluated for controlled release in aqueous buffer.

Furthermore, studies by Allender and coworkers[123] showed that slow permeation of a drug through the pores of a MIP before being released from the carrier system is another factor contributing to the prolongation of release time. In the study, they used a propranolol imprinted MIP and it was shown that when compared to a

non-imprinted polymer, the time required for a certain amount of propranolol to be released nearly doubled. The time course of drug release has also been studied by Sreenivasan.[173] He demonstrated the competitive binding of hydrocortisone (template) and testosterone (drug to be delivered) and found that the release of testosterone from the MIP was considerably slower. In addition, MIPs have been shown to be capable of differentiating between the enantiomers of a racemic mixture. Work conducted by Suedee *et al*.[174],[175] examined imprinted polymers as excipients for the controlled delivery of the more pharmaceutically active (*S)*-propranolol from a racemic mixture.

Asunama *et al*.[176] have developed a new molecular imprinting technique based on the ability of cyclodextrins to form inclusion complexes in water with relatively hydrophobic drugs. Cyclodextrins are non-toxic cyclic oligomers of 6-9 glucopyranose units, which present a hydrophilic outer surface and a non-polar cavity.[177] Similar works in terms of cyclodextrins have been proposed by Piletsky *et al*.[62] In their study, they combined the cyclodextrins with ionic monomers to enhance the affinity to amphiphilic molecules containing both hydrophobic and ionic groups.

Imprinted soft contact lenses are an illustration of the potential utility of imprinted hydrogels as drug delivery devices. In general, the drug loading capacity of conventional soft contact lenses is insufficient and, therefore, they have rarely been employed for ophthalmic drug delivery.[178],[179] To overcome this drawback, the application of molecular imprinting technology in the design of soft contact lenses has been shown to be particularly useful. The swelling and shrinking of hydrogels can also be responsive to external stimuli, such as pressure changes,

temperature or variations in concentration of a certain substance, and can be exploited in sophisticated controlled release protocols. Recently, Alvarez-Lorenzo and coworkers[180],[181],[182] developed an imprinting technique to create soft contact lenses which were able to reload and release drugs in a controlled way for the treatment of ocular pathologies.

1.7 References

[1] E. Caro, R. M. Marcé, F. Borrull, P. A. G. Cormack and D. C. Sherrington, *TrAC*. **2006**, *25*, 143-154.

[2] S. Wei, M. Jakusch and B. Mizaikoff, *Anal. Chim. Acta*. **2006**, *578*, 50-58.

[3] A. E. Mahjoub and C. Staub, *J. Chromatogr. B*. **2000**, *742*, 381-390.

[4] R. A. Anderson, M. M. Ariffin, P. A. G. Cormack and E. I. Miller, *Forensic Sci. Int*. **2008**, *174*, 40-46.

[5] G. Theodoridis, A. Kantifes, P. Manesiotis, N. Raikos and H. Tsoukali-Papadopoulou, *J. Chromatogr. A*. **2003**, *987*, 103-109.

[6] R. J. Ansell, *Adv. Drug Deliver. Rev*. **2005**, *57*, 1809-1835.

[7] R. Thoelen, R. Vansweevelt, J. Duchateau, F. Horemans, J. D'Haen, L. Lutsen, D. Vanderzande, M. Ameloot, M. VandeVen, T. J. Cleij and P. Wagner, *Biosens. Bioelectron*. **2008**, *23*, 913-918.

[8] N. A. O'Connor, D. A. Paisner, D. Huryn and K. J. Shea, *J. Am. Chem. Soc*. **2007**, *129*, 1680-1689.

[9] P. A. G. Cormack and A. Z. Elorza, *J. Chromatogr. B*. **2004**, *804*, 173-182.

[10] G. Wulff, T. Gross, R. Schönfeld, T. Schrader and C. Kirsten in *Molecular Imprinting for the Preparation of Enzyme-Analogous Polymers*, *703* ACS Symposium Series, **1998**, 10-28.

[11] K. Haupt and K. Mosbach, *Chem. Rev*. **2000**, *100*, 2495-2504.

[12] F. G. Tamayo, E. Turiel and A. Martín-Esteban, *J. Chromatogr. A*. **2007**, *1152*, 32-40.

[13] B. Sellergren, *TrAC*. **2003**, *22*, xii-xxii.

[14] E. Fischer, *Ber. Dtsch. Chem. Ges.* **1894**, *27*, 2985-2993.

[15] J. D.E. Koshland, *Angew. Chem. Int. Ed. Engl* **1994**, *33*, 2375-2378.

[16] L. Stryer, *Biochemistry*, W. H. Freeman New York, **1988**.

[17] M. V. Polyakov, L. Kuleshina and I. Neimark, *Zh. Fiz. Khim*, **1937**, *10*, 100-112.

[18] L. Pauling, *J. Am. Chem. Soc.* **1940**, *62*, 2643-2657.

[19] B. Dirion, Z. Cobb, E. Schillinger, L. I. Andersson and B. Sellergren, *J. Am. Chem. Soc.* **2003**, *125*, 15101-15109.

[20] F. H. Dickey, *J. Phys. Chem. US* **1955**, *59*, 695-707.

[21] G. Wulff and A. Sarchan, *Angew. Chem. Int. Edit.* **1972**, *11*, 341-347.

[22] R. Arshady and K. Mosbach, *Macromol. Chem. Phys.* **1981**, *182*, 687-692.

[23] B. Sellergren and L. I. Andersson, *Methods* **2000**, *22*, 92-106.

[24] M. J. Whitcombe, M. E. Rodriguez, P. Villar and E. N. Vulfson, *J. Am. Chem. Soc.* **1995**, *117*, 7105-7111.

[25] G. Wulff, W. Vesper, R. Grobe-Einsler and A. Sarhan, *Makromol. Chem.* **1977**, *178*, 2799-2816.

[26] G. Wulff, T. Gross and R. Schőnfeld, *Angew. Chem. Int. Edit.* **1997**, *36*, 1962-1964.

[27] C. Alexander, C. R. Smith, M. J. Whitcombe and E. N. Vulfson, *J. Am. Chem. Soc.* **1999**, *121*, 6640-6651.

[28] J. Yan, G. Springsteen, S. Deeter and B. Wang, *Tetrahedron* **2004**, *60*, 11205-11209.

[29] G. Wulff and A. Biffis, *Molecularly Imprinted Polymers: Man-Made Mimics of Antibodies and their Applications in Analytical Chemistry*, Elsevier, Amsterdam, **2001**, 71-111.

[30] K. J. Shea and G. J. Stoddard, *Macromolecules* **1991**, *24*, 1207-1209.

[31] G. Wulff, *Angew. Chem. Int. Ed.* **1995**, *34*, 1812-1832.

[32] K. Mosbach and R. Mosbach, *Acta. Chem. Scand.* **1966**, *20*, 2807-2810.

[33] B. Sellergren, *TrAC*. **1997**, *16*, 310-320.

[34] B. Sellergren, *Tech. and Instr. Anal Chem.* **2000**, *23*, 113-184.

[35] M. Yan and O. Ramström, *Molecular Imprinted Materials : Science and Technology, Marcel Dekker, New York*, **2005**.

[36] J. F. Wang, P. A. G. Cormack, D. C. Sherrington and E. Khoshdel, *Pure Appl. Chem.* **2007**, *79*, 1503-1517.

[37] H. Kempe and M. Kempe, *Anal. Chem.* **2006**, *78*, 3659-3666.

[38] J. Y. N. Philip, J. Buchweishaija, L. L. Mkayula and L. Ye, *J. Agr. Food Chem.* **2007**, *55*, 8870-8876.

[39] J. Yang, Y. Hu, J.-B. Cai, X.-L. Zhu and Q.-D. Su, *Anal. Bioanal. Chem.* **2006**, *384*, 761-768.

[40] A. Zurutuza, S. Bayoudh, P. A. G. Cormack, L. Dambies, J. Deere, R. Bischoff and D. C. Sherrington, *Anal. Chim. Acta.* **2005**, *542*, 14-19.

[41] P. T. Vallano and V. T. Remcho, *J. Chromatogr. A.* **2000**, *887*, 125-135.

[42] M. Kempe and K. Mosbach, *J. Chromatogr. A.* **1994**, *664*, 276-279.

[43] B. Sellergren, Å. Zander, T. Renner and A. Swietlow, *J. Chromatogr. A.* **1998**, *829*, 143-152.

[44] A. Bereczki, A. Tolokán, G. Horvai, V. Horváth, F. Lanza, A. J. Hall and B. Sellergren, *J. Chromatogr. A.* **2001**, *930*, 31-38.

[45] A. Flores, D. Cunliffe, M. J. Whitcombe and E. N. Vulfson, *J. Appl. Polym. Sci.* **2000**, *77*, 1841-1850.

[46] E. Caro, R. M. Marcé, F. Borrull, P. A. G. Cormack and D. C. Sherrington, *J. Chromatogr. A.* **2002**, *963*, 169-178.

[47] S. H. Cheong, S. McNiven, A. Rachkov, R. Levi, K. Yano and I. Karube, *Macromolecules* **1997**, *30*, 1317-1322.

[48] P. Villar, M. J. Whitcombe and E. N. Vulfson, *Polymer* **2007**, *48*, 1483-1489.

[49] M. Lübke, M. J. Whitcombe and E. N. Vulfson, *J. Am. Chem. Soc.* **1998**, *120*, 13342-13348.

[50] M. A. Khasawneh, P. T. Vallano and V. T. Remcho, *J. Chromatogr. A.* **2001**, *922*, 87-97.

[51] J. U. Klein, M. J. Whitcombe, F. Mulholland and E. N. Vulfson, *Angew. Chem. Int. Edit.* **1999**, *38*, 2057-2060.

[52] N. Kirsch, C. Alexander, M. Lübke, M. J. Whitcombe and E. N. Vulfson, *Polymer* **2000**, *41*, 5583-5590.

[53] B. Sellergren, *TrAC.* **1999**, *18*, 164-174.

[54] K. Yoshimatsu, K. Reimhult, A. Krozer, K. Mosbach, K. Sode and L. Ye, *Anal. Chim. Acta.* **2007**, *584*, 112-121.

[55] A. Martín-Esteban, Fresen. *J. Anal. Chem.* **2001**, *370*, 795-802.

[56] K. Karim, F. Breton, R. Rouillon, E. V. Piletska, A. Guerreiro, I. Chianella and S. A. Piletsky, *Adv. Drug Deliver. Rev.* **2005**, *57*, 1795-1808.

[57] B. Sellergren, *Molecularly Imprinted Polymers : Man-Made Mimics of Antibodies and Their Applications in Analytical Chemistry*, Elsevier, Amsterdam, **2001**, 113-184.

[58] C. Yu and K. Mosbach, *J. Chromatogr. A.* **2000**, *888*, 63-72.

[59] E. Yilmaz, K. Mosbach and K. Haupt, *Anal. Commun.* **1999**, *36*, 167-170.

[60] M. Kempe and K. Mosbach, *Tetrahedron Lett.* **1995**, *36*, 3563-3566.

[61] M. Kempe, *Anal. Chem.* **1996**, *68*, 1948-1953.

[62] S. A. Piletsky, H. S. Andersson and I. A. Nicholls, *Macromolecules* **1999**, *32*, 633-636.

[63] S. A. Piletsky, H. Matuschewski, U. Schedler, A. Wilpert, E. V. Piletska, T. A. Thiele and M. Ulbricht, *Macromolecules* **2000**, *33*, 3092-3098.

[64] C. Lubke, M. Lubke, M. J. Whitcombe and E. N. Vulfson, *Macromolecules* **2000**, *33*, 5098-5105.

[65] L. Malmusi, S. Franchini, A. Mucci, L. Schenetti, U. Gulini, G. Marucci, L. Brasili, H. Asanuma, M. Kakazu, M. Shibata, T. Hishiya and M. Komiyama, *Supramol. Sci.* **1998**, *5*, 417-421.

[66] K. Yoshizako, K. Hosoya, Y. Iwakoshi, K. Kimata and N. Tanaka, *Anal. Chem.* **1998**, *70*, 386-389.

[67] K. Haupt, A. Dzgoev and K. Mosbach, *Anal. Chem.* **1998**, *70*, 628-631.

[68] D. Janiak and P. Kofinas, *Anal. Bioanal. Chem.* **2007**, *389*, 399-404.

[69] S. L. Brown, J. Vos, P. A. G. Cormack and B. D. Moore, *Amer. Chem. Soc.*, **2006**, *Abstracts of Papers, 232nd ACS National Mtg.*, BIOT-026.

[70] C. Alexander, H. S. Andersson, L. I. Andersson, R. J. Ansell, N. Kirsch, I. A. Nicholls, J. O'Mahony and M. J. Whitcombe, *J. Mol. Recognit.* **2006**, *19*, 106-180.

[71] G. P. Gonz´alez, P. F. Hernando and J. S. D. Alegra, *Anal. Chim. Acta.* **2006**, *557*, 179-183.

[72] J. O'Mahony, A. Molinellib, K. Nolan, M. R. Smyth and B. Mizaikoff, *Biosens. Bioelectron.* **2006**, *21*, 1383-1392.

[73] X. Pang, G. Cheng, R. Li, S. Lu and Y. Zhang, *Anal. Chim. Acta.* **2005**, *550*, 13-17.

[74] M. Kawaguchi, Y. Hayatsu, H. Nakata, Y. Ishii, R. Ito, K. Saito and H. Nakazawa, *Anal. Chim. Acta.* **2005**, *539*, 83-89.

[75] J. Haginaka and C. Kagawa, *J. Chromatogr. A.* **2002**, *948*, 77-84.

[76] M. Nakamura, M. Ono, T. Nakajima, Y. Ito, T. Aketo and J. Haginaka, *J. Pharmaceut. Biomed.* **2005**, *37*, 231-237.

[77] K. Hosoya, Y. Kageyama, K. Kimata, T. Araki, N. Tanaka and J. M. J. Fréchet, *J. Polym. Sci. A1* **1996**, *34*, 2767-2774.

[78] J. Haginaka and Y. Sakai, *J. Pharmaceut. Biomed.* **2000**, *22*, 899-907.

[79] N. Pérez, M. J. Whitcombe and E. N. Vulfson, *J. Appl. Polym. Sci.* **2000**, *77*, 1851-1859.

[80] K. Li and H. D. H. Stöver, *J. Polym. Sci. A1* **1993**, *31*, 3257-3263.

[81] W.-H. Li and H. D. H. Stöver, *Macromolecules* **2000**, *33*, 4354-4360.

[82] W. H. Li, K. Li and H. D. H. Stöver, *J. Polym. Sci. Pol. Chem.* **1999**, *37*, 2295-2303.

[83] N. Pérez-Moral and A. G. Mayes, *Anal. Chim. Acta.* **2004**, *504*, 15-21.

[84] M. F. Ellis, T. W. Taylor, V. Gonzalez and K. F. Jensen, *AIChE Journal* **1988**, *34*, 1341-1353.

[85] A. G. Mayes and K. Mosbach, *Anal. Chem.* **1996**, *68*, 3769-3774.

[86] A. G. Strikovsky, D. Kasper, M. Grün, B. S. Green, J. Hradil and G. Wulff, *J. Am. Chem. Soc.* **2000**, *122*, 6295-6296.

[87] D. Silvestri, C. Borrelli, P. Giusti, C. Cristallini and G. Ciardelli, *Anal. Chim. Acta.* **2005**, *542*, 3-13.

[88] C. Baggiani, L. Anfossi, P. Baravalle, C. Giovannoli and C. Tozzi, *Anal. Chim. Acta.* **2005**, *531*, 199-207.

[89] B. Sellergren and K. J. Shea, *J. Chromatogr. A.* **1995**, *690*, 29-39.

[90] H. Yan and K. H. Row, *Int. J. Mol. Sci.* **2006**, *7*, 155-178.

[91] A. G. Mayes, *Molecularly Imprinted Polymers: Man Made Mimics of Antibodies and their Application in Analytical Chemistry*, Elsevier Science B.V, New York, **2001**.

[92] A. Flores, D. Cunliffe, M. J. Whitcombe and E. N. Vulfson, *J. Appl. Polym. Sci.* **2000**, *77*, 1851-1859.

[93] J. Damen and D. C. Neckers, *J. Org. Chem.* **1980**, *45*, 1382-1387.

[94] A. Strikovsky, J. Hradil and G. Wulff, *React. Funct. Polym.* **2003**, *54*, 49-61.

[95] S. G. Hu, S. W. Wang and X. W. He, *Analyst* **2003**, *128*, 1485-1489.

[96] D. W. Zhu, *Macromolecules* **1996**, *29*, 2813-2817.

[97] H. Meinert, *Macromol. Sy.* **1994**, *82*, 201-214.

[98] K. Hosoya, K. Yoshizako, Y. Shirasu, K. Kimata, T. Araki, N. Tanaka and J. Haginaka, *J. Chromatogr. A.* **1996**, *728*, 139-147.

[99] J. Haginaka, *Anal. Bioanal. Chem.* **2004**, *379*, 332-334.

[100] J. Haginaka, H. Takehira, K. Hosoya and N. Tanaka, *J. Chromatogr. A.* **1998**, *816*, 113-121.

[101] J. Haginaka, H. Sanbe and H. Takehira, *J. Chromatogr. A.* **1999**, *857*, 117-125.

[102] K. Yoshizako, Y. Shirasu, K. Hosoya, K. Kimata, T. Araki and N. Tanaka, *Chem. Lett.* **1996**, *8*, 717-718.

[103] N. Pérez-Moral and A. G. Mayes, *Macromol. Rapid Comm.* **2007**, *28*, 2170-2175.

[104] L. Ye and E. Yilmaz in *Molecularly Imprinted Polymer Beads, Vol.* CRS Press, **2004**, pp. 435-454.

[105] A. G. Mayes and M. J. Whitcombe, *Adv. Drug Deliver. Rev.* **2005**, *57*, 1742-1778.

[106] S. Carter and S. Rimmer, *Adv. Mater.* **2002**, *14*, 667-670.

[107] F. Barahona, E. Turiel, P. A. G. Cormack and A. Martín-Esteban, *J. Sep. Sci.* **2011**, *34*, 217-224.

[108] L. Schweitz, P. Spégel and S. Nilsson, *Analyst* **2000**, *125*, 1899-1901.

[109] L. Ye, P. A. G. Cormack and K. Mosbach, *Anal. Commun.* **1999**, *36*, 35-38.

[110] J. Wang, P. A. G. Cormack, D. C. Sherrington and E. Khoshdel, *Angew. Chem. Int. Edit.* **2003**, *42*, 5336-5338.

[111] A. Beltran, E. Caro, R. M. Marcé, P. A. G. Cormack, D. C. Sherrington and F. Borrull, *Anal. Chim. Acta.* **2007**, *597*, 6-11.

[112] E. Amut, Q. Fu, Q. Fang, R. Liu, A. Xiao, A. Zeng and C. Chang, *J. Polym. Res.* **2010**, *17*, 401-409.

[113] A. Dobashi, S. Nishida, K. Kurata and M. Hamada, *Anal. Sci.* **2002**, *18*, 35-39.

[114] H. Zhang, L. Ye and K. Mosbach, *J. Mol. Recognit.* **2006**, *19*, 248-259.

[115] L. Andersson, B. Sellergren and K. Mosbach, *Tetrahedron Lett.* **1984**, *25*, 5211-5214.

[116] C. Yu and K. Mosbach, *J. Org. Chem.* **1997**, *62*, 4057-4064.

[117] M. Kato, M. T. Dulay, B. Bennett, J. R. Chen and R. N. Zare, *Electrophoresis* **2000**, *21*, 3145-3151.

[118] L. Schweitz, *Anal. Chem.* **2002**, *74*, 1192-1196.

[119] L. Fischer, R. Mueller, B. Ekberg and K. Mosbach, *J. Am. Chem. Soc.* **1991**, *113*, 9358-9360.

[120] L. I. Andersson, *Anal. Chem.* **1996**, *68*, 111-117.

[121] L. Andersson, A. Paprica and T. Arvidsson, *Chromatographia* **1997**, *46*, 57-62.

[122] O. Ramström, C. Yu and K. Mosbach, *J. Mol. Recognit.* **1996**, *9*, 691-696.

[123] C. J. Allender, C. Richardson, B. Woodhouse, C. M. Heard and K. R. Brain, *Int. J. Pharm.* **2000**, *195*, 39-43.

[124] B. R. Hart, D. J. Rush and K. J. Shea, *J. Am. Chem. Soc.* **2000**, *122*, 460-465.

[125] N. Maier and W. Lindner, *Anal. Bioanal. Chem.* **2007**, *389*, 377-397.

[126] K. Sparnacci, M. Laus, L. Tondelli, L. Magnani and C. Bernardi, *Macromol. Chem. Physic.* **2002**, *203*, 1364-1369.

[127] M. Glad, O. Norrlöw, B. Sellergren, N. Siegbahn and K. Mosbach, *J. Chromatogr. A.* **1985**, *347*, 11-23.

[128] T. Shiomi, M. Matsui, F. Mizukami and K. Sakaguchi, *Biomaterials* **2005**, *26*, 5564-5571.

[129] D. F. Tai, C. Y. Lin, T. Z. Wu and L. K. Chen, *Anal. Chem.* **2005**, *77*, 5140-5143.

[130] X. Liu and K. Mosbach, *Am. Biotech. Lab.* **1998**, *16*, 90.

[131] J. Liao, Y. Wang and S. Hjertén, *Chromatographia* **1996**, *42*, 259-262.

[132] S. Hjertén, J. Liao, K. Nakazato, Y. Wang, G. Zamaratskaia and H. Zhang, *Chromatographia* **1997**, *44*, 227-234.

[133] D. Tong, C. Heényi, Z. Bikádi, J. Gao and S. Hjertén, *Chromatographia* **2001**, *54*, 7-14.

[134] N. Minouraa, A. Rachkov, M. Higuchi and T. Shimizu, *Bioseparation* **2001**, *10*, 399-407.

[135] B. D. Moore, M. C. Parker, P. J. Halling, J. Partridge and H. N. E. Stevens in *Rapid Dehydration of Protein*, *WO0069887* **2000**.

[136] M. Kreiner, B. D. Moore and M. C. Parker, *Chem. Commun.* **2001**, 1096-1097.

[137] A. A. Bawazir, B. D. Moore and J. D. S. Gaylor, *J. Med. Devices* **2009**, *3*, 27524.

[138] S. L. Brown, J. Vos, P. A. G. Cormack and B. D. Moore, *Amer. Chem. Soc.* **2006**, *Abstracts of Papers, 232nd ACS National Mtg.*, BIOT-026.

[139] J. M. Mollerup, *Fluid Phase Equilibr.* **2006**, *241*, 205-215.

[140] M. M. Ariffin, *PhD Thesis, University of Glasgow, Glasgow*, **2006**.

[141] Å. Zander, P. Findlay, T. Renner, B. Sellergren and A. Swietlow, *Anal. Chem.* **1998**, *70*, 3304-3314.

[142] K. Farrington, E. Magner and F. Regan, *Anal. Chim. Acta.* **2006**, *566*, 60-68.

[143] B. Bjarnason, L. Chimuka and O. Ramström, *Anal. Chem.* **1999**, *71*, 2152-2156.

[144] L. I. Andersson, *Bioseparation* **2001**, *10*, 353-364.

[145] B. Sellergren, *Anal. Chem.* **1994**, *66*, 1578-1582.

[146] P. Martin, I. D. Wilson and G. R. Jones, *J. Chromatogr. A.* **2000**, *889*, 143-147.

[147] M. T. Muldoon and L. H. Stanker, *Anal. Chem.* **1997**, *69*, 803-808.

[148] J. Matsui, K. Fujiwara and T. Takeuchi, *Anal. Chem.* **2000**, *72*, 1810-1813.

[149] J. Yang, Y. Hu, J. B. Cai, X. L. Zhu, Q. D. Su, Y. Q. Hu and F. X. Liang, *Food Chem. Toxicol.* **2007**, *45*, 896-903.

[150] J. Olsen, P. Martin and I. D. Wilson, *Anal. Commun.* **1998**, *35*, 13-14.

[151] M. M. Ariffin, E. I. Miller, P. A. G. Cormack and R. A. Anderson, *Anal. Chem.* **2007**, *79*, 256-262.

[152] N. Harun, R. Anderson and P. A. G. Cormack, *Anal. Bioanal. Chem.* **2010**, *396*, 2449-2459.

[153] L. I. Andersson, *J. Chromatogr. B.* **2000**, *745*, 3-13.

[154] A. Ellwanger, C. Berggren, S. Bayoudh, C. Crecenzi, L. Karlsson, P. K. Owens, K. Ensing, P. A. G. Cormack, D. C. Sherrington and B. Sellergren, *Analyst* **2001**, *126*, 784-792.

[155] M. Yan and A. Kapua, *Anal. Chim. Acta.* **2001**, *435*, 163-167.

[156] C. H. Weng, W. M. Yeh, K. C. Ho and G.-B. Lee, *Sensor. Actuat. B-Chem.* **2007**, *121*, 576-582.

[157] Y. Yoshimi, R. Ohdaira, C. Iiyama and K. Sakai, *Sensor. Actuat. B-Chem.* **2001**, *73*, 49-53.

[158] C. I. Lin, A. K. Joseph, C. K. Chang and Y. D. Lee, *J. Chromatogr. A.* **2004**, *1027*, 259-262.

[159] K. Yano and I. Karube, *TrAC.* **1999**, *18*, 199-204.

[160] A. M. Riederer, R. E. Hunter Jr, S. W. Hayden and P. B. Ryan, *Environ. Sci. Technol.* **2009**, *44*, 483-490.

[161] N. R. Walker, M. J. Linman, M. M. Timmers, S. L. Dean, C. M. Burkett, J. A. Lloyd, J. D. Keelor, B. M. Baughman and P. L. Edmiston, *Anal. Chim. Acta.* **2007**, *593*, 82-91.

[162] A. L. Hillberg, K. R. Brain and C. J. Allender, *Adv. Drug Deliver. Rev.* **2005**, *57*, 1875-1889.

[163] L. Ye and K. Haupt, *Anal. Bioanal. Chem.* **2004**, *378*, 1887-1897.

[164] M. J. Whitcombe, C. Alexander and E. N. Vulfson, *Synlett* **2000**, *2000*, 0911-0923.

[165] C. Alexander, L. Davidson and W. Hayes, *Tetrahedron* **2003**, *59*, 2025-2027.

[166] G. Wulff, *Chem. Rev.* **2002**, *102*, 1-28.

[167] J. M. Kim, K. D. Ahn and G. Wulff, *Macromol. Chem. Phys.* **2001**, *202*, 1105-1108.

[168] W. Chen, D. K. Han, K. D. Ahn and J. M. Kim, *Macromol. Research* **2002**, *10*, 122-126.

[169] B. Sellergren and C. J. Allender, *Adv. Drug Deliver. Rev.* **2005**, *57*, 1733-1741.

[170] C. Beneke, A.Viljoen and J. Hamman, *Molecules* **2009**, *14*, 2602-2620.

[171] D. Cunliffe, A. Kirby and C. Alexander, *Adv. Drug Deliver. Rev.* **2005**, *57*, 1836-1853.

[172] M. C. Norell, H. S. Andersson and I. A. Nicholls, *J. Mol. Recognit.* **1998**, *11*, 98-102.

[173] K. Sreenivasan, *Angew. Makromol. Chem.* **1997**, *246*, 65-69.

[174] R. Suedee, T. Srichana and G. P. Martin, *J. Control. Release* **2000**, *66*, 135-147.

[175] R. Suedee, T. Srichana and T. Rattananont, *Drug Deliv.* **2002**, *9*, 19 - 30.

[176] H. Asanuma, T. Akiyama, K. Kajiya, T. Hishiya and M. Komiyama, *Anal. Chim. Acta.* **2001**, *435*, 25-33.

[177] D. C. Bibby, N. M. Davies and I. G. Tucker, *Int. J. Pharm.* **1999**, *187*, 243-250.

[178] C. C. S. Karlgard, N. S. Wong, L. W. Jones and C. Moresoli, *Int. J. Pharm.* **2003**, *257*, 141-151.

[179] T. P. Heyman, M. L. McDermott, J. L. Ubels and H. F. Edelhauser, *J. Cat. Ref. Surg.* **1989**, *15*, 169.

[180] C. Alvarez-Lorenzo, O. Guney, T. Oya, Y. Sakai, M. Kobayashi, T. Enoki, Y. Takeoka, T. Ishibashi, K. Kuroda, K. Tanaka, G. Wang, A. Y. Grosberg, S. Masamune and T. Tanaka, *Macromolecules* **2000**, *33*, 8693-8697.

[181] C. Alvarez-Lorenzo, H. Hiratani, J. L. Gómez-Amoza, R. Martínez-Pacheco, C. Souto and A. Concheiro, *J. Pharm. Sci.* **2002**, *91*, 2182-2192.

[182] H. Hiratani, Y. Mizutani and C. Alvarez-Lorenzo, *Macromol. Biosci.* **2005**, *5*, 728-733.

CHAPTER 2

AIMS AND SCOPE OF RESEARCH

2.1 Introduction to the PhD Study

Molecular imprinting is a rapidly developing technique for the preparation of polymeric materials that are capable of molecular recognition for selective separation and chemical analysis, amongst other applications. Besides their remarkable molecular recognition properties, MIPs are physically-robust, insoluble macromolecules that can be packed, in particulate and beaded forms, into columns for direct use as liquid chromatography (LC) stationary phases and solid-phase extraction (SPE) sorbents. Their inherent selectivity in SPE has already been proven repeatedly, but their potential use as selective polymeric HPLC stationary phases has not yet been exploited fully, although polymeric stationary phases for SPE are now produced commercially. In this area, chiral selectivity would be a valuable adjunct to the properties of a stationary phase. The format of a separation system, whether it is traditional High Performance Liquid Chromatography (HLPC), Ultra Performance Liquid Chromatography (UPLC), capillary chromatography, electrochromatography or electrophoresis, presents both opportunities and challenges for the application of MIPs.

Other physical formats for MIPs besides particulate forms have also been reported, *e.g.*, imprinted capillaries and membranes. Of direct relevance to the current work is the fact that imprinted materials are stable in use, are recyclable, and that inexpensive, commodity monomers and crosslinkers are normally used in their

preparation. Furthermore, it is recognised that there is still room for improvement in the properties of the current generation of imprinted polymers, in terms of format synthesis and optimisation, imprinting and binding in aqueous media, binding capacity and binding site distributions.

In this study, work was directed towards the synthesis of novel imprinted materials that will enable high performance separations in analytical science. Free radical polymerisation (FRP) is one of the main techniques used industrially for the production of polymeric materials. Although this synthetic technique has allowed the preparation of advanced polymers for use in diverse fields, it does not provide good/tight control over the molar mass, molar mass distribution and architecture of the polymer being synthesised. With the evident growth in the molecular imprinting field, innovative synthetic approaches which allow better control over these features are very desirable. To overcome the disadvantages of free radical polymerisation, a range of so-called living/controlled radical polymerisation (CRP) techniques has been developed.

It is well understood that CRP processes offer many benefits. These include the ability to control molecular weight and polydispersity, and to prepare block copolymers and other polymers of complex architecture. As an alternative to the use of conventional FRP for the production of MIPs, our hypothesis was that the controlled nature of 'living' (controlled) radical polymerisation would translate into MIPs with properties superior to those displayed by MIPs prepared by conventional FRP, *e.g.*, improved homogeneity of binding sites and enhanced chromatographic performance.

In another distinct branch of the study, a computational modelling approach was explored to allow a prediction of the binding isotherm of a MIP in a qualitative manner prior to synthesis. The focus of this area was the development of a detailed understanding of the molecular recognition phenomena and its resulting effect on the adsorption behaviour of molecularly imprinted polymers.

2.2 Outline of the Thesis

This thesis consists of three main works, all focussed upon enhancing the properties and utility of molecularly imprinted polymers. The aim of each chapter of the Thesis is outlined below.

Chapter 1: Introduction

In this chapter, a brief overview of the history and development of molecularly imprinted polymers is outlined. The approaches to MIP synthesis are discussed in detail, with selected examples provided for each approach. Furthermore, attention is drawn to a number of factors pertaining to the template molecules and the selection of suitable functional monomers, crosslinkers, solvents, initiators and general polymerisation procedures. In addition, recent applications of MIPs are also discussed.

Chapter 2: Aim and Scope of Research

In this section, a brief general outline of the thesis is provided, including the scientific motivations for the study.

Chapter 3: Molecularly Imprinted Polymers in Forensic Toxicology

In Chapter 3, a brief introduction to, and the problems associated with, ketamine, which is an internationally-controlled drug, are discussed. A new analytical method, referred to as MILC-MS/MS for the detection of ketamine, has been developed. Previous reports on ketamine detection were based on the MISPE method. A key requirement for the new method is the production of ketamine imprinted polymer particulates in an appropriate physical format for the direct packing of the imprinted materials into chromatography columns, which are then hyphenated to a mass spectrometer. Several such polymers were synthesised and their molecular recognition properties characterised using liquid chromatography techniques. Promising preliminary results on the new approach of ketamine detection (MILC-MS/MS) are discussed.

Chapter 4: Controlled/Living Radical Polymerisation

Chapter 4 contains a brief discussion about polymerisation in general, the chemistry of conventional free radical polymerisation (FRP) and living/controlled radical polymerisation (CRP). CRP techniques have attracted great attention in the last decade. These techniques have opened avenues to the synthesis of tailor-made macromolecules. CRP is discussed in detail; atom transfer radical polymerisation (ATRP), nitroxide-mediated radical polymerisation (NMRP) and reversible addition-fragmentation chain-transfer polymerisation (RAFT) are introduced. RAFT polymerisation is discussed in the greatest detail as it is the method employed in this study. Procedures for the RAFT agent synthesised for this study are discussed. Furthermore, a brief introduction to, and the advantages of post-polymerisation chemical modification with 2-hydroxyethyl-methacrylate (HEMA) are discussed.

Chapter 5: Towards the Rational Design of Molecularly Imprinted Polymers

Chapter 5 describes the synthetic part of a collaborative research study where the aim of the research was to develop a computational model for MIPs which will predict the qualitative binding isotherm of a MIP synthesised *in silico*. However, in order to test the predictive power of the model, the data generated has been compared to binding isotherm data generated for real imprinted polymers. Therefore, imprinted polymers have been synthesised and their binding isotherms have been measured with BET analysis in order to test the validity of the predictive model. To this end, pyridine imprinted and non-imprinted polymers have been synthesised in monolithic form. Thereafter, the monoliths were ground and the properties of the template-free products were evaluated.

Chapter 6: General Conclusions and Further Works

Chapter 6 comprises a general discussion of all the work performed over the course of this study. Conclusions based on the successes and failures during the study will be drawn, and suggestions for logical extensions of the work will be outlined.

CHAPTER 3

MOLECULAR IMPRINTING IN FORENSIC TOXICOLOGY

3.1 Introduction to Forensic Toxicology

Forensic toxicology is a discipline of forensic science dealing with the medical and legal aspects of the harmful effects of toxic substances or poisons on human beings.[1] It is the study of the chemical composition, preparation and identification of poisons, commonly alcohol, drugs and chemicals. It also includes knowledge about the adsorption, distribution and elimination characteristics of such substances in the body.[2]

Toxicology is the study of the toxic or harmful effects of chemicals, particularly on living systems.[3] It is concerned with how toxins act, when their harmful effects occur, and what the symptoms and treatments are for poisoning. It also involves the identification of the substances involved.

Bioanalysis is the process of analysing drugs and chemicals in order to gain more information about them, to enable drug discovery and development.[4] The most frequently analysed biological samples are urine, blood, plasma or serum, hair, saliva and tissues.[5] Currently, the development of scientific techniques for the analysis of drug and non-drug substances is important and advancing rapidly. To understand drug action, one must know where and how the effects occur in the body.[6]

3.2 Forensic Toxicology Issues and Possible Solutions

The future may provide greater and greater toxicological information, but it is not a certainty that this will add interpretive clarity for the forensic toxicologist.[7] Every generation of forensic toxicologist has had to endure numerous challenges outside of those already expressed.

Today, toxicologists have to develop new methods and techniques to identify new drugs or new drug derivatives since these species continue to emerge. The most popular drugs now are the synthetic drugs, such as those in the amphetamines group,[8],[9] and benzodiazepines,[10],[11] but can be any other illicit substance, cannabis,[12],[13] cocaine[14],[15] and the opiates.[16],[17] The discipline requires high levels of skill in analytical techniques, with a solid knowledge of pharmacology and pharmacokinetics. It is illogical to use only one extraction method to isolate all types of drugs from a sample. In response to this issue, a few distinct methods have been developed and published.[18],[19],[20] The critical issue is the sensitivity and selectivity of the analytical methods or techniques used to detect trace levels of drugs even in the presence of other drugs.

The second big issue in forensic toxicology is the type of specimens used for analyses. Typically, blood and urine are used as samples. They are relatively easy samples to obtain and can be obtained relatively rapid and non-invasively. The analysis of such samples can show substances even several weeks after their ingestion. However, alternative specimens such as oral fluid, hair and vitreous humor can be used as a sample which gives toxicologists a wider scope for obtaining information and providing evidence. For this reason, guidelines have been published by the Society of Hair Testing (SOHT)[21] and the Society of

Forensic Toxicologists (SOFT)[22] which include these alternative specimens. This is to ensure that the method validation and the issues of good laboratory practice can be accepted by law.

To overcome the sensitivity and selectivity problems, numerous extraction techniques have been developed. The most classical technique is liquid-liquid extraction (LLE). However, from an environmental point of view, the use of large amounts of organic solvents, and often chlorinated solvents, makes this technique unfavourable. As a result, there is a demand for highly sensitive and selective systems that can be used in high-throughput analysis. Thus, various new techniques, such as supercritical fluid extraction (SFE), solid-phase extraction (SPE) and solid-phase microextraction (SPME) have been developed in order to replace the LLE technique.

With current technology, it is possible to improve the extraction of basic drugs and minimise the number of co-extracted interferences. Recently, the use of solid-phase extraction (SPE) methods for the isolation of analytes from biological matrices has been applied routinely.[23],[24] The SPE method is simple and reproducible and has reduced the volume of organic solvents used in LLE methods. With SPE, many of the problems associated with LLE can be prevented, such as incomplete phase separations, less-than-quantitative recoveries, use of expensive and breakable speciality glassware.

The development of SPE began in the mid 20th century using adsorbents such as Amberlite XAD-2 resin (a polystyrene material).[25] Then, the silica-based materials used as SPE sorbents, first appeared in the 1980s and were invented by Professor

Michael Burke from Arizona University; they were introduced onto the market by Analytichem.[26]

In the 1990s, mixed-mode sorbents such as Certify™ were introduced and showed an improvement in drug extraction efficiency and minimised the number of co-extracted interferences. A few years later, polymeric sorbents such as Strata™ X were introduced, and these showed no residual surface silanol groups, unlike the substituted silica sorbents. A major breakthrough in SPE occurred in the past few years when molecularly imprinted polymers (MIPs) were used as SPE sorbents. The extraction method based upon these sorbents is known as molecularly imprinted solid-phase extraction (MISPE).[27],[28] It was first reported by Sellergren in 1994.[29]

MIPs are no longer new materials. More than three decades have passed since the early Wulff studies and the technology is rapidly coming of age. However, just what lies ahead for molecular imprinting is far from clear. A search of the literature reveals that researchers have applied molecular imprinting strategies to almost every conceivable problem requiring a molecular recognition solution.

Imprinted polymers have high selectivities and affinities,[28] and they can be tailored towards a particular analyte or class of compounds in terms of solid-phase extraction strategies. This selectivity is exploited during the extraction procedure, where harsh washing conditions can be employed during extraction for the removal of interferences. This leads, in turn, to cleaner extracts, lower detection limits and more efficient sample clean-up processes. This new method provides the analyst with an attractive alternative to the SPE and LLE methods which have been used routinely for a long time.

In the context of MISPE and forensic toxicology, Anderson and coworkers,[30],[31] developed a method for the detection of benzodiazepines in hair by using a molecularly imprinted polymer in SPE protocols. The results showed that MISPE could be used as a complementary method to classical SPE for the analysis of benzodiazepines in hair samples. Furthermore, Harun *et al*.[32] described a similar method for the detection of ketamine in hair samples.

Chromatography plays a crucial role in analytical techniques applied to the analysis of forensic biological samples. In conventional methods, gas chromatography (GC) has been used with detectors such as flame ionisation detectors (GC/FID), nitrogen phosphorus detectors (GC/NPD) and mass spectrometry (GC-MS), however the most widely used is high performance liquid chromatography (HPLC) with ultraviolet detection (HPLC/UV) and LC-MS/MS to detect toxic substances in samples.

The development of the liquid chromatography-tandem mass spectrometry (LC-MS/MS) technique has generated great interest among forensic toxicologists. As discussed by Maurer,[33] this equipment is both a good supplement and complement to GC-MS for multi-analyte procedures for the screening and quantification of drugs. In addition, LC-MS eliminates the need for the time-consuming derivatisation steps which are often required in GC-MS. This technique has now become a valuable tool for the routine analysis of forensic samples and as an alternative to immunoassay.[34],[35]

3.3 Aims of Study

There were two main aims of this particular study. The first aim was to deliver polymer beads suitable for packing into LC column in readiness for molecularly imprinted liquid chromatography (MILC). For this purpose, precipitation polymerisation was used in order to produce MIP microspheres suitable for use as the stationary phases. When such microspheres are applied as stationary phases in chromatography for the evaluation of an imprinting effect, they are expected to give higher efficiency and better separation than particles derived from suspension polymerisations or the grinding of polymer monoliths. In this study, ketamine was selected as template and used to generate ketamine-imprinted polymer beads. The intention was to study the imprinting effects through HPLC analyses of the MIP stationary phases and then to use the same columns to develop a new method for ketamine analysis. All the synthetic work and the stationary phase evaluation work were carried out at the University of Strathclyde.

The second aim of the study was the development of a new analytical method (MILC-MS/MS) for the detection of ketamine, an internationally-controlled drug, in hair samples. A ketamine-imprinted polymer was synthesised in monolithic form, ground into particles and then packed into an LC column. The molecular recognition properties were assessed *via* the new analytical method. The principal intended application was hair analysis. This work was carried out by the author at the University of Glasgow.

3.4 Ketamine

Ketamine is a dissociative anaesthetic which has analgesic properties in sub-anaesthetic doses.[36] Ketamine hydrochloride was first reported by Calvin Stevens in 1962 as part of an effort to find a safer anaesthetic alternative to phencyclidine (PCP), which is likely to cause hallucinations, neurotoxicity and seizures.[37] Ketamine, also known as Special K, Vitamin K or Cat Valiums, is an injectable anaesthetic. Today, it is most commonly used by veterinarians on large animals.

In the 1980s, ketamine began to be used recreationally as an intoxicant. It is similar in chemical structure to PCP and thus creates similar effects, including numbness, loss of coordination, sense of invulnerability, muscle rigidity, aggressive/violent behaviour, slurred or blocked speech, exaggerated sense of strength, and a blank stare.[38] Since ketamine is an anaesthetic, it stops the user from feeling pain, which could lead the user to inadvertently cause injury to themselves. Ketamine may relieve tension and anxiety, is purported to be a sexual stimulant, and intensifies colours and sounds.[39]

Ketamine (Figure 3.1) contains a stereogenic centre at C2 of the cyclohexyl ring and has two enantiomers, (*S*)-(+)-ketamine **7** and (*R*)-(-)-ketamine **8**. In systematic nomenclature it is known as 2-(2-chlorophenyl)-2-(methylamino)cyclohexanone, an arylcycloalkylamine, $C_{13}H_{16}ClNO$ with molecular weight of 237.74 g/mol.[40] It is available either as a racemic mixture or as the pure enantiomers. Ketamine is obtained primarily in a powder form and is administered through snorting or the inhaling of lines. Other forms of ingestion include intramuscular injection and oral consumption in tablet form.[36]

Ketamine hydrochloride is a white crystalline powder, which is soluble in water, methanol and chloroform. Most pharmaceutical preparations of ketamine are of the racemic compound. The (±)-ketamine hydrochloride standard in methanol is available commercially as an analytical standard. The melting point in its free base form is 92-93 °C while the melting point of its hydrochloride form is 262-263 °C.[41],[42]

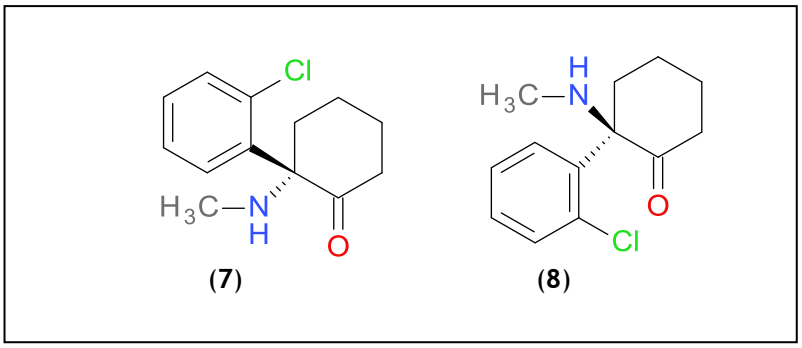

Figure 3.1 Molecular structures of: (a) (*S*)-(+)-ketamine and (b) (*R*)-(-)-ketamine

Ketamine manufactured by pharmaceutical companies must follow the guidelines and meet the standard of Good Manufacturing Practice (GMP) to ensure the purity and quality of the product. The racemic form is used for pharmaceutical purposes as the hydrochloride salt, prepared in aqueous solution and packaged in small glass vials. It is marketed as Ketalar®, Ketolar®, Ketaject®, Ketanest®, Ketavet®, Ketavet 100®, Ketalin®, Vetalar®, Kalipsol®, Calipsol®, Substania®, Ketamine Panpharma®, Ketamine UVA®, Chlorketam® and Imalgene®.

The (*S*)-(+)-enantiomer **7** of ketamine appears to have a favourable cardiovascular profile and neuroprotective effect.[40],[43] The dose required for (*S*)-(+)-ketamine **7** is less than that required for the racemic mixture and has fewer side effects and a shorter recovery time.[44],[45] White *et al.*[46] found that (*S*)-(+)-ketamine **7** was

approximately four times as potent as (*R*)-(-)-ketamine **8**. Furthermore, (*S*)-(+)-ketamine **7** is the enantiomer that causes the psychotomimetic effects of ketamine, although sub-anaesthetic doses of (*R*)-(-)-ketamine **8** may induce a state of relaxation.[47],[48]

When used recreationally, ketamine is known as K, Ket, Special K, Riddle, Horse, Spesh, Vitamin K (not to be confused with the true vitamin K), Smack K, Kit-Kat, Keller, Jeremy Powder, Barry Keddle, HOSS, The Hoos, Hossalar, Kurdamin, Kitty, Wonk, Wonky, 'tekno smack, Regreta, tranq, and D-rod.[51] It is available in tablet and powder form, and as a vaporiser of unknown purity and quality.

There are a number of analytical procedures for the detection and identification of ketamine and its metabolites in biological fluids. The method chosen depends on a number of factors, such as cost, time, sensitivity, workload, specificity and reliability. Most screening methods are immunoassay techniques. Immunoassays are based on the principle of competition between labelled and unlabelled antigen (drug) for the binding sites on a specific antibody.[52] There are many types of immunoassay analysis, such as enzyme immunoassay (EIA), fluorescent polarisation immunoassay (FPIA) and radio-immunoassay (RIA).

3.5 Impact of Ketamine Misuse

Legally produced ketamine will be pure but illegally produced tablets are commonly found with ephedrine added (which is commonly used for allergies and asthma treatment). Sometimes these are passed off as ecstasy.[53]

Ketamine misuse was first identified in the early 1970s on the West Coast of the USA.[54] Ketamine sold illicitly is often converted from a liquid form to a powder form utilising a simple evaporation process. The liquid ketamine is dried in a variety of ways, such as by microwave oven, conventional oven or sun-dried until a residue remains. This crystal residue is ground into a powder form to give a fine powdery material similar to cocaine and heroin. In this form it is convenient to be marketed.

Over the past decade, there have been a growing number of reports on the non-medical, unauthorised use of ketamine in the United Kingdom.[55],[56] The misuse of ketamine has also been reported in Sweden,[57] Taiwan,[58] Australia,[59],[60],[61] USA,[62],[54] China,[63] Singapore,[64] and has recently has been found in the urine samples of suspected drug users in Malaysia.[65]

Research accounts indicate that the recreational use of ketamine has widened in the context of nightclubs, dance parties and 'raves', thus leading to increasing public concern about the potential hazards of this drug. Ketamine is also commonly injected intramuscularly among the youth, involving multiple injections, shared bottles of ketamine and use of the same syringes from secondary sources. These practices therefore increase the risk of transmitting infectious diseases such as HIV and Hepatitis C.[68]

3.6 Free Radical Polymerisation

MIPs have been synthesised mainly by free radical polymerisation as this is a relatively simple and easy process to carry out. Free radical polymerisation is a technique for the conversion of monomer into polymer that has been well

exploited in both industrial and academic research laboratories. Numerous vinyl monomers can be polymerised effectively in excellent yield and it is realisable commercially at low cost. The technique has a number of advantages including its tolerance to impurities in the system (*e.g.,* water) and its applicability to a broad range of monomers and experimental conditions. Generally, it can be carried out at atmospheric pressure and moderate temperatures, typically in the range 20-150 °C, and polymers with high molar masses can be obtained within short reaction times. Due to these various reasons, it has been used as a method of choice for preparing molecularly imprinted polymers.

Free radical polymerisation consists of three distinct stages (Figure 3.2): (1) initiation, (2) propagation, and (3) termination. The initiation step is started by a radical initiator such as a peroxide or azo compound, normally either by photolytic or thermal decomposition.[70] Normally, initiators are used at low levels compared to the monomer, *e.g.,* 1 wt % or 1 mol % with respect to the number of moles of polymerisable double bonds. The initiator radical reacts with the monomer in the initiation process and initiates the growth of a polymer chain. Initiation is followed by chain propagation, in which the newly formed monomer radical reacts with monomer in a chain-growth process. Typically, in free radical polymerisation, the rate of propagation is much faster than the rate of initiation. In the termination reactions, two free radicals react with each other to produce 'dead' polymer. Termination is normally either by combination or by disproportionation.

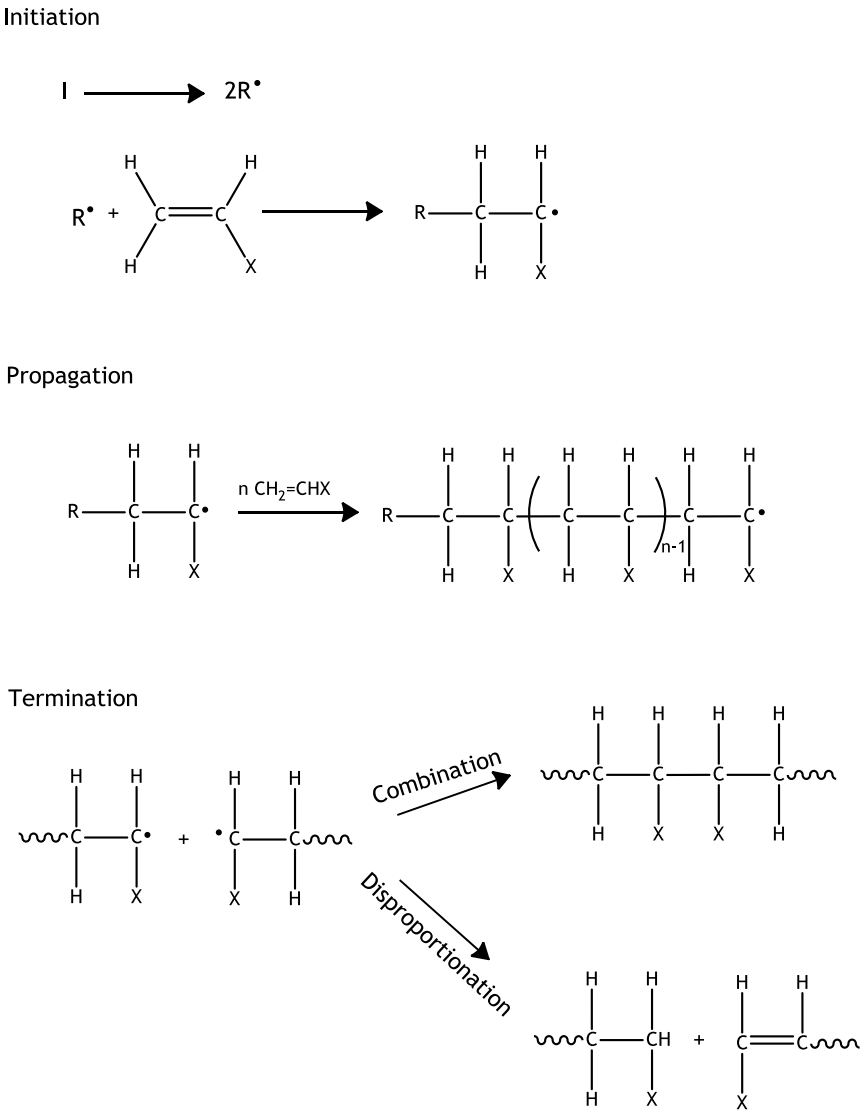

Note: Free radical (formed from the initiator, I) is denoted as R• and the vinyl monomer as CH_2=CHX

Figure 3.2 Schematic representation of free radical polymerisation showing the initiation, propagation and termination steps

3.7 Polymerisation Methods

Different uses and potential applications of imprinted polymers demand different properties from the polymers. Many different methods for the preparation of imprinted polymers have been reported. The main methods employed are monolith synthesis and bead synthesis *via* precipitation polymerisation. In this

Chapter, both of these polymerisation methods were employed for MIP preparation with ketamine as template. In the first part of the investigation, ketamine-imprinted polymers prepared *via* precipitation polymerisation were used as stationary phases in HPLC analyses to evaluate the imprinting effect. In the second part of the investigation, ketamine-imprinted polymers were prepared *via* the monolith method and used in a newly developed method, MILC-MS/MS, for the purposes of forensic toxicology studies.

3.7.1 Precipitation Polymerisation

Precipitation polymerisation is one of the most promising synthetic methods to produce molecularly imprinted polymers in the form of uniformly-sized spherical beads (as described in Chapter 1).[71],[72],[73] This method gives high yields of useful material when compared to monolith synthesis. The bead surfaces are free from stabilisers and surfactants and, additionally, the beads can be removed easily from the reaction medium by filtration. This method has been developed over a number of years in our laboratory and is now an established and well-studied system.[74],[75] The application of precipitation polymerisation in molecular imprinting was further investigated by Wang *et al*.[76] and Ferguson *et al*..[77] In the present work, the particle sizes of all the microspheres prepared were in the range of 1.0 μm to 3.5 μm. Thus, when applied as stationary phases in chromatography for the evaluation of imprinting effects, short columns of 4.6 I.D x 50 mm were used. This was to avoid high back pressures arising from the use of relatively small particles packed into the columns.

3.7.2 Monolith Synthesis

The first polymerisation method employed to synthesise imprinted polymers was based on the formation of a monolith.[78],[79],[80] The term monolith describes a macroporous, highly crosslinked and therefore rigid, monolithic material which acts as a support for the stationary phase in a separation process. The definition is used in the context of functional solid materials for separation purposes.[81] However, polymer monoliths are increasingly finding roles as sorbents for a much wider range of chromatographic applications and formats. There are a number of applications of porous monolithic stationary phases, as has been reported as mentioned in Chapter 1. In a relevant, recent report Harun *et al.*[32] synthesised a ketamine imprinted polymer in monolithic format which was then broken down by grinding to give polymer particles suitable for MISPE. This provided a starting point for the current investigation.

3.8 Experimental Section (Part I)

3.8.1 Chemicals and Materials

(±)-Ketamine.HCl and (*S*)-(+)-ketamine.HCl were purchased from Sigma (1.0 mg/mL ± 5% in methanol and 5 g in solid form). Methacrylic acid, MAA (99.0 %), HPLC grade acetonitrile (ReagentPlus®, 99.0 %), toluene (Anhydrous, 99.8 %), acetone (99.0 %) and 2,2'-azobisisobutyronitrile, AIBN (98.0 %) were purchased from Aldrich. Dichloromethane, DCM (ACS reagent, ≥99.5 %), sodium bicarbonate, $NaHCO_3$ (dry powder, ≥99.5 %), anhydrous sodium sulfate, Na_2SO_4 (ACS reagent, anhydrous powder, ≥99.0 %), methanol (ACS reagent, ≥99.8 %) and anhydrous magnesium sulfate, $MgSO_4$ (anhydrous, ReagentPlus®, ≥99.5 %) were purchased from Sigma-Aldrich. Commercial divinylbenzene-80, DVB-80 (technical grade, mixture of isomers, 80 %) was purchased from Fluka.

Toluene, acetone and acetonitrile were used as received. MAA (34 °C/5 mmHg) was purified by drying over anhydrous sodium sulfate and then distilled under vacuum prior to use. DVB-80 was passed through a short column packed with neutral activated alumina prior to use. AIBN was recrystallised from methanol at low temperature.

3.8.2 Converting Ketamine.HCl into Ketamine Free Base

For the purposes of imprinting, ketamine (the template) must be present in its free base form. Most commercial ketamine standards are sold as the ketamine hydrochloride salt which must be converted to the free base form to serve as a template in the polymerisation process. The steps in converting the ketamine.HCl to the free base form were as follows. (±)-Ketamine (1.0 g) was partitioned between saturated aqueous bicarbonate (20 mL) and DCM (20 mL). The DCM layer was separated from the aqueous layer and then washed twice with saturated aqueous sodium bicarbonate (2 x 20 mL) and once with water (20 mL). The DCM layer was dried over anhydrous magnesium sulfate and the drying agent was removed by vacuum filtration. The DCM was removed under reduced pressure on a rotary evaporator and the crystalline residue dried *in vacuo* at 40 °C to constant mass (0.611 g, 70 %, Mp 92-93 °C).[82] The (*S*)-(+)-Ketamine **7** free base was prepared in an analogous fashion (0.613 g, 71 %, Mp 120 °C).[83]

3.8.3 Synthesis of Ketamine MIPs and Non-Imprinted Polymers (NIPs) *via* Precipitation Polymerisation

The ketamine MIPs were prepared *via* a precipitation polymerisation method. The compounds used as templates were (±)-ketamine and (*S*)-(+)-ketamine **7**. The

precipitation polymerisation method has been introduced and discussed in detail in Chapter 1 and, briefly in Section 3.7.1.

A series of polymers were prepared in a mixture of acetonitrile and toluene as the porogenic solvent. The feed compositions of template, functional monomer, crosslinker, porogen and initiator are shown in Table 3.1.

In general, the template, (±)-ketamine or (*S*)-(+)-ketamine **7**, was dissolved in a mixture of acetonitrile and toluene (3/1, v/v) in either a 50 mL Kimax© culture tube fitted with a screw cap or in a Nalgene bottle. This was followed by addition of the functional monomer, MAA, and the crosslinker, DVB-80. Finally, the initiator, AIBN, was added.

The solution was deoxygenated by bubbling nitrogen gas through the solution for about 20 minutes at ice-bath temperature and the reaction vessel then sealed under nitrogen. The reaction vessel was then placed on a low-profile roller housed inside a temperature-controlled incubator. The temperature was ramped from room temperature to 60 °C over a period of approximately 2 hours and then kept constant at 60 °C for 48 hours thereafter. The monomer solutions turned milky within two hours after reaching 60 °C and the polymerisations proceeded smoothly.

After 48 hours at 60 °C, a sample of the polymer suspension was spotted onto a microscope slide and the bead size estimated under an optical microscope. If the bead size was too small (less than 1 µm), the vessel contents were deoxygenated again, sealed under nitrogen and polymerisation allowed to continue in the

incubator. If the beads formed were of the desired size, the reaction vessel was cooled to room temperature and a few crystals of hydroquinone added to the milky suspension of polymer particles which had formed. The polymer was filtered off on a polyamide membrane filter (0.2 μm), washed with acetonitrile (2 x 20 mL) and then methanol (20 mL).

The polymer was transferred to a pre-weighed vial and dried to constant mass *in vacuo* at 40 °C. The yields of all particles prepared in this way were determined gravimetrically. All polymerisations were carried out in duplicate, with a non-imprinted (control) polymer (NIP) being prepared in the absence of template.

The apparatus used in the precipitation polymerisations is shown in Figure 3.3. The reaction vessels rolled about their long axes at a controllable speed. The polymerisation temperature can be easily varied from room temperature up to 60°C.

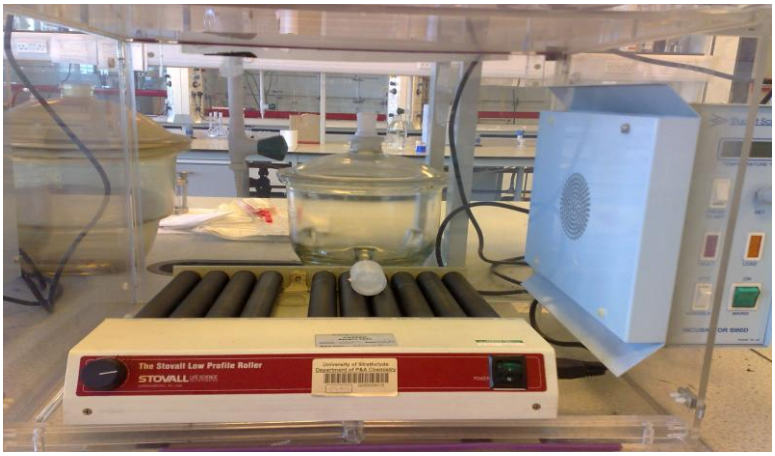

Figure 3.3 Stovall Flat-Bed Roller Incubator set-up

Table 3.1 Precipitation polymerisation conditions for ketamine-imprinted polymers

Polymer code	Mole ratio of T:M:X	Ketamine (g), (mmol)	MAA (mL), (mmol)	DVB-80 (mL), (mmol)	MeCN/toluene (3/1, v/v), (mL)	AIBN (g), (mmol)	Yield (%)
PP1	0:4:20	---- (-)	0.23 (2.71)	1.91 (13.57)	75 / 25	0.0980 (0.60)	74
PP2	1:4:20	0.1613 (0.68)	0.23 (2.71)	1.91 (13.57)	75 / 25	0.0980 (0.60)	67
PP3	1:4:20	0.1613 (0.68)	0.23 (2.71)	1.91 (13.57)	75 / 25	0.0980 (0.60)	70
PP4	0:8:40	---- (-)	0.12 (1.36)	0.97 (6.78)	18.75 / 6.25	0.0735 (0.44)	69
PP5	1:8:40	0.0403 (0.17)	0.12 (1.36)	0.97 (6.78)	18.75 / 6.25	0.0735 (0.44)	58
PP6	1:8:40	0.0403 (0.17)	0.12 (1.36)	0.97 (6.78)	18.75 / 6.25	0.0735 (0.44)	82

Notes:

1) PP1 - NIP; PP2 - (±)-ketamine ; PP3 - (*S*)-(+)-ketamine in 4:20 system
2) PP4 - NIP; PP5 - (±)-ketamine; PP6 - (*S*)-(+)-ketamine in 8:40 system
3) T is template, M is functional monomer, X is crosslinker and MeCN is acetonitrile
4) The initiator used for PP1, PP2 and PP3 was at a level of 2 mol% with respect to the total number of moles of polymerisable double bonds and the monomer concentration used was 2 % (w/v) with respect to solvent.
5) The initiator used for PP4, PP5 and PP6 was at a level of 3 mol% with respect to the total number of moles of polymerisable double bonds and the monomer concentration used was 4 % (w/v) with respect to solvent.

3.8.4 Scanning Electron Microscopy (SEM)

SEM images were acquired at the SEM unit, Chemistry Department, University of Glasgow, on a Jeol 6400. A small quantity of the polymer powder was sputter-coated with gold prior to SEM measurements. SEM was used to image the size and shape of microspheres.

3.8.5 In-House Column Packing and Off-Line Column Washing

Column packing: An Alltech Model 1666 Slurry Packer was used to pack the polymers into empty LC columns using procedures recommended by the manufacturer. The MIPs and NIPs were packed into stainless-steel LC columns of dimension 0.46 cm I.D.d x 5 cm fitted with 0.2 μm frits. Approximately 0.5 g of polymer was sufficient to pack each column. Acetone was used as the slurry solvent. The columns were packed at an air pressure of 15 psi and a solvent pressure of 500 psi over a period of around 30 minutes. Figure 3.4 shows the column packer used to pack the polymers.

Column Washing: The columns were washed off-line using a Gilson Model 303 HPLC pump using a mixture of acetonitrile and acetic acid (95/5, v/v) at a flow-rate of 1.0 mL/min and a pressure of 120 psi (Figure 3.5). The NIP column was washed first, followed by the (*S*)-(+)-ketamine column and then the (±)-ketamine column to minimise the likelihood of any cross-contamination with template.

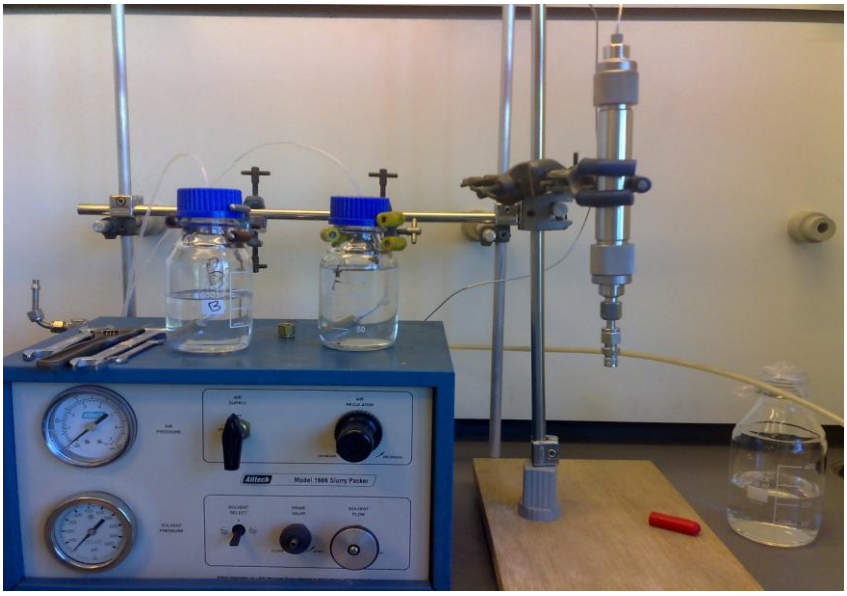

Figure 3.4 Column Packer: Alltech Model 1666 Slurry Packer

Figure 3.5 Column washing using a Model Gilson 303 HPLC pump

3.8.6 High Performance Liquid Chromatography (HPLC) Analysis

Analysis of the packed columns was carried out on a Waters HPLC system. The system comprised a Waters 1535 binary pump, a Waters 717 autosampler and a Waters 2487 Dual Wavelength absorbance detector. The software used for operation of the system and data handling was Waters Breeze.

The analyses were performed under isocratic conditions. The mobile phase was 100 % acetonitrile in Channel A at a flow rate of 0.5 mL/min. The sample volume used was 10 µL and the detector wavelength was 220 nm. The analytes injected onto the columns were, in order of injection: pure acetone; 10 mM (*S*)-(+)-ketamine in acetonitrile; 10 mM (±)-ketamine in acetonitrile. Imprinting factors were calculated by comparing the retention factors on the imprinted and non-imprinted columns. The peak areas were also compared.

The retention factors (*k'*) were calculated according to Equation 3.1 and standard chromatographic theory.

$$k' = (t_r - t_o) / t_o \qquad \text{----------} \quad \textbf{3.1}$$

Where t_o is the retention time of the void marker (acetone) on the column, and t_r is the retention time of the analyte on the same column.

The imprinting factors (IF) were calculated using Equation 3.2:

$$IF = k'_{MIP} / k'_{NIP} \qquad \text{----------} \quad \textbf{3.2}$$

Where k'_{MIP} is the retention factor of the analyte on the MIP and k'_{NIP} is the retention factor of the analyte on the NIP. Figure 3.6 shows a typical HPLC chromatogram illustrating elution of the void marker and the analyte.

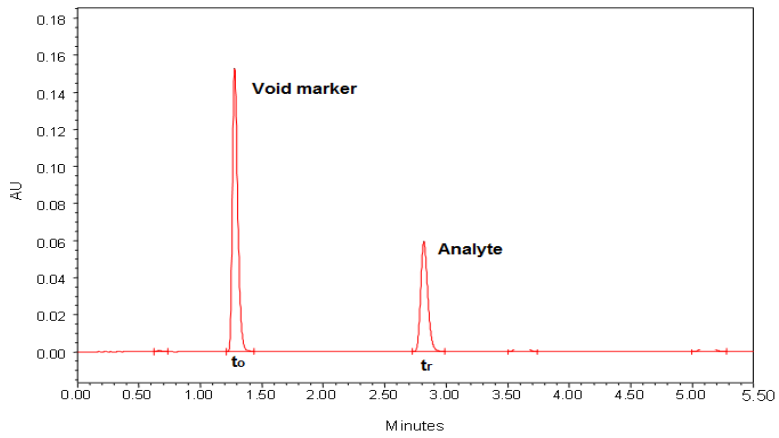

Figure 3.6 Typical HPLC chromatogram showing elution of the void marker at t_o and elution of the analyte at t_r

3.9 Results and Discussion (Part I)

Precipitation polymerisation begins with a homogeneous solution of monomer in solvent. As polymerisation proceeds, growing oligomers aggregate and crosslink to form stable particles which precipitate out of solution as monodisperse, spherical gel particles. Then, these gel particles grow by capturing other oligomers and monomers from the reaction medium.[84] With this particular polymerisation approach, monodisperse polymer microspheres can be produced, typically in the size range 1-10 µm. However, for the purposes of HPLC work, beads in the size range 3-5 µm are preferable. This is because particles in this size range are relatively easy to pack into columns and give acceptable back pressures. Furthermore, they ought to give better separation efficiencies than larger particles thereby leading to better overall chromatographic performance.

The synthetic strategies for polymer microspheres imprinted with ketamine were based on methods developed originally in our laboratory by Linsey Ferguson.[77] Methacrylic acid has been shown to be an effective functional monomer in forming non-covalent interactions with a number of templates and was therefore employed in the ketamine system as a functional monomer together with divinylbenzene (DVB-80) as the crosslinker to produce rigid, macroporous beads. Acetonitrile was used in combination with toluene as porogen. The presence of toluene, which is a thermodynamically 'good' solvent, helps to delay the onset of phase separation and leads to particles with higher specific surface areas.

In this study, two polymerisation strategies were evaluated as shown in Table 3.1, previously. These differed in the ratio of template (T): functional monomer (M): crosslinker (X); T:M:X ratios of 1:4:20 and 1:8:40 were used, respectively. Additionally, the initiator and the monomer concentrations were increased in the case of the polymerisations using a T:M:X ratio of 1:8:40. Based on work reported by Wang *et al.*,[75] it was expected that when the concentrations of the monomers and the initiators were increased simultaneously, the average diameters of the beads produced would increase and the products would be obtained in good yields.[76]

3.9.1 Synthesis of ketamine-imprinted polymers

For the 1:4:20 case, polymerisations were carried out on a 2 g monomer scale, with the concentration of AIBN at 2 % (with respect to the number of moles of polymerisable double bonds in the monomers) and the monomer concentration at 2 % (w/v). Three precipitation polymerisations were performed in total; NIP (PP1), (±)-ketamine MIP (PP2) and (*S*)-(+)-ketamine MIP (PP3), as shown in Table 3.2. The

polymerisations were conducted in 125 mL Nalgene bottles, with the bottles being rotated slowly about their long axes on a low profile roller housed within a temperature-controlled incubator.

Table 3.2 Precipitation polymerisation conditions and the yields of products for the 1:4:20 series of polymerisations with ketamine as template

Polymer Code[1]	**Concentration of monomer (%)**[2]	**Concentration of initiator (mol %)**[3]	**Microsphere yield (%)**
PP1	2	2	74
PP2	2	2	67
PP3	2	2	70

Notes:

1. PP1 - NIP; PP2 - (±)-ketamine MIP; PP3 - (*S*)-(+)-ketamine MIP
2. With respect to porogenic solvent (w/v)
3. With respect to the total number of moles of polymerisable double bonds in the monomers

The polymerisations were run for 48 hours at 60 °C. However, the filtration processes were problematic for each of the polymerisations as the particles formed after the polymerisations were too small to allow effective filtration on a 0.2 μm membrane filter. Ferguson reported the same problem when working with ketamine-imprinted polymers produced by precipitation polymerisation.[77] However, in spite of the difficulties, the polymers were eventually isolated in

good yields, with the NIP (PP1) being isolated in the highest yield (74 %). After washing and drying, the polymers were then analysed by SEM.

The SEM images of the products (Figure 3.7) show that particles were produced in each case. Many of the particles were spherical, however the particles were not monodisperse and the quality of the particles, and in particular the imprinted particles, was considered to be not sufficiently high for the intended HPLC analyses. The particles ranged in diameter from ~3 μm (PP1, best quality), to ~2 μm (PP3, intermediate quality) to ~1 μm (PP2, lowest quality).

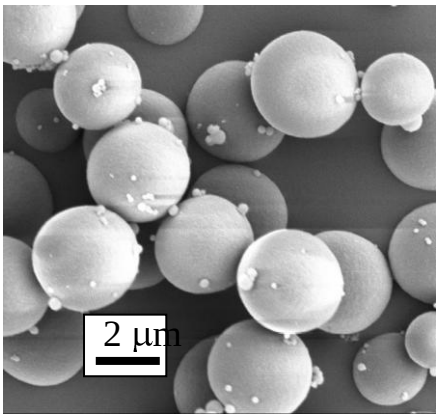

(a) PP1 mean diameter ~ 3 μm

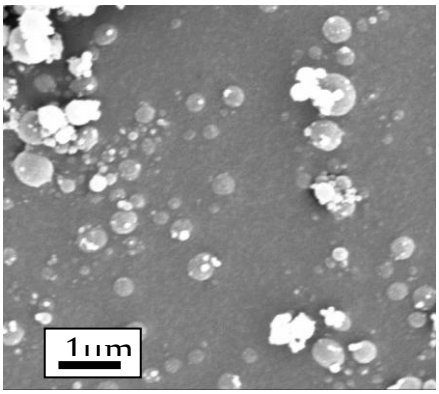

(b) PP2 mean diameter ~ 1 μm

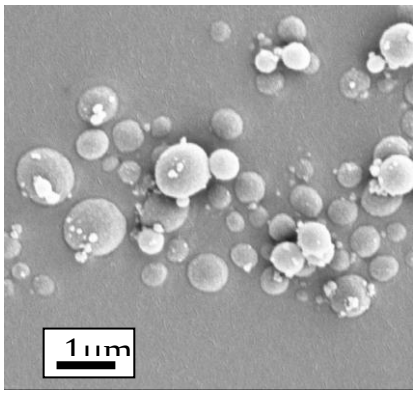

(c) PP3 mean diameter ~ 2 μm

Figure 3.7 SEM images of: (a) PP1, (b) PP2 and (c) PP3

T:M:X mole ratio used was 1: 4: 20

The differences in diameter and quality of particles might be due to the presence of template, in this case ketamine. The quality of particles where template was absent (PP1) was better than quality of the imprinted particles. This clearly showed that the presence of template had an effect upon the course of the polymerisations.

Since the particles formed using a T:M:X ratio of 1:4:20 were of low quality and too small to be useful for HPLC work, a second series of polymers was synthesised using a T:M:X ratio of 1:8:40. Table 3.3 details the new polymerisation conditions for this 1:8:40 series and lists the yields of microspheres produced. The initiator was used at a level of 3 mol % with respect to the total number of moles of polymerisable double bonds, and the monomer concentration was increased from 2 to 4 % (w/v), with respect to solvent. The rationale for moving from a ratio of 1:4:20 to a ratio of 1:8:40, at the same time as increasing the initiator and monomer concentrations, was that an increase in the average diameters of the particles and an enhancement in the quality of the beads produced was expected. The concentration of the template was kept low as this contributed to the quality of the end products. Three polymerisations were carried out, namely PP4 (NIP), PP5 ((±)-ketamine MIP) and PP6 ((*S*)-(+)-ketamine MIP).

The 1:8:40 series of polymerisations were carried out on a 1 g monomer scale in Kimax® culture tubes, instead of Nalgene bottles, for 48 hours at 60 °C. In a study carried out by O'Donnell,[85] it was observed that differences in reactor volume and reactor type had an influence on the formation of the beads in some precipitation polymerisations, which is why glass Kimax culture tubes were used in place of Nalgene bottles on this occasion. As can be seen in Table 3.3, the isolated

yields of products were good to excellent, with the PP6 polymer being obtained in the highest yield (82 %).

Table 3.3 Precipitation polymerisation conditions and yields of the products for the 1:8:40 series of polymerisations with ketamine as template

Polymer Code[1]	**Concentration of monomer (%)**[2]	**Concentration of initiator (mol %)**[3]	**Microsphere yield (%)**
PP4	4	3	69
PP5	4	3	58
PP6	4	3	82

Notes:

1. PP4 - NIP; PP5 - (±)-ketamine MIP; PP6 - (*S*)-(+)-ketamine MIP
2. With respect to porogenic solvent (w/v)
3. With respect to the total number of moles of polymerisable double bonds in the monomers

SEM analyses were carried out to image the particles produced (Figure 3.8). It can be seen that, compared to the polymers prepared using the 1:4:20 ratio of T:M:X, the product quality was better, the average particle diameter was slightly higher and the majority of the particles were spherical. Even although they were not monodisperse, the particles were considered to be of a high enough quality and of a sufficient size to be packed into LC columns.

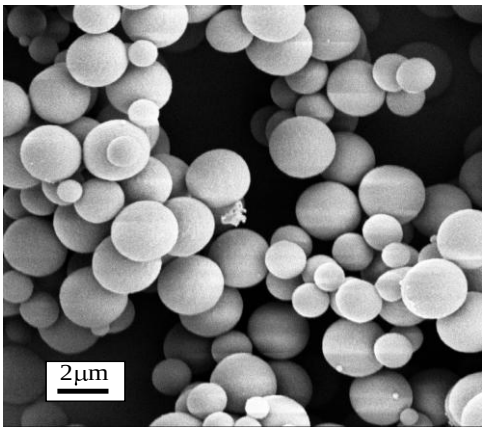

(a) PP4 mean diameter ~ 3 μm

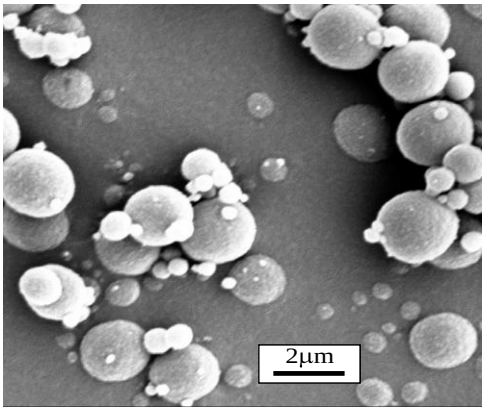

(b) PP5 mean diameter ~ 3 μm

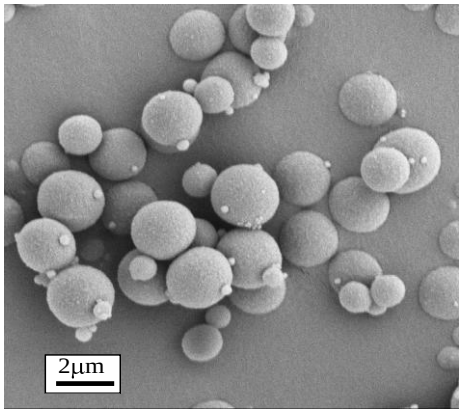

(c) PP6 mean diameter~ 3 μm

Figure 3.8 The SEM images of: (a) PP4, (b) PP5, and (c) PP6.

T: M: X mole ratio used was 1: 8: 40

3.9.2 HPLC analyses

Chromatographic evaluations of columns packed with ketamine imprinted and non-imprinted polymers were carried out using HPLC, with UV as the detection method. Based on the SEM analyses, the polymers from the 1:8:40 series were selected for packing into LC columns because the sample quality was higher and the particles had higher average diameters than those polymers from the 1:4:20

series. The procedure for packing and washing of the columns was described in Section 3.8.5.

During the packing process, PP4 (the NIP) packed easily within less than one hour with the solvent and air pressure at 500 psi and 15 psi, respectively, as would be expected for good quality particles of around 3 μm in diameter. However, there were packing problems for PP5 and PP6. For these two MIPs, only PP6 could be packed into a column, however the packing process required a period of approximately 6 hours with the solvent and air pressure at 500 psi and 15 psi, respectively, even after the fines had been removed.

After equilibrating the PP4 and PP6 columns with acetonitrile, the elution of 10 mM samples of the (*S*)-(+)-ketamine **7** and the (±)-ketamine standards were performed in isocratic mode at a flowrate of 0.5 mL/min with 100 % acetonitrile as mobile phase. The detector wavelength was set at 220 nm based on a previous study of ketamine detection by HPLC.[86] The retention factors on the imprinted (k'_{MIP}) and non-imprinted (k'_{NIP}) stationary phases, as well as the imprinting factors, were calculated.

The PP4 and PP6 columns were injected with acetone as a void marker in addition to the 10 mM (*S*)-(+)-ketamine **7** and (±)-ketamine standards (n=3). Acetone is a neutral molecule and was used as a void marker due to its expected low affinity towards the polymers. Furthermore, the acetone peak shape can indicate any problems within the column packing. Symmetrical and narrow peak shapes of acetone on the NIP (PP4) and MIP (PP6) columns would indicate that the columns had been packed well.

Figure 3.9 and Figure 3.10 show the chromatograms obtained from the columns packed with polymers PP4 (**NIP**) and PP6 (**MIP**), respectively, as the stationary phase materials. The retention factors (*k'*) and the imprinting factors (IF) for the MIP and NIP columns were calculated according to Equations 3.1 and 3.2, using the average retention times from duplicate injections, and are shown in Table 3.4.

In typical LC chromatograms derived from NIP and MIP stationary phases, the acetone peak for both columns should be very sharp and appear at almost the same retention time. Secondly, the retention times of template on the MIP should be longer than on the NIP for the same concentration of analyte (template).

Unfortunately, the anticipated chromatographic results for PP6 were not realised. Based on Figures 3.9 and 3.10, the acetone peak on the NIP and MIP are obviously different. The PP4 column has a very sharp peak with a retention time of 1.3 minutes, whereas the PP6 column has a broader, less well-defined peak with front tailing for acetone and a retention time of 1.7 minutes (Table 3.4) suggestive of problems with the packing of the stationary phase. The corresponding *k'* values were higher for the MIP than the NIP, demonstrating the existence of an imprinting effect. Furthermore, the MIP column gave broader peaks with extensive tailing when injected with the analytes, as one would expect from an imprinted stationary phase.

As can be seen from the NIP and MIP chromatograms, the (*S*)-(+)-ketamine **7** and the (±)-ketamine had very similar retention times to one other and did not show any obvious sign of enantioseparation. For the MIP column, injection with (*S*)-(+)-

ketamine **7** gave a nice broad peak and a stable baseline compared to (±)-ketamine.

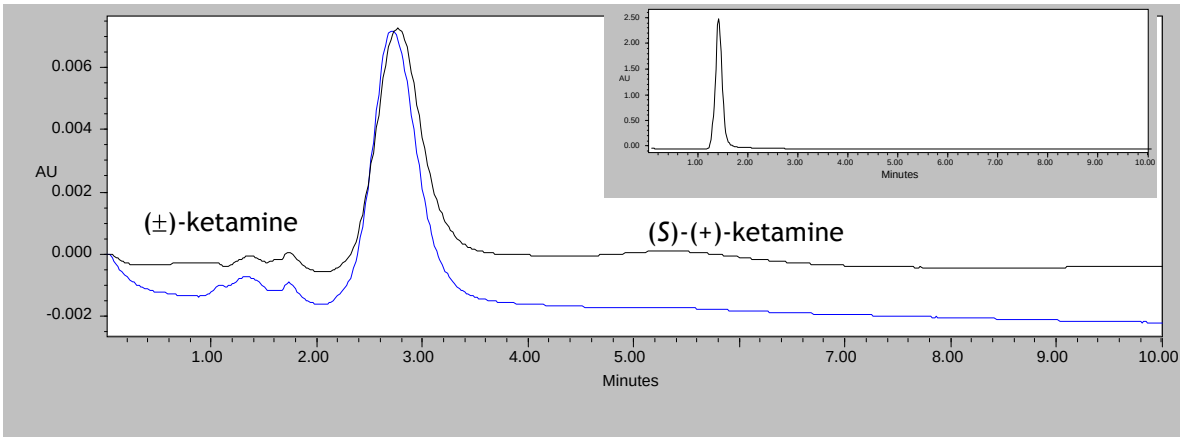

Figure 3.9 Chromatogram of acetone (small window), and overlay chromatograms of 10 mM (*S*)-(+)-ketamine (black) and (±)-ketamine (blue) standards on PP4 (NIP) column

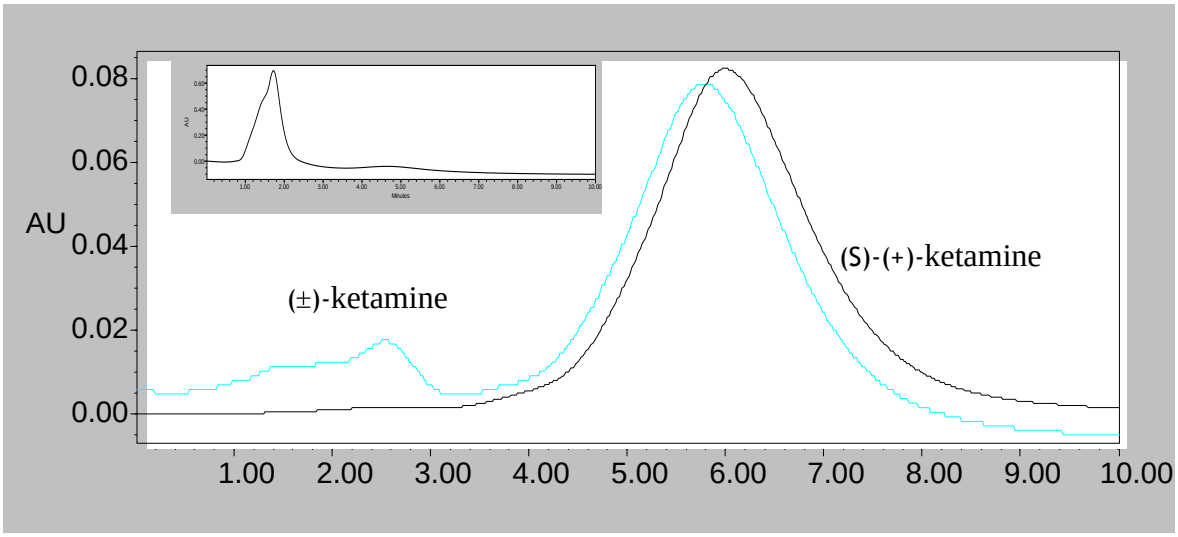

Figure 3.10 Chromatogram of acetone (small window), and overlay chromatograms of 10 mM (*S*)-(+)-ketamine (black) and (±)-ketamine (blue) standards on PP6 (MIP) column

The chromatogram for (±)-ketamine on the MIP column showed an unstable baseline and gave a broad peak at around 6 minutes. In spite of these observations, ketamine would appear to be retained more strongly by the MIP (PP6) than by the NIP (PP4), as judged from the calculated IF values (Table 3.4). Whilst it was very pleasing to obtain chromatographic data supporting the imprinting effect, it was obvious that the physical form of the MIP in particular was not ideal for LC work.

Table 3.4 Chromatographic characteristics of the PP4 and PP6 packed columns

Column	Analyte (10 µL injected)	Retention time, (min)	Retention factors, (*k'*)	Imprinting factors, (IF)
PP4 (**NIP**)	Acetone	1.32	-	-
	10 mM (*S*)-(+)-ketamine	2.86	1.2	-
	10 mM (±)-ketamine	2.71	1.1	-
PP6 (**MIP**)	Acetone	1.72	-	-
	10 mM (*S*)-(+)-ketamine	5.99	2.5	2.1
	10 mM (±)-ketamine	5.83	2.4	2.2

The IF for (*S*)-(+)-ketamine **7** and (±)-ketamine was calculated to be 2.1 and 2.2, respectively, demonstrating a modest imprinting effect of the polymers based on

the chromatograms shown. Bearing in mind the intended application (MILC) moderate IF values in combination with non-ideal chromatographic performance for PP6 did not give us confidence to continue with these particular polymers. As an example of a non-related MILC study in which the IF values and chromatographic performance were deemed to be acceptable, Turiel *et al.*[87] demonstrated high IF values reaching a maximum value of 273, for thiabendazole in a mobile phase containing 4 % (v/v) acetic acid.

3.10 Conclusion (Part I)

In this work, spherical molecularly imprinted polymers for (±)-ketamine and (*S*)-(+)-ketamine **7** have been prepared using two different T:M:X ratios; 1:4:20 and 1:8:40. However, only the polymers from the 1:8:40 series were considered to be of a quality suitable for packing into LC columns. With the imprinted material as the HPLC stationary phase, the selective recognition of ketamine by the imprinted material was demonstrated clearly.

It was found, that the MIP was not sufficiently good to be used as a stationary phase in MILC, with low IF values and insufficiently good chromatographic performance being observed. However, on a positive note, ketamine-imprinted beads were obtained successfully in the 1:8:40 series. For the purposes of real ketamine analysis in forensic toxicology, we had to take a step backwards, where polymer particles prepared from the grinding of monoliths would be the stationary phase of choice since they have already been used to good effect previously in ketamine analysis using MISPE.[82] When applied as stationary phases in LC, those polymer particles gave higher IF values than PP6.

3.11 Experimental Section (Part II)

The experiments described in Part II were carried out by the author at the University of Glasgow. Three in-house produced LC columns were used in this study. The columns were prepared in our group by Norlida Harun as part of a separate study where the focus was MISPE.[32] The columns were packed with polymer particles obtained by the grinding of polymer monoliths. The methods used for column preparation were based on methods reported elsewhere in the literature.[75],[82],[88]

3.11.1 Chemicals and Materials

Dichloromethane, (ACS reagent, ≥99.5 %), HPLC grade acetonitrile (ReagentPlus®, 99.0 %), methanol (ACS reagent, 99.8 %) and acetic acid (ACS grade, 99.7 %) were purchased from BDH Chemicals Ltd., and sodium dodecyl sulfate (SDS) (ACS reagent, ≥99.0 %) was purchased from Sigma-Aldrich. Sodium hydrogen phosphate (ACS, anhydrous, 99.0 %) and sodium dihydrogen phosphate (technical grade, 98.0 %) were purchased from Alfa Aesar, UK. (±)-Ketamine standard (1 mg/mL in methanol) and internal standard (±)-ketamine-D4 (0.1 mg/mL in methanol) were purchased from Promochem, Teddington, UK.

3.11.2 Preparation of Ketamine MIPs and Non-Imprinted Polymer (NIP)

The ketamine MIPs and NIP were prepared *via* a solution polymerisation method.[82] The templates used were (±)-ketamine and (*S*)-(+)-ketamine **7**. A series of polymers were prepared on a 5 g monomer scale with the feed ratios of template, functional monomer and crosslinker set at 1:4:20. In this study, toluene was used as porogen. The NIP was prepared in similar manner to the MIPs but in the absence of template.

3.11.3 Preparation of Solutions

(a) Preparation of Standard Stock Solution

(±)-Ketamine standard working solution: Measured exactly 0.05 mL of 1.0 mg/mL standard (±)-ketamine, and methanol was added to make exactly 50 mL to give a concentration of 1 μg/mL. (±)-Ketamine-D4 standard working solution: Measured exactly 0.1 mL of 0.1 mg/mL standard (±)-ketamine-D4, and methanol was added to make exactly 10 mL to give a concentration of 1 μg/mL. Stock and working solutions had a nominal shelf life of 6 months and were kept refrigerated (4 °C) when not in use and replaced on an as-needed basis.

(b) Preparation of pH 6.0 Phosphate Buffer

Sodium hydrogen phosphate (1.70 g) and sodium dihydrogen phosphate (12.14 g) were weighed into a 1 L volumetric flask and made up to volume with deionised water. The pH was adjusted to pH 6.0 using phosphoric acid.

(c) Mobile phase

A mobile phase consisting of 99 % acetonitrile and 1 % acetic acid (v/v) was prepared.

3.11.4 Hair samples

(a) Preparation of hair samples

The analyses of hair samples were divided into two parts. The first part was the preparation of standard samples as references, while the second part was the preparation of samples of spiked hair. The methods used for hair washing and hair incubation were based on those reported by Miller *et al.*[89] for the

detection of amphetamines, benzodiazepines, cocaine and opiates and their metabolites from hair, and by Harun *et al.*[32] for the detection of ketamine.

(i) Standard samples were prepared by adding 100 ng of (±)-ketamine and 100 ng of internal standard (IS) ketamine-D4 in methanol to 1.5 mL of 0.1 M phosphate buffer (pH 6.0) in weighing bottles prior to the incubation. The samples in the weighing bottles were capped and left to incubate for 18 hours at 45 °C. Then the solutions were cooled and transferred into clean glass vials. The solution samples were blown down to dryness at 40 °C under a stream of nitrogen and reconstituted in 100 μL of DCM. 20 μL of this sample was injected for analysis.

(ii) Samples of spiked hair were prepared in the following manner: Blank hair samples were collected from volunteers in the laboratory. The 0.5 cm-tip sections were weighed out into vials for analysis and each cut into two 2-3 mm segments using a pair of clean scissors. The hair samples were washed with 1 mL of 0.1 % sodium dodecyl sulfate (SDS), 2 x 1 mL deionised water and 2 x 1 mL dichloromethane, in each case with ultrasonication for 10 minutes. Then, the hair samples were left to dry in air at room temperature overnight.

Washed hair samples weighing 20 ± 0.1 mg were transferred into weighing bottles by adding 1.5 mL of 0.1 M phosphate buffer (pH 6.0). (±)-Ketamine standard and IS (ketamine-D4) were added to the weighing bottles prior to incubation. The samples were left to incubate for 18 hours at 45 °C. Then, the hair extracts were cooled and transferred into clean glass vials. The same procedures were applied as for the standard samples, where the extracted

samples were blown down to dryness under a stream of nitrogen at 40 °C and reconstituted in 100 μL of DCM. 20 μL of this sample was injected for analysis.

3.11.5 Operational Principle of LC-ESI-MS

LC-MS/MS analysis of ketamine was carried out using a Thermo Finnigan LCQ™ Deca XP (Thermo Finnigan, San Jose CA, USA) equipped with a Surveyor autosampler (AS 3000) and MS pump system. The instrument was attached to a computer system with XCalibur 1.3 software for data acquisition and processing. The instrument has three main components, *i.e*, the HPLC system, an electrospray interface (ESI) as ionisation source and a mass spectrometer (the ion trap mass analyser). The main advantage of the ion trap MS method is its ability to perform multiple stages of isolation and fragmentation of ions (MS^n), thus facilitating the identification of unknowns.

LC-MS/MS Conditions

LC analyses were carried out using a mobile phase containing 99 % acetonitrile and 1 % acetic acid at a flow rate of 0.2 mL/min. The elution programme used was isocratic mode with an analysis run time of 20 minutes. Chromatographic separation was performed using in-house packed columns (0.46 cm i.d x 5 cm fitted with 0.2 μm frits). Ionisation of analyte was performed using electrospray ionisation (ESI) in the positive ion mode, and data was collected in the Selective Reaction Monitoring (SRM) mode. The data was then processed using XCalibur™ Software version 1.3 from Thermo Finnigan.

The LC-MS/MS method was based on a published method for the analysis of ketamine[32] and multiple drugs in hair, including amphetamine,

benzodiazepines, cocaine and opiates.[89] The capillary temperature, sheath and auxiliary gas flow and collision energies were optimised during tuning for the analyte. The probe voltage used was 4.5 kV. Internal standard data was collected in selected ion monitoring (SIM) mode. Analytes were identified on the basis of their retention time and full MS/MS spectra. The product ion ratios were monitored to gain further qualitative identification data.

3.11.6 Limits of Detection (LOD) and Lower Limits of Quantification (LLOQ)

(a) Introduction of LOD and LLOQ

The limit of detection (LOD) is defined as the lowest concentration that can be detected by using an optimised method but not necessarily quantified as an exact value.[90],[91] The lower limit of quantification (LLOQ) is defined as the lowest concentration of the analyte of interest that can be quantified with acceptable precision and accuracy. LLOQ is recommended in most guidelines to be determined as a signal to noise ratio of 10:1.[92],[93],[94]

LOD and LLOQ values can be determined using more than one procedure. In the most commonly used method, the LOD and LLOQ values are determined by the value of signal to noise (S/N) ratios of 3 and 10, respectively, of the analyte peak to matrix background noise.[95] The LLOQ also can be defined as the lowest calibration standard that can be measured with acceptable precision and accuracy.

In this study, the LOD and LLOQ values were calculated statistically from the regression line of the calibration curve. The LOD was calculated using 3 times

the standard error of the regression line using Equation 3.3 and Equation 3.4,[95] where Y_B is the intercept, S_B is the standard error of the regression line and m is the gradient.

$$Y_{LOD} = Y_B + 3S_B \quad \text{---------- 3.3}$$

$$LOD = (Y_{LOD}-Y_B)/m \quad \text{---------- 3.4}$$

LLOQ values were calculated using the same method but using 10 times the standard error of the regression line (Equation 3.5 and Equation 3.6). The calculation was easy and fit for the purpose of method validation in this study, and has also been used previously.[82],[96]

$$Y_{LLOQ} = Y_B + 10S_B \quad \text{---------- 3.5}$$

$$LLOQ = (Y_{LLOQ}-Y_B)/m \quad \text{---------- 3.6}$$

(b) LOD and LLOQ sample preparation

The LOD and LLOQ values were determined using spiked blank hair samples. 20 ± 0.1 mg quantities of blank decontaminated hair samples were spiked with 1, 5, 10, 15 and 25 ng of (±)-ketamine; 100 ng of the internal standard, ketamine-D4, was then added. The samples were then extracted based on the method in Section 3.11.4 (a-ii) and analysed by LC-MS/MS. Calibration curves were constructed by plotting the peak area ratios of standard/IS against the spike analyte concentrations, and were subjected to linear regression analysis. Two replicate analyses were carried out for each concentration to get the LOD

and LLOQ values. The LOD and LLOQ were calculated from the regression lines as the concentrations which gave signal-to-noise ratios of 3 and 10, respectively.

3.12 Results and Discussion (Part II)

3.12.1 Synthesis of MIPs and NIP

In this work, the polymers under study were synthesised in monolithic form and then broken down by grinding into particulate form prior to packing into LC columns.[82] Two MIPs, with (±)-ketamine and (*S*)-(+)-ketamine **7** as templates, respectively, and a corresponding NIP, were synthesised for the purposes of the study. The ketamine MIPs were synthesised using a combination of functional monomer, crosslinker, initiator and porogen expected to give rise to MIPs with high affinity and rebinding selectivity for the analyte.

The MIPs and NIP produced were stable and could be stored at ambient temperature before being used for analyses. The polymers were packed successfully into LC columns; hereafter, the three packed columns are referred to as the NIP, (*S*)-Ket and (±)-Ket columns.

3.12.2 Hair Sample Analyses for Ketamine Detection

Over 30 years ago, the group of Baumgartner carried out the first toxicology testing using hair samples for determining opiate abuse histories.[97] Generally, in forensic drug analysis, samples of tissues and body fluids such as blood and urine were used. However, these samples are only able to provide information about drug exposure within the period 1-5 days prior to sample collection.[98] Thus, the use of other unconventional samples such as hair and nails became a more

important practice to gain long-term information on the drug use. Sectional analysis of hair samples also provides a reliable guide to the duration of drug ingestion. Besides, the collection of hair samples is also less invasive compared to blood or urine in terms of sample collection, and offers further advantages in respect of storage and transportation. Hair samples become more important especially when the crimes are reported more than 24 hours after consumption, where blood or urine samples are no longer appropriate. Another advantage is that hair analysis may help to determine the time of drug exposure. Furthermore, hair contains a relatively high parent drug to metabolite ratio. Therefore, it is normally easy to identify the parent drug and the metabolites.[99]

Hair samples are suitable for determining drug abuse histories because, when ingested, drugs will circulate in the bloodstream including the blood vessel of the hair bulb. Then, they can diffuse out of the blood vessel and become entrapped in the core of the hair shaft as it grows out from the hair follicle. The life span of a single hair varies from about 4 months to 4 years.

There are a few published reports on ketamine hair testing as an individual drug or in combination with other drugs using a GC-MS/MS method.[100],[101] In a recent study reported by Harun *et al.*,[32] a radical approach was pioneered in which a MIP was used as a sorbent for solid-phase extraction (SPE) in tandem with LC-MS/MS for the detection of ketamine and its metabolites in the forensic toxicology field. In this study, direct injection from an in-house prepared SPE column packed with a MIP was used with LC-MS/MS for the detection of ketamine. This technique has great potential for hair testing, and the purpose of the study was to develop a useful testing method for the determination of the drug in hair which involved a

simpler preparation and a more sensitive analytical procedure. LC-MS/MS was used to provide reliable results, sensitivity and selectivity. Identification of ketamine was based on retention time and full MS/MS spectra. Data collection was obtained from the selected reaction monitoring (SRM) where one parent ion and two daughter ions were selected for each analyte, which fulfilled the requirements of the European Union for identification and confirmation of illicit drugs.[102]

In the present study, where the aim was to remove the need for sample clean-up prior to the (MI)LC step, the role of the acid in the mobile phase was to suppress non-specific binding events and to reduce the retention times of ketamine on the columns. The analyses of ketamine were conducted under isocratic conditions as it gave better results compared to gradient elution conditions. According to the SPE study reported by Harun *et al.*,[82] when ketamine is introduced to the ketamine MIP sorbent the binding is best in chloroform, followed by DCM, acetonitrile and toluene. However, due to the environmental issues aspect, the use of chloroform has been changed to DCM to reconstitute the samples.

3.12.3 Study on the Standard Ketamine Solution

Studies using a standard ketamine solution were a key reference to ascertain whether the columns had the potential to be developed as a new analytical method for ketamine detection. In this study, the analyte used was a mixture of (±)-ketamine and (±)-ketamine-D4 as an internal standard (IS) without hair samples. Deuterated versions of drugs and their metabolites for use as internal standards are vital tools for laboratories conducting accurate determinations of these compounds in biological and environmental matrices.[103] Many authorities, such as the Society of Forensic Toxicology's "Forensic Toxicology Laboratory

Guidelines" and the "European Laboratory Guidelines for Legally Defensible Workplace Drug Testing" (EWDTS) recommend or require the use of deuterated standards.[104]

Figure 3.11 shows SRM chromatograms from the NIP column for a standard (±)-ketamine solution at a concentration of 100 ng/mL. Surprisingly, the SRM chromatogram did not show sharp peaks, as would be expected for ketamine on a NIP column (n=5). In principle, the ketamine peaks eluting from a NIP column should be very sharp peak and appear at shorter retention times than on a MIP column. This is due to the NIP column not having any specific binding events. Based on the chromatograms obtained in this study, the ketamine peaks were broad, less well-defined with a retention time of 11 minutes.

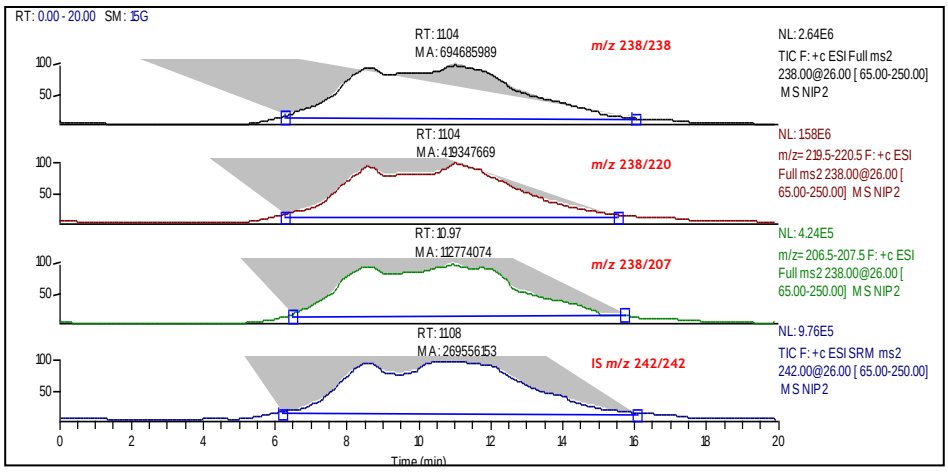

Figure 3.11 SRM chromatograms of quantitation ions for (±)-ketamine standard injected onto the NIP column at a concentration of 100 ng/mL. *RT* retention time; *MA* manual area.

The (±)-Ket column was first injected with analyte dissolved in 100 % acetonitrile. Unfortunately, no peaks appeared after 40 minutes of injection. Therefore, 1 % acetic acid was added to the mobile phase, as acetic acid would be expected to suppress the non-specific binding events and to reduce the retention times of ketamine on the column. Based on the SRM chromatograms for the (±)-Ket column (Fig. 3.12), ketamine peaks were clearly observed at a retention time of 5.01 minutes and 4.89 minutes for (±)-ketamine and IS ketamine-D4, respectively (n=5). As expected, there was no separation on the (±)-Ket column for the racemic ketamine analyte. The presence of the analyte was confirmed by MS.

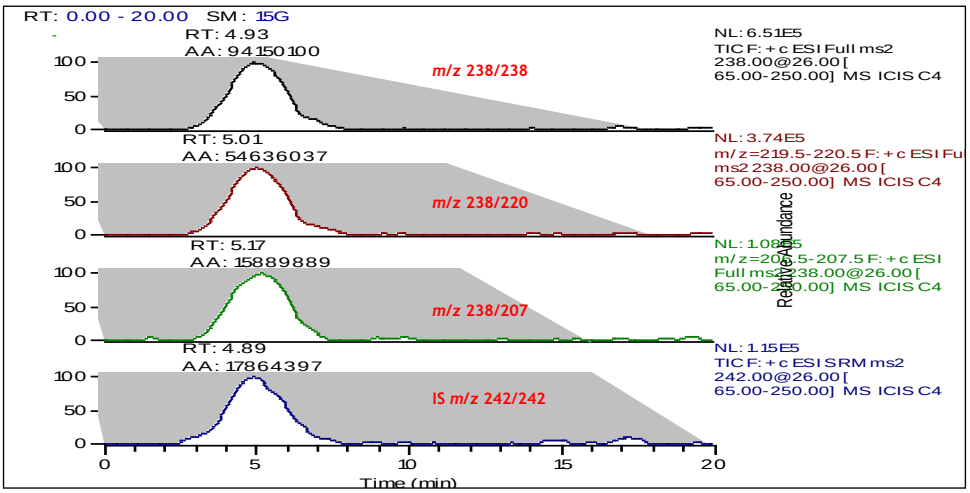

Figure 3.12 SRM chromatograms of quantitation ions for (±)-ketamine standard at a concentration of 100 ng/mL injected onto the (±)-Ket column. *RT* retention time; *AA* automatic area.

Interestingly, chromatograms from the (*S*)-Ket column (Figure 3.13), showed clear evidence of peak splitting when injected with the (±)-ketamine standard (n=5), suggestive of enantioseparation and indicative of chiral selectivity by the (*S*)-Ket

column. In Figure 3.13, the first peak (RT at 3.69) was assigned to a mixture of (*S*)-ketamine and (*R*)-ketamine while the second peak (RT at 5.33) was assigned to (*S*)-(+)-ketamine **7**. Both peaks were confirmed as ketamine by MS data. Results obtained in this study were in agreement with the HPLC results from the study by Harun *et al.*[82]

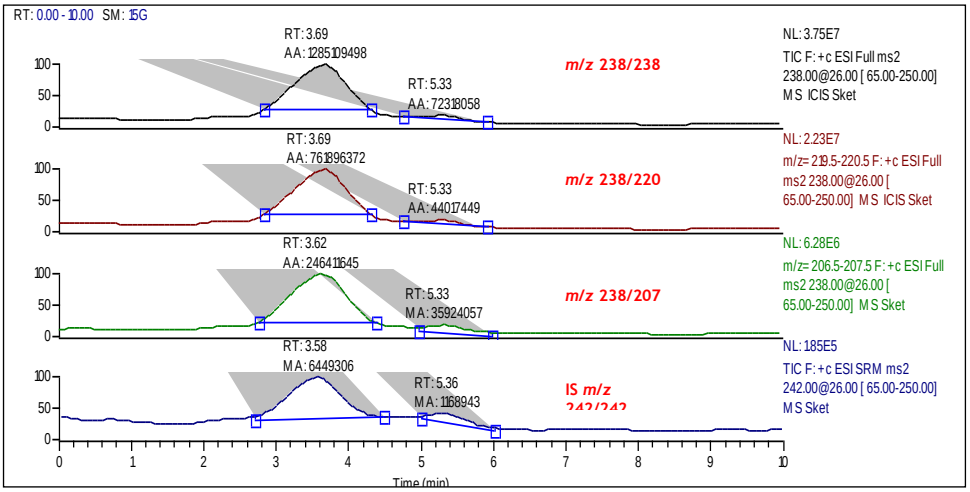

Figure 3.13 SRM chromatograms of quantitation ions for (±)-ketamine standard at a concentration of 100 ng/mL injected onto the (*S*)-Ket column. *RT* retention time; *AA* automatic area; *MA* manual area.

In Figure 3.13, it can be seen from the relative peak areas that the enantioseparation was incomplete (peak area ratio ~ 90:10). Further optimisation of the chromatographic conditions and/or the polymer synthesis conditions would be expected to give better enantioseparation, however this was beyond the scope of the present study, not least of all because forensic toxicology studies normally target racemic ketamine (*i.e.*, enantioseparation is not essential). For this reason, in the subsequent studies involving spiked hair samples the (±)-Ket column was

used to provide binding selectivity towards ketamine, however studies with the (*S*)-Ket column were also carried out for completeness.

3.12.4 Study on spiked hair samples

Spiked hair samples were prepared as described in Section 3.11.4(a-ii). The same procedures used in the study of the standard ketamine solutions were used to analyse the ketamine in spiked hair samples. Analyses were first performed on the NIP column (n=5). The retention time of the analyte was recorded at around 5 minutes, with broad peaks appearing in the chromatograms as shown in Figure 3.14. Analyses using spiked hair samples gave poor chromatograms without a stable baseline being established, as observed previously; therefore investigations using the NIP column were not pursued any further.

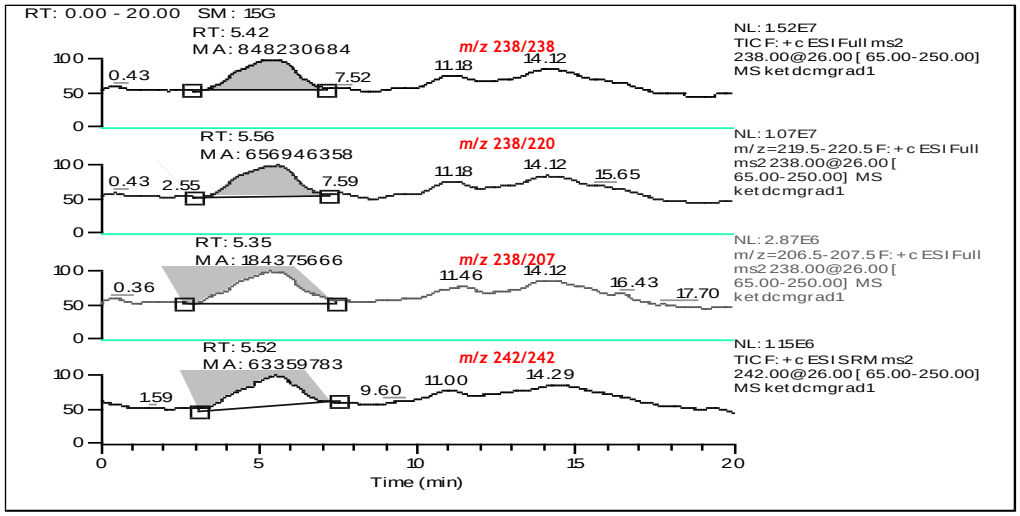

Figure 3.14 SRM chromatograms of quantitation ions for (±)-ketamine standard injected onto the NIP column at a concentration of 100 ng/mL. *RT* retention time; *MA* manual area.

Figure 3.15 shows SRM chromatograms of spiked hair samples on the (±)-Ket column (n=5). The retention time recorded was almost identical to the time recorded in the standard ketamine study. The retention time was 5.53 minutes for standard ketamine and 6.24 minutes for IS ketamine-D4. The baselines obtained in this study were unstable, and the peaks which appeared were broad and tailing due to the imprinting effect, however the results were reproducible and represented an important step in the demonstration of proof-of-principle.

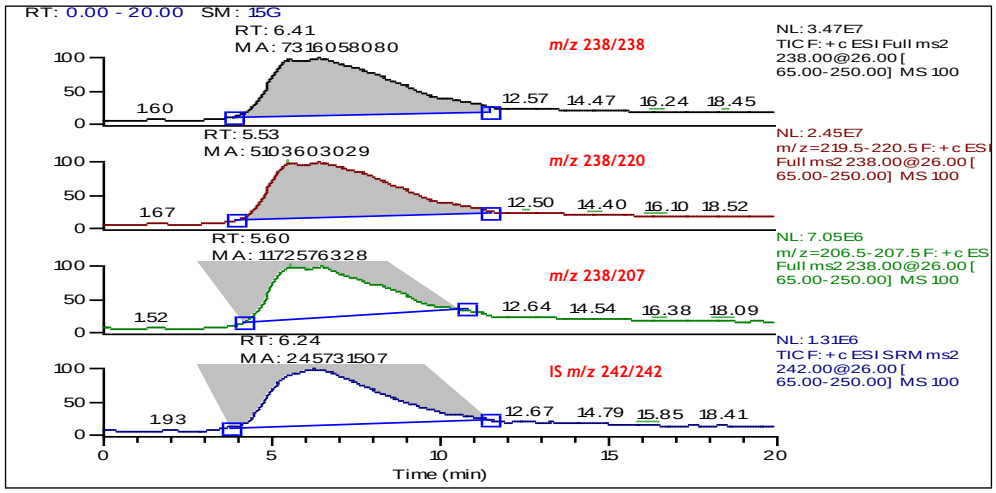

Figure 3.15 SRM chromatograms of spiked hair samples at a concentration of 100 ng/mL injected onto the (±)-Ket column. *RT* retention time; *MA* manual area.

For spiked hair samples on the (*S*)-Ket column, two ketamine peaks appeared in the chromatograms (Figure 3.16), as had been observed for the (*S*)-Ket column when using ketamine standards, indicating enantioseparation (n=5). The retention time of ketamine was 3.86 minutes, with the peak at 8.61 minutes being assigned to (*S*)-(+)-ketamine. For IS ketamine-D4, the corresponding retention times were 3.96 and 8.92 minutes. These results arise because (*S*)-(+)-ketamine binds stronger than (*R*)-(-)-ketamine on the (*S*)-Ket column and is therefore retained longer on the column. Yet again, it was clear that the enantioseparation was incomplete.

An important point to note is that Harun *et al.*[32],[82] successfully developed a MIP-based extraction method for ketamine in hair samples using a combination of MISPE and LC-MS/MS. The method was found to be both selective and sensitive, and also showed less matrix effects than a conventional SPE method. Nevertheless, enantioseparation was not reported. To our knowledge, there is no study in the literature related to the direct injection of racemic ketamine onto a bespoke column and which leads to enantioseparation in the context of a forensic toxicology study. Our preliminary results in this area show good potential for the enantioseparation of ketamine, although further optimisation work would ideally be required.

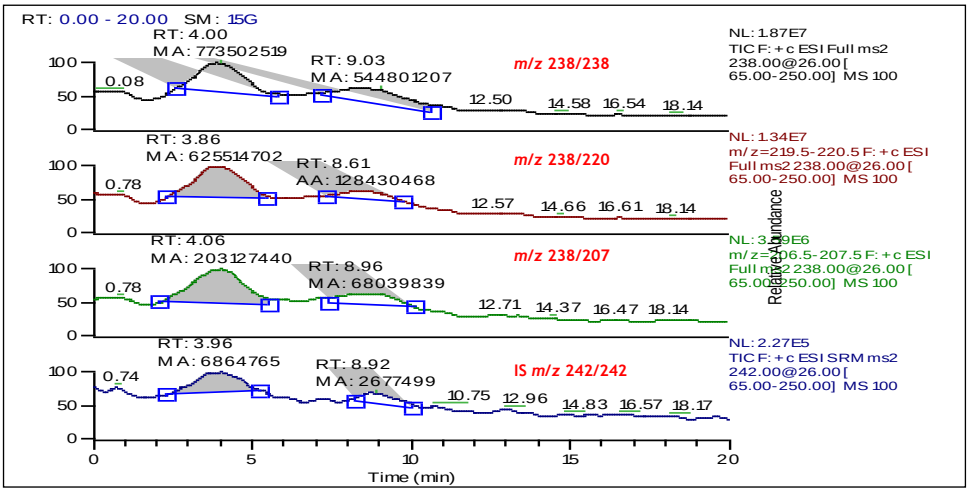

Figure 3.16 SRM chromatograms of spiked hair samples at a concentration of 100 ng/mL injected onto the (*S*)-Ket column. *RT* retention time; *MA* manual area.

Mass spectral data acquired for ketamine and its deuterated internal standard were based on electrospray (ESI) in positive ion mode which produced protonated molecular ions, $[M+H]^+$. Figure 3.17 and Figure 3.18 show the MS spectra for ketamine and ketamine-D4, respectively. The mass spectrum of standard ketamine was first acquired in full-scan mode (150-400 *m/z*) by infusion of a

reference solution. From these spectra, the precursor ions were selected and fragmented, acquiring the full-scan MS/MS spectra. Fragmentation of the selected precursor ions was performed by collision-induced dissociation with helium, which fills the ion trap. Finally, the most intense product ions were chosen and each compound was analysed in single reaction monitoring (SRM) mode to obtain the best sensitivity and specificity.

The precursor ion for ketamine was the $[M+H]^+$ ion at *m/z* 238 and the daughter ions were at *m/z* 220, 207 and 179, while the precursor for ketamine-D4 was at *m/z* 242 and its daughter ions were at *m/z* 224, 211 and 183. In this study, MS specta from the (±)-Ket and (*S*)-Ket column studies showed the same fragmentation of ions. Therefore, it could not be used as a method to determine the peaks of ketamine enantiomers in the enantioseparation.

The MS spectrum of ketamine (Fig. 3.17) at 238 $[M+H]^+$ revealed an initial loss of H_2O to give a fragment at 220, and loss of CH_3NH_2 to give a fragment at 207 followed by loss of H_2O or CO to give fragments at 189 and 179. The ketamine-D4 MS spectrum (Fig. 3.18) monitoring 242 $[M+H]^+$ showed fragmentations at 224, 211, 193 (barely visible), 183 and 129. The fragmentations of ketamine and ketamine-D4 in tandem mass spectrometry were in agreement with chemical ionisation (CI) data reported by Kochhar,[105] except for the fragments at 125 and 129. The most prominent fragment at 125 for ketamine and 129 for ketamine-D4 indicated chlorobenzonium ion and chlorobenzonium-D4 ion fragments.[106] A proposed mechanism for this decomposition is shown in Figure 3.19.

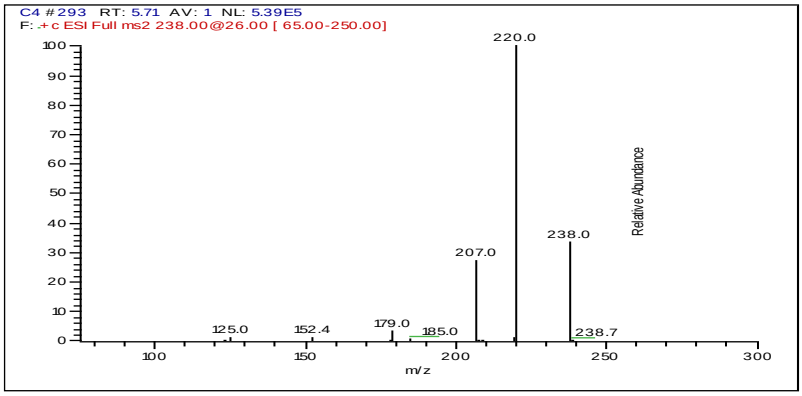

Figure 3.17 Mass spectrum of ketamine

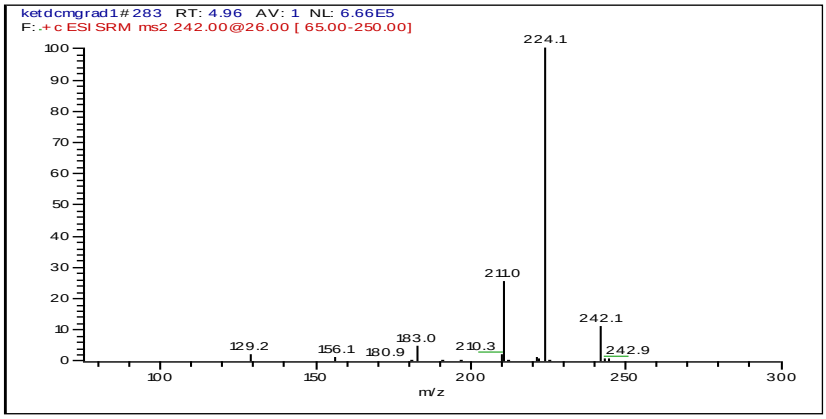

Figure 3.18 Mass spectrum of ketamine-D4

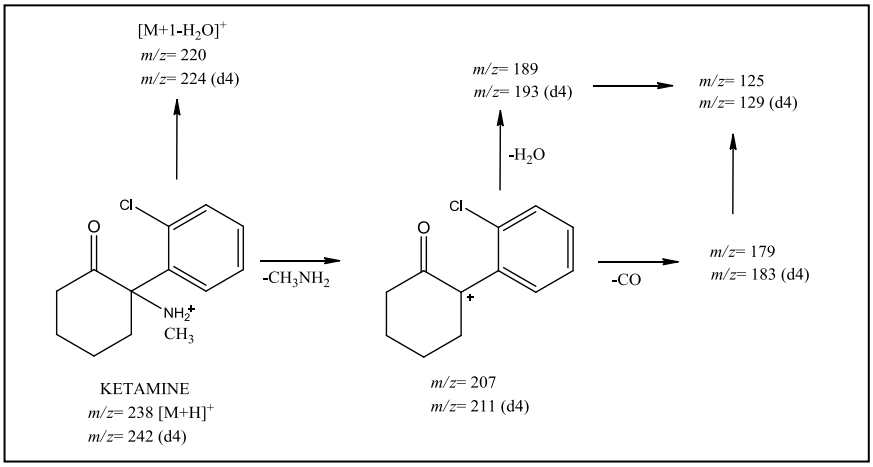

Figure 3.19 Suggested fragmentation of ketamine[106]

3.12.5 Study on the LOD and LLOQ

Thus far, it has been demonstrated that MILC-MS/MS can be used to detect ketamine in spiked hair samples. The next step was to establish the LOD and LLOQ values. The LOD and LLOQ values for both columns were calculated based on Equations 3.4 and 3.6, respectively. Standard calibration curves were obtained using 20 mg of spiked hair samples with standard solution and 100 ng of IS ketamine-D4. Calibration curves were obtained with five calibration points. The sensitivity of the method was determined by calculation of the LOD and the LLOQ.

The LOD and LLOQ values of ketamine on the (*S*)-Ket column were calculated to be 2.1 ng/mg and 6.9 ng/mg, respectively, while for the (±)-Ket column the LOD and LLOQ values were calculated to be 3.0 ng/mg and 10.0 ng/mg, respectively. Although the LOD and LLOQ values for both columns used in this study were higher than the values reported by Harun *et al.*[32] in a MISPE-LC-MS/MS study (0.1 ng/mg (LOD) and 0.18 ng/mg (LLOQ) for (±)-Ket column) it is important to stress the point that the new MILC-MS/MS method does not require a clean-up step prior to LC so offers time savings. The sensitivity of this method is still not as good as obtained in other published works, but yet again it should be stressed that it is a streamlined method and that it offers the potential of enantioseparation.[32],[82],[99] Although further column optimisation is required ideally, already the correlation coefficients for the calibration curves for both columns were better than 0.99, confirming a good linearity in the range of 1-25 ng/mg (Table 3.5).

Table 3.5 Analytical characteristic of MILC-ESI-MS method for ketamine

Column	Linear range (ng/mg hair)	Regression line equation	Correlation coefficient (R^2)	LOD (ng/mg hair)	LLOQ (ng/mg hair)
(*S*)-Ket	1 - 25	Y = 0.0575x + 1.0775	0.9958	2.1	6.9
(±)-Ket	1 - 25	Y = 0.0646x + 1.6198	0.9914	3.0	10.0

3.13 Conclusion (Part II)

In this study, a new analytical method for ketamine in hair has been proposed and developed. The method is known as Molecularly Imprinted Liquid Chromatography-tandem Mass Spectrometry (MILC-MS/MS). A key requirement for this method is the production of ketamine-imprinted polymer particulates in an appropriate physical format for direct packing into LC columns, which could then be hyphenated to mass spectrometer. Polymer particles were synthesised and packed into three different columns, to give namely the NIP, (*S*)-Ket and (±)-Ket columns.

MILC-MS/MS chromatograms of spiked hair samples showed that both imprinted columns were able to detect the presence of ketamine in less than 10 minutes and without the need for any clean up step prior to LC. There is also a suggestion that the (*S*)-Ket column can be used to provide information about the enantiomeric purity of ketamine in hair.

The LOD and LLOQ values were low (< 10 ng/mg hair) for both columns investigated in this study, and good linearity of the calibration curves in the range 1-25 ng/mg were obtained, with R^2 values better than 0.99.

The results from this preliminary study suggest strongly that the MILC-MS/MS method can be applied for the detection of ketamine. Since the method is a general one, we believe that it can be applied more widely in the field of forensic toxicology, and beyond.

3.14 References

[1] C. D. Klaassen, *Casarett & Doull's Toxicology: The Basic Science of Poisons*, New York, McGraw-Hill, **2001**.

[2] L. Langman and B. Kapur, *Clin. Biochem.* **2006**, *39*, 498-510.

[3] S. E. Manahan in *Toxicological Chemistry and Biochemistry, Third Ed.* CRC Press, Florida, **2003**.

[4] V. Cirimele, P. Kintz and B. Ludes, *J. Chromatogr. B.* **1997**, *700*, 119-129.

[5] R. Venn and R. Goody in *Methodological surveys in bioanalysis of drugs*, *25* Eds. E. Reid, H. Hill and I. Wilson, Elsevier, Netherlands, **1998**, 13-20.

[6] *http://www.forcon.ca/learning/forensic_toxicology.html. Accessed on July, 2010.*

[7] R. A. Middleberg, *Forensic Magazine* **2008**, *5*, 16-23.

[8] E. Ellinwood, G. King and T. Lee in *Chronic Amphetamine Use and Abuse*, Neurophsychopharmacol., 5th Generation of Progress, Durham, **2000**.

[9] G. Lawyer, P. Bjerkan, A. Hammarberg, N. Jayaram-Lindstrom, J. Franck and I. Agartz, *BMC Pharmacol.* **2010**, *10*, 5.

[10] J. Drews, *Science* **2000**, *287*, 1960-1964.

[11] E. Costa and A. Guidetti, *Trends Pharmacol. Sci.* **1996**, *17*, 192-200.

[12] J. D. Grant, M. T. Lynskey, J. F. Scherrer, A. Agrawal, A. C. Heath and K. K. Bucholz, *Addict. Behav.* **2010**, *35*, 35-41.

[13] T. P. Ellingstad, L. C. Sobell, M. B. Sobell, L. Eickleberry and C. J. Golden, *Addict. Behav.* **2006**, *31*, 519-530.

[14] J. M. Witkin, *Neurosci. Biobev. Rev.* **1994**, *18*, 121-142.

[15] S. M. White and C. J. T. Lambe, *J. Clin. Forensic Med.* **2003**, *10*, 27-39.

[16] P. E. Davis, H. Liddiard and T. M. McMillan, *Drug Alcohol Depen.* **2002**, *67*, 105-108.

[17] R. Kronstrand, R. Grundin and J. Jonsson, *Forensic Sci. Int.* **1998**, *92*, 29-38.

[18] T. Ishida, K. Kudo, H. Inoue, A. Tsuji, T. Kojima and N. Ikeda, *J. Anal. Toxicol.* **2006**, *30*, 468-477.

[19] K. Robert, N. Ingrid, S. Joakim and D. Henrik, *Forensic Sci. Int.* **2004**, *145*, 183-190.

[20] J. Feng, L. Wang, I. Dai, T. Harmon and J. T. Bernert, *J. Anal. Toxicol.* **2007**, *31*, 359-368.

[21] *http://www.soht.org/pdf/Consensus_on_Hair_Analysis.pdf. Accessed on July,2010.*

[22] *http://www.soft-tox.org/docs/Guidelines%202006%20Final.pdf. Accessed on July, 2010.*

[23] *http://www.sigmaaldrich.com/Graphics/Supelco/objects/4600/4538.pdf. Accessed on August, 2010.*

[24] S. McClean, E. O'Kane, J. Hillis and W. F. Smyth, *J. Chromatogr. A.* **1999**, *838*, 273-291.

[25] A. K. Burnham, G. V. Calder, J. S. Fritz, G. A. Junk, H. J. Svec and R. Willis, *Anal. Chem.* **1972**, *44*, 139-142.

[26] G. Cooper, *PhD Thesis,* University of Glasgow, Glasgow, **1999**.

[27] B. Sellergren, *TrAC*. **1999**, *18*, 164-174.

[28] J. Olsen, P. Martin and I. D. Wilson, *Anal. Commun.* **1998**, *35*, 13-14.

[29] B. Sellergren, *Anal. Chem.* **1994**, *66*, 1578-1582.

[30] R. A. Anderson, M. M. Ariffin, P. A. G. Cormack and E. I. Miller, *Forensic Sci. Int*. **2008**, *174*, 40-46.

[31] M. M. Ariffin, E. I. Miller, P. A. G. Cormack and R. A. Anderson, *Anal. Chem.* **2007**, *79*, 256-262.

[32] N. Harun, R. Anderson and P. A. G. Cormack, *Anal. Bioanal. Chem.* **2010**, *396*, 2449-2459.

[33] H. H. Maurer, *Clin. Biochem.* **2005**, *38*, 310-318.

[34] G. N. Leung, D. K. Leung, T. S. Wan and C. H. Wong, *J. Chromatogr. A.* **2007**, *1156 (1-2)*, 271-279.

[35] T. Yamashita, Y. Dohta, T. Nakamura and T. Fukami, *J. Chromatogr. A.* **2008**, *1182 (1)*, 72-76.

[36] L. Muetzelfeldt, S. K. Kamboj, H. Rees, J. Taylor, C. J. A. Morgan and H. V. Curran, *Drug Alcohol Depen.* **2008**, *95*, 219-229.

[37] F. G. Bonanno, *Injury* **2002**, *33*, 323-327.

[38] A. A. Weinbroum, *Anesth. Analg.* **2003**, *96*, 789-795.

[39] K. Eun-mi, L. Ju-seon, C. Sang-kil, L. Mi-ae and C. Hee-sun, *Forensic Sci. Int.* **2008**, *174*, 197-202.

[40] A. T. Bhutta, *Semin. Perinatol.* **2007**, *31*, 303-308.

[41] R. L. Schmid, A. N. Sandler and J. Katz, *Pain* **1999**, *82*, 111-125.

[42] *WHO Expert Committee, Critical review of Ketamine*, 34th ECDD, **2006**.

[43] D. Reich and G. Silvay, *Can. J. Anaesth.* **1989**, *36*, 186-197.

[44] H. Koinig and P. Marhofer, *Pediatr. Anesth.* **2003**, *13*, 185-187.

[45] C. Pees, N. A. Haas, P. Ewert, F. Berger and P. E. Lange, *Pediatr. Cardiol.* **2003**, *24*, 424-429.

[46] P. F. White, J. Schuttler, A. Shafer, D. R. Stanski, Y. Horai and A. J. Trevor, *Br. J. Anaesth.* **1985**, *57*, 197-203.

[47] W. Engelhardt, K. Stahl, A. Marouche and E. Hartung, *Der Anaesthesist* **1998**, *47*, 184-192.

[48] F. X. Vollenweider, P. Vontobel, I. Øye, D. Hell and K. L. Leenders, *J. Psychiat. Res.* **2000**, *34*, 35-43.

[49] J. Copeland and P. Dillon, *Int. J. Drug Policy.* **2005**, *16*, 122-131.

[50] *http://www.drugstraining.co.uk/drugsterms.html. Accessed on August, 2010.*

[51] *http://www.zhion.com/drug/Ketamine.html. Accessed on June*, 2010.

[52] H. Schütz, A. Paine, F. Erdmann, G. Weiler and M. Verhoff, *Forensic Sci. Med. Pathol.* **2006**, *2*, 75-83.

[53] *http://www.mainliners.org.uk/pages/information-on-substance-misuse-139.html. Accessed on July*, 2010.

[54] R. Siegel, *NIDA Res. Monogr.* **1978**, *21*, 119-147.

[55] P. J. Dalgarno and Shewan, *J. Psychoactive Drugs.* **1996**, *28(2)*, 191-199.

[56] S. C. E. Riley and E. Hayward, *Drugs: Education, Prevention and Policy* **2004**, *11*, 243-262.

[57] K. Skovmand, *The Lancet.* **1996**, *348*, 122.

[58] A. C. Lua, H. R. Lin, Y. T. Tseng, A. R. Hu and P. C. Yeh, *Forensic Sci. Int.* **2003**, *136*, 47-51.

[59] P. Dillon and L. Degenhardt, *J. Subst. Use*. **2001**, *6*, 11-15.

[60] P. Dillon, J. Copeland and K. Jansen, *Drug Alcohol Depen.* **2003**, *69*, 23-28.

[61] J. M. White and C. F. Ryan, *Drug Alcohol Rev.* **1996**, *15*, 145-155.

[62] *Ketamine abuse increasing*, Drug Enforcement Agency,**1997**. Assecced on July 2010.

[63] C. Zhao, Z. Liu, D. Zhao, Y. Liu, J. Liang, Y. Tang, Z. Liu and J. Zheng, *Ann. NY. Acad. Sci.* **2004**, *1025*, 439-445.

[64] H. S. Leong, N. L. Tan, C. P. Lui and T. K. Lee, *J. Anal. Toxicol.* **2005**, *29*, 314-318.

[65] N. Harun, R. A. Anderson and E. I. Miller, *J. Anal. Toxicol.* **2009**, *33(6)*, 310-321.

[66] A. M. Mattison, M. W. Ross, T. Wolfson and D. Franklin, *J. Subst. Abuse.* **2001**, *13*, 119-126.

[67] M. W. Ross, A. M. Mattison and D. R. Franklin, *Subst. Use Misuse.* **2003**, *38*, 1173-1183.

[68] S. Lankenau and M. Clatts, *J. Urban Health.* **2004**, *81*, 232-248.

[69] J. M. Van Leeuwen, C. Hopfer, S. Hooks, R. White, J. Petersen and J. Pirkopf, *J. Commun. Health.* **2004**, *29*, 217-229.

[70] M. P. Stevens in *Polymer Chemistry: An Introduction*, Oxford University Press, New York, **1999**.

[71] K. Hosoya, K. Yoshizako, Y. Shirasu, K. Kimata, T. Araki, N. Tanaka and J. Haginaka, *J. Chromatogr. A.* **1996**, *728*, 139-147.

[72] A. G. Mayes and K. Mosbach, *Anal. Chem.* **1996**, *68*, 3769-3774.

[73] M. Nakamura, M. Ono, T. Nakajima, Y. Ito, T. Aketo and J. Haginaka, *J. Pharmaceut. Biomed.* **2005**, *37*, 231-237.

[74] J. Wang, P. A. G. Cormack, D. C. Sherrington and E. Khoshdel, *Angew. Chem. Int. Ed.* **2003**, *42*, 5336-5338.

[75] J. F. Wang, PhD Thesis, University of Strathclyde, Glasgow, **2004**.

[76] J. F. Wang, P. A. G. Cormack, D. C. Sherrington and E. Khoshdel, *Pure Appl. Chem.* **2007**, *79*, 1503-1517.

[77] L. Ferguson, MSci Thesis, University of Strathclyde, Glasgow, **2007**.

[78] A. G. Mayes and K. Mosbach, *TrAC.* **1997**, *16*, 321-332.

[79] F. Svec, *J. Sep. Sci.* **2005**, *28*, 729-745.

[80] F. Svec and C. G. Huber, *Anal. Chem.* **2006**, *78*, 2100-2107.

[81] O. G. Potter and E. F. Hilder, *J. Sep. Sci.* **2008**, *31*, 1881-1906.

[82] N. Harun, PhD Thesis, University of Glasgow, Glasgow, **2010**.

[83] R. Yokoyama, S. Matsumoto, S. Nomura, T. Higaki, T. Yokoyama and S. I. Kiyooka, *Tetrahedron* **2009**, *65*, 5181-5191.

[84] W.-H. Li and H. D. H. Stöver, *Macromolecules* **2000**, *33*, 4354-4360.

[85] E. A. O'Donnell, PhD thesis, University of Strathclyde, Glasgow, **2007**.

[86] H. Y. Aboul-Enein and M. M. Hefnawy, *Talanta* **2005**, *65*, 67-73.

[87] E. Turiel, J. L. Tadeo, P. A. G. Cormack and A. Martin-Esteban, *Analyst* **2005**, *130*, 1601-1607.

[88] A. G. Strikovsky, D. Kasper, M. Grün, B. S. Green, J. Hradil and G. Wulff, *J. Am. Chem. Soc.* **2000**, *122*, 6295-6296.

[89] E. I. Miller, F. M. Wylie and J. S. Oliver, *J. Anal. Toxicol.* **2008**, *32*, 457-469.

[90] F. T. Peter, *Anal. Bioanal. Chem.* **2007**, *388*, 1505-1519.

[91] A. C. Moffat, M. D. Osselton, B. Widdop and L. Y. Gallichet in *Clarke's Analysis of Drugs and Poisons*, 3rd Edition, Pharmaceutical Press, London, **2004**.

[92] V. Shah, K. Midha, J. Findlay, H. Hill, J. Hulse, I. McGilveray, G. McKay, K. Miller, R. Patnaik, M. Powell, A. Tonelli, C. T. Viswanathan and A. Yacobi, *Pharmaceut. Res.* **2000**, *17*, 1551-1557.

[93] T. P. Frank, H. D. Olaf and M. Frank, *Forensic Sci. Int.* **2007**, *165*, 216-224.

[94] A. G. Gonzalez and M. A. Herrador, *TrAC.* **2007**, *26*, 227-238.

[95] J. N. Miller and J. C. Miller, *Statistics and chemometrics for analytical chemistry,* Pearson Prentice Hall, Harlow, **2005**.

[96] H. J. Torrance, PhD Thesis, University of Glasgow, Glasgow, **2005**.

[97] A. M. Baumgartner, P. F. Jones, W. A. Baumgartner and C. T. Black, *J. Nucl. Med.* **1979**, *20*, 748-752.

[98] R. Laurent, *Clin. Endocrinol.* **2000**, *14*, 147-165.

[99] M. Tabernero, M. Felli, A. Bermejo and M. Chiarotti, *Anal. Bioanal. Chem.* **2009**, *395*, 2547-2557.

[100] Y. H. Wu, K. L. Lin, S. C. Chen and Y. Z. Chang, *J. Chromatogr. B.* **2008**, *870*, 192-202.

[101] C. H. Wu, M. H. Huang, S. M. Wang, C. C. Lin and R. H. Liu, *J. Chromatogr. A.* **2007**, *1157*, 336-351.

[102] L. Rivier, *Anal. Chim. Acta.* **2003**, *492*, 69-82.

[103] *http://www.lgcstandards.com. Accessed on August, 2010.*

[104] S. C. Turfus, M. C. Parkin, D. A. Cowan, J. M. Halket, N. W. Smith, R. A. Braithwaite, S. P. Elliot, G. B. Steventon and A. T. Kicman, *Drug Metab. Dipos.* **2009**, *37*, 1769-1778.

[105] M. M. Kochhar, *Clin. Toxicol.* **1977**, *11*, 265-275.

[106] W. Kaung-Chaun, S. Tuo-Shi and C. Sheaw-Guey, *Forensic Sci. Int.* **2005**, *147*, 81-88.

CHAPTER 4

CONTROLLED/LIVING RADICAL POLYMERISATION IN THE SYNTHESIS OF MOLECULARLY IMPRINTED POLYMERS (MIPs)

4.1 Introduction

Molecular imprinting is a facile and versatile approach for the generation of synthetic receptors with tailor-made recognition sites.[1] They are normally prepared by conventional free radical polymerisation (FRP) due to the tolerance of FRP for a wide range of functional groups in the monomers and templates, but also because conventional FRP can normally be carried out in a facile manner under mild reaction conditions. MIPs have a broad range of potential applications in separation science,[2],[3] catalysis,[4] sensing[5],[6] and drug delivery.[7] However, conventional FRP allows for only limited control over the polymer growth processes with regard to chain propagation and termination, as well as the chemical structures of the polymeric products,[8],[9] plus polymer networks with heterogeneous structures are normally produced when such networks are synthesised using FRP. The presence of heterogeneity within the network structures of MIPs, especially heterogeneity within the population of binding sites, translates, at least in part, to the inherent drawbacks of MIPs, including broad, asymmetric peaks in LC analyses.[10]

The necessity to overcome these limitations urged synthetic polymer chemists to develop new concepts, which would permit for the preparation of MIPs with more

homogeneous network structures, a better understanding of the structure-property relationship of MIPs, and for obtaining MIPs with improved binding properties.[1] In this respect, controlled/living radical polymerisation (CRP) techniques have been evolved and it is well understood that CRP processes offer many benefits. They have attracted significant attention because they provide simple and robust routes to the synthesis of well-defined polymers and have now become one of the most rapidly developing areas in the field of polymer science.[11],[12],[13] These include the ability to control molecular weight and polydispersity, and to prepare block copolymers and other polymers of complex architecture.[14] A living process implies that all polymer chains start growing simultaneously, while during chain growth no termination or chain transfer takes place and the chains remain active once all monomer has been consumed. Consequently, all chains grow for a similar period of time and a narrow molecular weight distribution is obtained. When all monomer has been consumed, the active centre persists and upon addition of a new batch of monomer, polymerisation continues to form a block copolymer. The CRP techniques that have received greatest attention recently are nitroxide-mediated radical polymerisation (NMRP),[15] atom transfer radical polymerisation (ATRP)[16],[17] and reversible addition-fragmentation chain transfer (RAFT) polymerisation.[18]

Living or controlled radical polymerisation offers a combination of the best features of living anionic polymerisation and radical polymerisation. As mentioned before, these methods allow the syntheses of tailor-made polymers with well-defined structures and functionalities, giving control over the macroscopic properties and an easy access to a large production scale. The recent emergence of techniques for implementing controlled radical polymerisations has provided a

new set of tools for polymer chemists which allow very precise control over the polymerisation processes while retaining much of the versatility of conventional free radical polymerisation.[17],[18],[19]

Yet again, the aim of controlled radical polymerisation (CRP) is to synthesise polymers with pre-determined molar masses and narrow molar mass distributions. The polymerisation methods are based on dynamic equilibria between propagating radicals and various dormant species, a characteristic feature which is a central to all controlled radical polymerisation systems.[20] Radicals may be either reversibly trapped in a deactivation/activation process (Figure 4.1) or they can be involved in a 'reversible transfer', degenerative exchange process (Figure 4.2). Examples of reversible deactivation/activation are NMRP[21] and ATRP,[10] while RAFT polymerisation[22] is an example of reversible transfer.

In reversible deactivation/activation, the polymer chain is end-capped with a moiety that can reversibly undergo homolytical cleavage. In NMRP, a nitroxide is the capping moiety, while in ATRP a halide is reversibly transferred to a transition-metal complex. Furthermore, in the reversible transfer process (*i.e,* RAFT), there is fast exchange of growing radicals *via* a transfer agent, where thiocarbonyl-containing compounds are normally responsible for this exchange which proceeds *via* an intermediate radical.

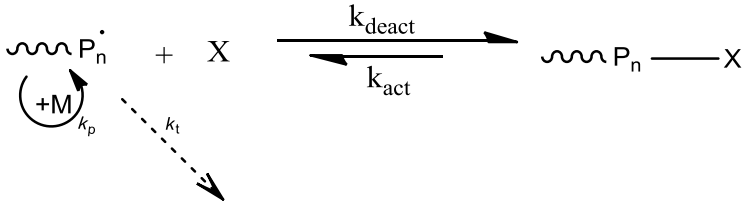

Figure 4.1 Reversible deactivation/activation process[21]

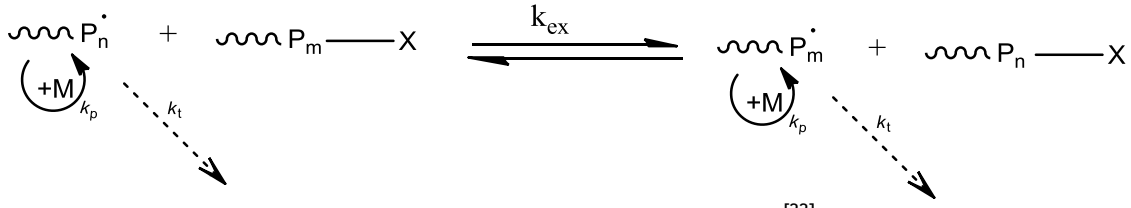

Figure 4.2 Reversible transfer process[22]

As an alternative to conventional FRP for the production of MIPs, our hypothesis was that the controlled nature of 'living' (controlled) radical polymerisation would translate into MIPs with properties superior to those displayed by MIPs prepared by conventional FRP, *e.g.*, improved homogeneity of binding sites and enhanced chromatographic performance when the MIPs are applied as stationary phases in HPLC.

Historically, porous organic polymers derived from vinyl monomers have been prepared almost exclusively by free radical polymerisation. In the late 1960s, these polymers were first prepared as macroporous beads through a suspension polymerisation technique.[23],[24] Macroporous beads are used widely not only as the basis of ion-exchange resins,[25] but also as catalytic surfaces and supports,[26],[27] separation and adsorbent media,[28],[29] chromatographic materials,[30] biomaterials[31] and electric insulators.[32] In column-based separation science, the normal procedure would be to pack the polymer particles into the

columns and then carry out the separation science. However, in 1992, Svec and Fréchet presented a new procedure to synthesise macroporous polymer monoliths directly inside columns for applications such as capillary electrochromatography and HPLC.[33]

Following the studies conducted by Svec and Fréchet on porous monolithic materials, the NMRP technique has been exploited extensively for the synthesis of narrow molecular-weight distribution homopolymers and block copolymers of styrene and acrylates.[21],[34] Svec *et al.*[35],[36] were the first to emphasise the advantages of the use of NMRP for the preparation of macroporous polymers by the direct copolymerisation of monovinyl and divinyl monomers in the presence of a porogenic solvent. However, there are a few drawbacks of the NMRP method: these include the long polymerisation times, the limit of the range of monomers that can be polymerised, and the relatively high polymerisation temperature (>125 °C). Later on, Hawker *et al.*[15],[37] introduced the unimolecular initiator concept, in which an alkoxyamine was used as the initiator, and this enabled the polymerisations to be performed at somewhat lower temperatures (< 100 °C). Porous poly(divinylbenzene) monoliths were prepared by Kanamori *et al.*[38] using a monomer/porogenic mixture containing divinylbenzene, 1,3,5-trimethylbenzene as well as dimethylsiloxane in the presence of an alkoxyamine initiator.

Recently, Zhang and coworkers applied the ATRP method to the synthesis of MIPs in monolithic form. They successfully generated MIPs with improved properties.[1] ATRP is more versatile than NMRP but it requires unconventional initiating systems that often have poor compatibility with polymerisation media,[39],[40],[41] however, metal contamination of the polymeric products can be problematic.

More recently, RAFT polymerisation has become established as a valuable method of controlled radical polymerisation, and is one of the most versatile ways to confer "living" characteristics onto radical polymerisations. The method relies on efficient chain-transfer processes which are mediated typically by thiocarbonyl-containing RAFT agents, *e.g.*, dithioesters.[42] Of the three methods available to mediate a controlled radical polymerisation, the RAFT process is arguably the most robust. It tolerates traces of impurities and is compatible with the broadest range of monomers and reaction conditions.[22],[43],[44] Moreover, the RAFT process is capable of controlling polymerisations in aqueous dispersion which NMRP and ATRP polymerisation are unable to do.[45],[46],[47]

In some circumstances, it is desirable to transform the thiocarbonyl-containing group for use in subsequent post-polymerisation processes or to set in place a different functionality. There are many examples which have been reported where RAFT- synthesised block or graft copolymers, functional nanoparticles and biopolymer conjugates, include effective strategies for the chemical transformation of the thiocarbonyl end-group as an integral part of the process. The latest reviews focusing on end-functional polymers and RAFT polymerisation include those by Moad *et al.*,[48] Willcock and O'Reilly[49] and Barner and Perrier.[50]

4.2 Aim of study

The main objective of the present work was to explore the potential benefits in applying RAFT polymerisation techniques towards the synthesis of MIPs, with caffeine as a model template. Caffeine was selected as template because it has been used previously in the production of molecularly imprinted polymers through conventional synthesis approaches, both in our laboratory and elsewhere. In the

present study, polymers were prepared *via* conventional free radical polymerisation and controlled radical polymerisation in the form of polymer monolith and polymer microspheres. The properties of these polymers were compared. HPLC was used for the purposes of analysis.

4.3 Free Radical Polymerisation and Controlled Radical Polymerisation

While living anionic vinyl polymerisation was being discovered and developed, conventional free radical polymerisation (FRP) was already flourishing. A comprehensive theory of radical polymerisation was developed and many new products were commercialised.[16],[51],[52] In fact, almost 50 % of all commercial polymers are produced in this way[53].

There are some similarities between CRP and FRP. CRP and FRP can polymerise a similar range of monomers and exhibit similar chemo-, regio- and stereo-selectivities. However, several important differences exist between them as summarised below.

1. The average lifetime of growing chains is longer in CRP than FRP due to the formation of dormant species and intermittent reversible activation.
2. In FRP the rate of initiation is slow relative to the rate of propagation. In CRP the rate of propagation is normally slower than the rate of propagation in FRP from the point of view of the growth of a single chain.
3. By the end of the polymerisation all chains are dead in the case of FRP, however in CRP the proportion of dead chains is usually less than 10 %.

4. In FRP, a steady state radical concentration is established with similar rates of initiation and termination, whereas in CRP a steady state is reached by balancing the rates of the activation and deactivation.

Additionally, by gaining better control over the polymerisation reaction, it was anticipated that improved molecular recognition with MIPs could be achieved.

4.4 Development of Controlled Radical Polymerisation

In the 1950s, the discovery of living anionic polymerisation by Michael Szwarc had a tremendous effect on polymer science.[54] His work led to major developments in both polymer physics and synthetic polymer chemistry. The studies enabled the production of polymers with predetermined molecular masses, narrow molar mass distributions and predetermined architectures. In addition to the discovery, it enabled the preparation of block copolymers and star-shaped polymers.[55]

The term 'Living Polymers', which was first introduced by Szwarc in a paper in *Nature,* was officially recognised by the IUPAC Macromolecular Nomenclature Committee.[54] Szwarc showed that anionic polymerisation can be carried out in the absence of termination reactions. Szwarc's discovery of living anionic polymerisation led many researchers all over the world to search for methods of extending the living polymerisation processes to other modes of polymerisation. Anionic polymerisation was the first and only example of a living polymerisation process for more than a decade after the proof of its 'livingness', but other living techniques have since been discovered.

Several years later, Stanislaw Penczek demonstrated the 'livingness' of the cationic ring-opening polymerisation (CROP) of tetrahydrofuran initiated by triflate esters.[56],[57],[58] Living CROP was further modified to include other heterocyclic monomers and this enabled the synthesis of many well-defined (co)polymers.[59],[60]

In the 1980s, inspired by Szwarc's discovery, a few other researchers developed living cationic polymerisation (Sawamoto & Higashimura 1984; Faust & Kennedy 1987). Sawamoto[61] demonstrated living cationic polymer using vinyl ethers and HI/I_2, and Kennedy[62] published the first example of living polymerisation of isobutylene. Approximately at the same time, the 'iniferter' (**ini**tiator-trans**fer**-**ter**mination) technique was introduced by Otsu & Tazaki[63] when upon revision of some of their older works and literature reports from others, they discovered that the addition of certain compounds (*e.g.*, dithiocarbamates or disulfides) to a radical polymerisation resulted in a system that exhibited some living characteristics, where the dithiocarbamates acted as initiators as well as transfer agents and termination agents.[64]

Finally, in the 1990s, living/controlled free-radical polymerisation techniques such as nitroxide-mediated radical polymerisation (NMRP), atom transfer radical polymerisation (ATRP) and reversible addition-fragmentation transfer (RAFT) polymerisation were introduced by Georges *et al.* (1993),[21] Wang & Matyjaszweski (1995)[65] and Moad & Solomon (1995)[66], respectively.

4.4.1 Nitroxide-Mediated Radical Polymerisation (NMRP)

Nitroxide-Mediated Radical Polymerisation (NMRP) is also known as stable free-radical polymerisation (SFRP), and was developed at the Commonwealth Scientific and Industrial Research Organisation (CSIRO) in the mid-1980s by Rizarrdo and coworkers.[67] Prior to the development of NMRP, nitroxides were known as radical scavengers, and various derivatives were used widely for polymer stabilisation. These applications were based typically on the property of nitroxides to efficiently trap carbon-centred radicals by combining with them at near diffusion-controlled rates.

In the period 1979-1990, various studies into the reactions of initiator-derived radicals with monomers were carried out, where nitroxides (*e.g.*, **9** and **10**) in Figure 4.3 were used as radical traps.[52],[68] It was observed that under some conditions the trapping of propagating radicals by the nitroxide was reversible, an observation that ultimately led to the development of NMRP. In 1985, the exploitation of alkoxyamines as polymerisation initiators and the use of NMRP for producing end-functional and block polymers were first described in a CSIRO patent.[69] Figure 4.3 shows examples of nitroxides which have been investigated.

Johnson *et al.*[70] introduced what is now known as the persistent radical effect (PRE)[71] and showed theoretically that NMRP could produced narrow polydispersity polymers. NMRP experiments were carried out by using (meth)acrylates with nitroxides, such as **11-13** as control agents. However, NMRP received greatest attention following a demonstration by Georges *et al.*[21] in 1993 in which they used 2,2,6,6-tetramethylpiperidinyloxy (TEMPO) **9** as the control agent for styrene

polymerisation; the preparation of polystyrene with a relatively narrow molecular weight distribution was demonstrated.

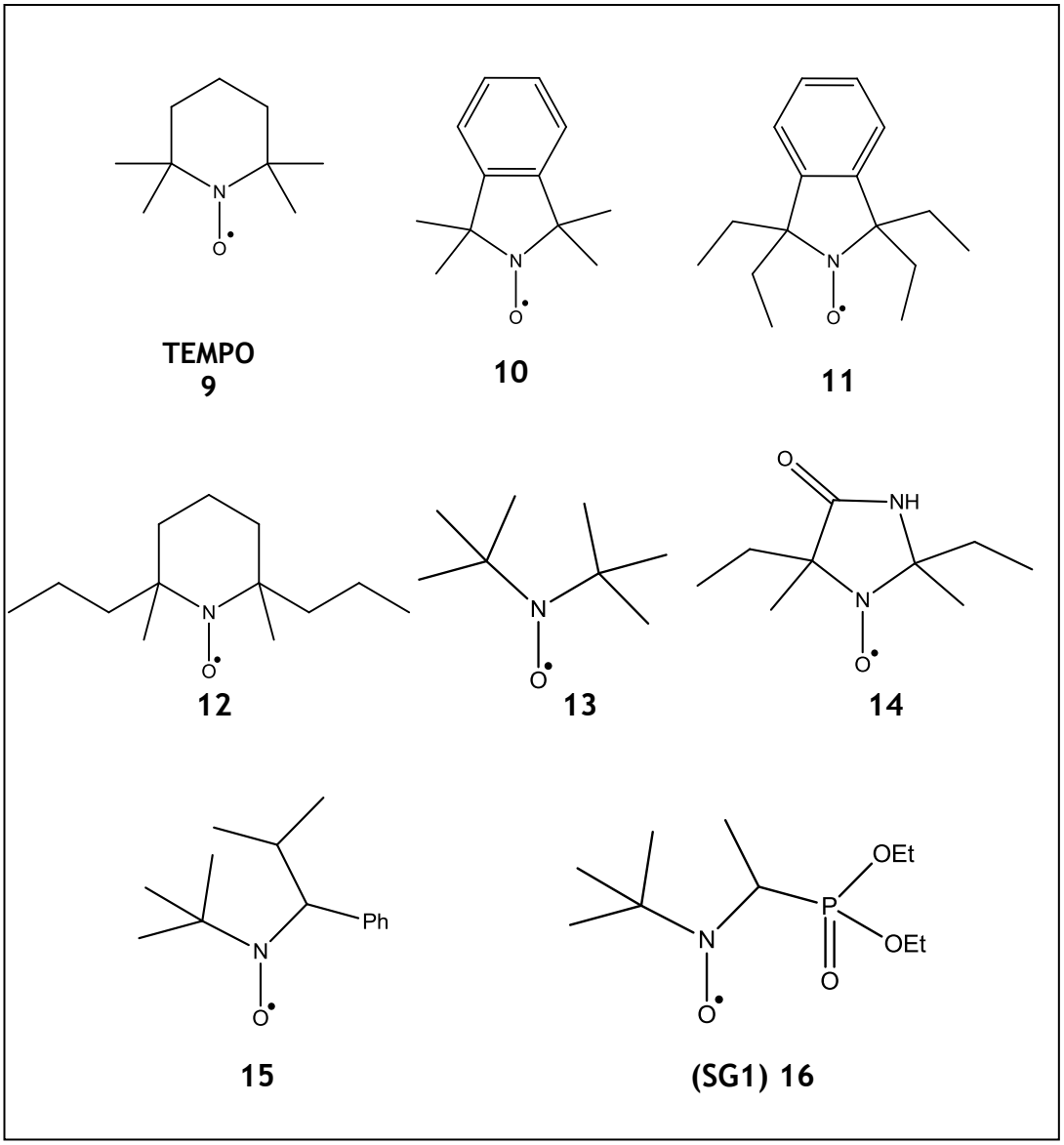

Figure 4.3 Examples of nitroxides used in the NMRP technique

There were two strategies to initiate NMRP. In the first approach, an alkoxyamine is used as the initiator. This approach was used in the original CSIRO work,[69]

however Hawker and coworkers also made use of this method and coined the term 'unimer' (unimolecular initiator) to describe these initiators.[15] In the second approach, the alkoxyamine is formed *in situ* from the nitroxide and radicals generated using a conventional initiator which decomposes in the presence of monomer.

A wide range of alkoxyamines and nitroxides has now been used in NMRP. The important parameters in NMRP are the activation-deactivation equilibrium constant *K*, and the values of K_{act} and K_{deac} (Figure 4.4).[72] Success is also dependent upon the significance of side reactions. In addition, the combination/disproportionation ratio for the reaction of the nitroxide with the propagating radical and the intrinsic stability of the nitroxide under the polymerisation conditions are also important.

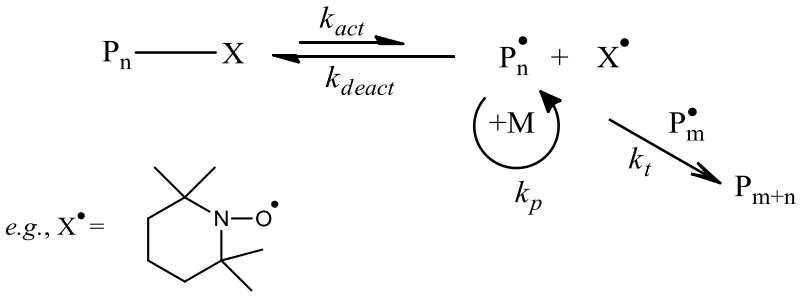

Figure 4.4 Reversible coupling-dissociation mechanism for NMRP[72]

To improve the rate of polymerisation in NMRP, there are two strategies which have been outlined. One is to decrease the rate of side reactions. For example, imidazolinone-derived nitroxides (*e.g.*, **14**) provide better control for polymerisation of (meth)acrylates when compared with TEMPO **9**. The second strategy is to use nitroxides that are somewhat unstable so that an excess of

nitroxide does not build up during polymerisation. Good examples for this latter approach are open-chain nitroxides (**15**) and SG1 (**16**), which are very effective at relatively low temperatures.

Although NMRP is a useful method of controlled radical polymerisation, it is mainly limited to styrene and its functional derivates.[17],[73] The polymerisation of methacrylates and vinyl acetate is still problematic for NMRP because of the increased chain end degradation due to hydrogen transfer.[74]

4.4.2 Atom Transfer Radical Polymerisation (ATRP)

Another controlled/living radical polymerisation technique based on reversible deactivation is atom transfer radical polymerisation (ATRP).[16],[65] It is one of the most successful methods available to polymerise styrenes, (meth)acrylates and a variety of other monomers in a controlled fashion.[75] The development of ATRP is derived from studies of atom transfer radical addition (ATRA) from the 1940s through the 1960s, initially by Kharasch[76] and later improved by Minisci[77] and Asscher & Vofsi.[78]

The mechanism for ATRA involves atom transfer from an organic halide (R-X) to a metal complex, addition to an alkene then atom transfer back to the organic radical (Figure 4.5). Generally, the addition step is rapid and the alkyl radical is more stabilised than the radical adduct $RCH_2^{\bullet}CHY$. As a result, mono-addition products are formed predominately.

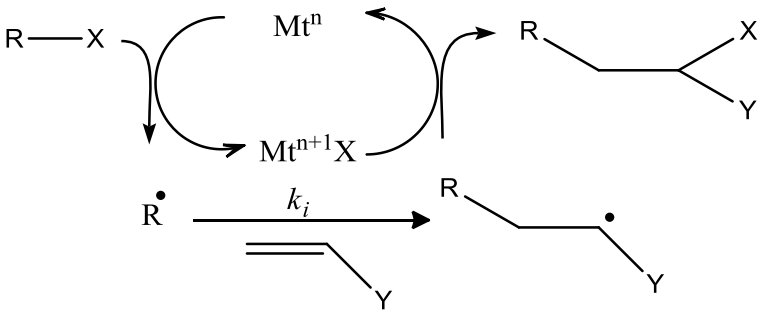

Figure 4.5 Mechanism of ATRA[76]

The first ATRA reactions were conducted in the presence of light or radical initiators. However, these conditions were then replaced by using halogen-transfer agents based on transition metals such as copper, iron, ruthenium and nickel. Large amounts of metal catalysts were needed to form the desired products.[79] The main difference between ATRA and ATRP is that the addition product (RCH_2CHXY, in Figure 4.5) is able to reactivate to a radical ($RCH_2^{\bullet}CHY$) and able to subsequently undergo propagation reactions with an excess of monomer to form a polymeric (or oligomeric) chain. Therefore, equilibrium is established between the dormant alkyl halide molecule and the active radical species, where the latter can propagate, terminate or deactivate.

Sawamoto[80] was the first to introduce a method of trapping radicals using an organometallic complex, and was followed by Matyjazewski[65] with his work on the optimisation of copper complexes in the 1990s. Indeed, a number of other groups, such as Kato *et al.*[81] and Perces & Barboiu,[82] published separately their own work on ATRP.

The ATRP systems are composed of initiator, monomer, catalyst (a transition metal and a suitable ligand) and solvent. Typically, the initiating molecule is an

alkyl halide, functionalized in the alpha position by an ester group or an aromatic ring. The halide is usually bromide or chloride although iodide based initiator has been reported as well. Various vinyl monomers such as styrene,[83],[84],[85] methyl methacrylate,[86],[87] acrylonitriles[88],[89] and acrylamides[90],[91] can be polymerised with ATRP. Certainly, ATRP gives good results for a greater number of monomers than NMRP.

ATRP uses a transition metal-halide as catalyst. Matyjaszewski and coworkers introduced copper (the two oxidation states are Cu^{I} and Cu^{II}) as a catalyst while the Sawamoto group used ruthenium(II)/ruthenium(III) in their work on ATRP. However, copper is the most common metal used in ATRP due to its versatility and relatively low cost. A large number of metal ion catalysts such as manganese, iron, nickel, palladium, rhenium and titanium have also proven successful for various monomers.[92],[93],[94] The metals ions are used in conjunction with a large variety of ligands. The ligands are an important part of the ATRP system. Firstly, ligands solubilise the metal ion in the reaction media. They also control selectivity by steric and electronic effects. Finally, they influenced the redox chemistry of the metal complex. Nitrogen or phosphine-based ligands are by far the most common ligands used in ATRP.[95],[96] It has been shown that polar solvents such as water, greatly affect the rate of the polymerisation.

In ATRP (Figure 4.6), when the halogen (X) in the alkyl halide is abstracted by the metal complex in a reversible redox process, an oxidised species ($Mt^{n+1}X$) and a carbon-centred radical $R^{\bullet}$ are formed. The reverse of this process is extremely fast, meaning that the radical only has a small amount of time to react with monomer before it is converted back into an alkyl halide and the lower oxidation

state metal complex. This radical can either react with the monomer M (generating polymer with the rate constant of propagation k_p), with another radical of the same type (termination with the rate constant k_t) or is rapidly deactivated by reaction with the oxidised transition metal halide complex to reform the lower oxidation state transition metal catalyst. The overall rate of the reaction is highly dependent on the redox potential of the metal complex.

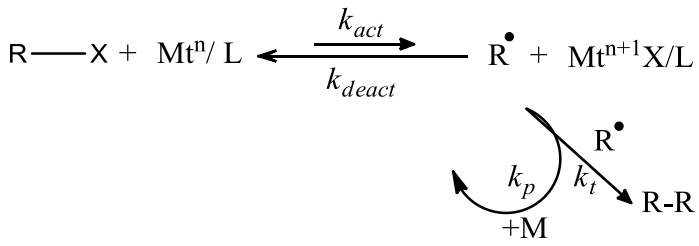

Figure 4.6 General mechanism of ATRP[16]

ATRP has numerous advantages when compared with NMRP. However, one drawback of classical ATRP is the use of high amounts of the catalysts during polymerisation.[65] Although the polymers obtained are well-defined in terms of chain-end functionality and molecular weight distribution, extra purification steps may be needed before being used in many applications.

This is a significant obstacle for the widespread use of ATRP in commercial processes. To alleviate this problem, several studies have been conducted on removing and recycling the catalysts efficiently by using different methods, for example by extraction, immobilisation, precipitation and biphasic systems.[97],[98]

Several promising techniques have been developed by the groups of Matyjaszewski, Percec and Haddleton with the aim of reducing the amounts of the

metal catalysts used, *i.e.*, reverse ATRP,[99] simultaneous reverse and normal initiation (SR&NI),[100] activators generated by electron transfer (AGET),[101] initiators for continuous activator regeneration (ICAR)[84] and activators regenerated by electron transfer (ARGET).[83] Different initiation mechanisms have been studied in detail by changing the polymerisation parameters, (*i.e.*, initiator, transition metal ion and ligands) and all of these systems are based on metal-mediated living radical polymerisation.

Nevertheless, there are currently two major classes of monomer which have not yet been successfully polymerised by the ATRP technique. Acidic monomers are not amendable to this technique since they can protonate ligands and form the corresponding carboxylate salts. The second class of monomers are halogenated alkenes, alkyl-substituted olefins and vinyl esters which are presently resistant to polymerisation by ATRP.

4.4.3 Reversible Addition-Fragmentation Chain Transfer (RAFT) Polymerisation

RAFT polymerisation is certainly the most recent of the CRP systems. It is now recognised as a valuable new method for the synthesis of polymers *via* CRP. It differs from other CRP techniques by its notable versatility towards the types of monomers it can polymerise, including (meth)acrylamides, styrenes, (meth) acrylates, acrylonitrile, vinyl formamide, vinyl chlorides and vinyl acetates, as well as a range of other vinyl monomers.[22],[102]

The first report, in 1988 by Zard and coworkers,[103] proposed xanthate esters and reversible chain transfer as a source of alkyl radicals, and applied it in the

synthesis of monoadducts to a monomer (a maleimide). When the synthesis involves a xanthate RAFT agent, it is called MADIX (macromolecular design by interchange of xanthate).[104] Reversible addition-fragmentation chain transfer chemistry involving xanthate esters has been known to organic chemists for quite some time. A numbers of xanthate applications in organic synthesis have been described in papers and reviewed by the Zard group.[105],[106]

The use of RAFT agents to control polymerisation was first reported by a Commonwealth Scientific and Industrial Research Organisation (CSIRO) group in the mid 1980s.[107],[108],[109] The RAFT agents used included macromonomers, allyl sulfide, allyl bromides, allyl peroxides, vinyl ethers and thioesters. However, in early 1998, living radical polymerisation using thiocarbonylthio RAFT agents was described in a patent.[110] The first paper and conference reports describing the process also appeared in 1998.[111] In January 2005, the first paper on RAFT had received more than 500 citations.

The key feature of the mechanism of RAFT polymerisation is a sequence of addition-fragmentation equilibria. Initiation and radical-radical termination occur as in conventional radical polymerisation. In the early stage of the polymerisation, addition of a propagating radical ($P^{\bullet}_n$) to the thiocarbonylthio compound [RSC(Z)=S] followed by fragmentation of the intermediate radical gives rise to a polymeric thiocarbonylthio compound [$P_nS(Z)C=S$] and a new radical ($R^{\bullet}$). Reaction of the radical ($R^{\bullet}$) with monomer forms a new propagating radical ($P^{\bullet}_m$). Rapid equilibrium between the active propagating radicals ($P^{\bullet}_n$ and $P^{\bullet}_m$) and the dormant polymeric thiocarbonylthio compounds provides equal probability for all chains to grow, and allows for the production of polymers with narrow polydispersity. When

the polymerisation is complete, most of chains retain the thiocarbonylthio end group and can be isolated as stable materials (Figure 4.7).[42]

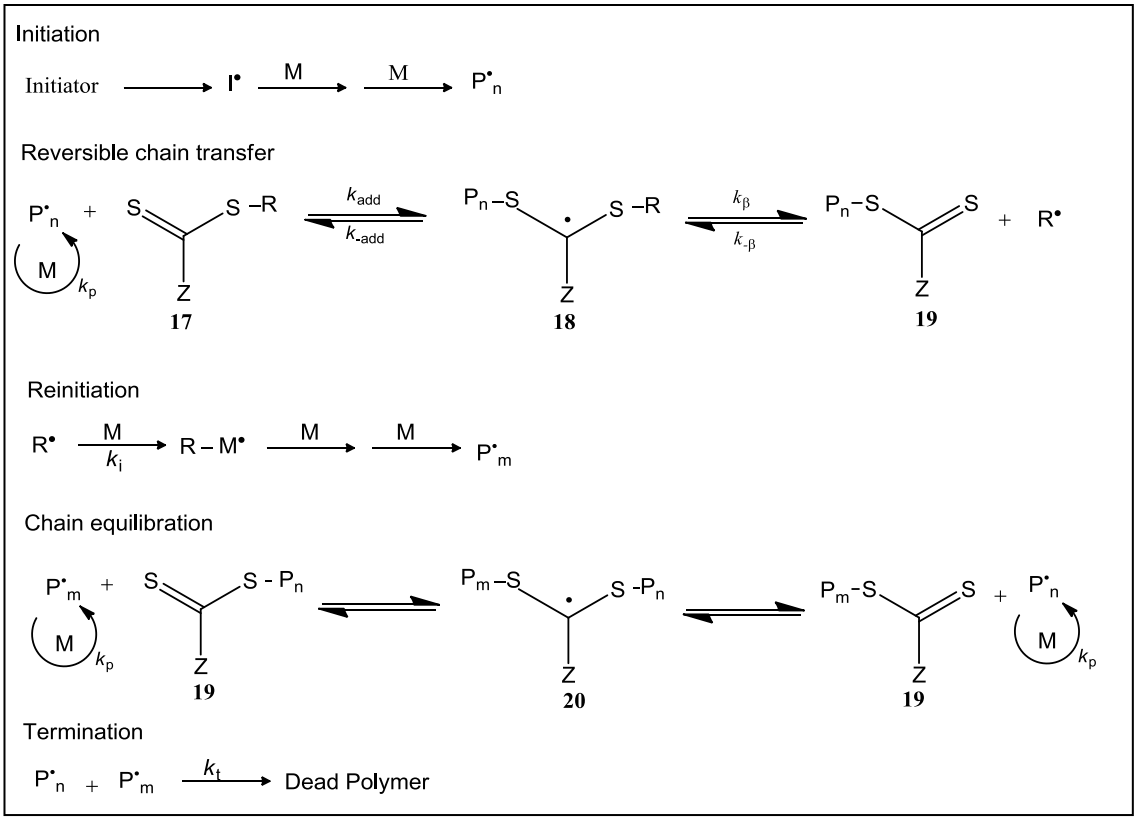

Figure 4.7 Mechanism of RAFT polymerisation

The effectiveness of RAFT agents depends on the monomer being polymerised but also depends strongly on the properties of the free-radical leaving group R and the Z group which can be chosen to activate or deactivate the thiocarbonyl double bond and modify the stability of the intermediate radicals (Figure 4.8).[112],[113]

For an efficient RAFT polymerisation, the RAFT agents should have a reactive C=S double bond, the intermediate radicals should fragment rapidly and give no side reactions, and the expelled radicals should efficiently re-initiate polymerisation. Dithioesters, more specifically dithiobenzoates and dithioacetates, were the first

compounds to be used as RAFT agents.[22] Dithioesters exhibit higher activity than trithiocarbonates, xanthates and dithiocarbamates.

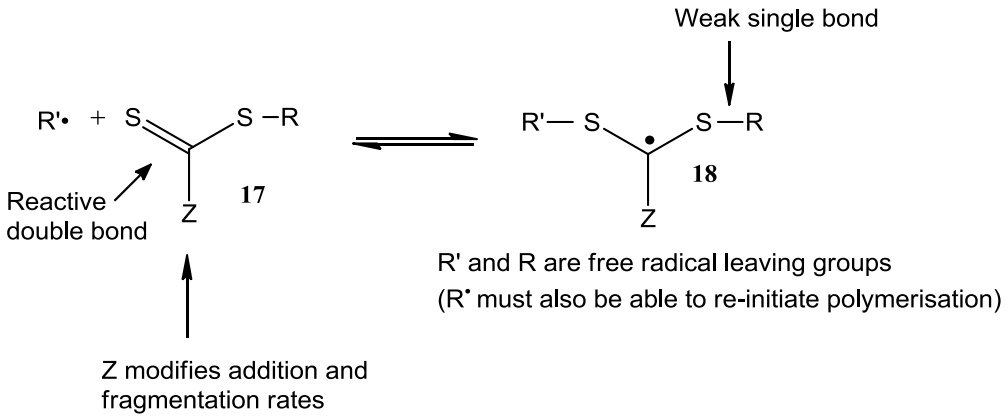

Figure 4.8 Structural features of a thiocarbonylthio RAFT agent and the intermediate formed on radical addition

A summary of RAFT agents of the thiocarbonylthio type and the factors which influence the polymerisation can be found in recent reviews.[114],[115],[116] A guide to the suitability of RAFT agents for controlling polymerisation is shown in Figure 4.9. For Z, addition rates decrease and fragmentation rates increase from left to right. For R, fragmentation rates decrease from left to right. A dashed line shows partial control (*i.e.*, control of molecular weight but poor control of polydispersity or substantial retardation in the case of VAc).[55]

RAFT polymerisation is different to all other techniques of controlled radical polymerisations in that it can be used to polymerise a particularly wide range of monomers, including those which are difficult to polymerise by other CRP methods, such as unprotected (meth)acrylic acids,[117],[118] acrylamide[117],[119] and vinyl acetate.[104] In addition to this, the RAFT technique allows a wide range of polymerisation conditions to be used. It has been successfully conducted over the

temperature range 20 to 150 °C in a broad range of solvents, including water, and using different synthetic methods (emulsion, bulk, suspension, *etc.*).

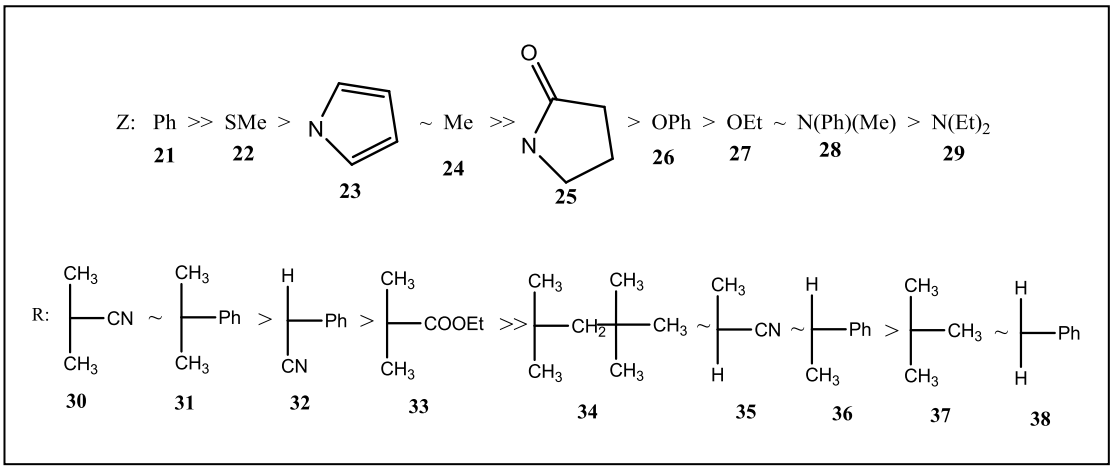

Figure 4.9 Rates of radical addition decrease and rates of fragmentation increase from left to right for RAFT agents with these Z group and order of R group leaving ability in RAFT

The use of the RAFT polymerisation technique allows control over the polymer molecular weight, polydispersity and, in the case of polymer brushes, polymer brush structure and film thickness. Furthermore, the synthesis of functional porous materials and micro-patterned thin films,[120] and the synthesis of comb and graft polymers[121] as well as star polymers, have been reported.

As mentioned earlier, MIPs are normally prepared by free radical polymerisation, which mostly results in polymer networks with heterogeneous structures due in part to the difficulty in controlling the chain propagation and termination steps.[10] In this respect, controlled radical polymerisation techniques are perfectly suited for this purpose. So far, RAFT polymerisation has shown potential in preparing MIPs with improved properties such as faster binding kinetics[122] and tailor-made

structures.[122],[123] However, its application in molecular imprinting is still limited and has not so far been studied in any detail for MIP preparation. Therefore, it is of importance to extend the application of RAFT polymerisation to the synthesis of MIPs with different formats, in order to demonstrate its versatility and take advantage of any benefits which may accrue from the use of CRP.

Recently, a combined use of RAFT polymerisation and precipitation polymerisation has been reported for the preparation of polymer microspheres.[124],[125],[126] In the study, the introduction of the RAFT mechanism into the precipitation polymerisation allowed the easy preparation of functional polymer microspheres with reactive dithioester groups on their surfaces.

In the present study, cyanoisopropyl dithiobenzoate (CPDB) **39** was selected as RAFT agent. This is due to its compatibility with most monomers polymerisable by radical polymerisation and monomers used routinely in MIP syntheses, and it is robust under a wide range of reaction conditions. The chemical structures, particle size and morphology, and template rebinding properties of the MIPs obtained in microsphere and in monolithic format were established, and they were compared with those MIPs prepared *via* conventional free radical polymerisation. In addition, MIPs with reactive dithioester groups on their surfaces are useful for further surface chemical modification, which has also been discussed as a means to prove the 'livingness' of the RAFT polymerisation.

4.5 Experimental Section

4.5.1 Chemicals and materials

Potassium ferricyanide (99.99 %), carbon disulfide (anhydrous, ≥99.0 %), diethyl ether (CHROMASOLV®Plus for HPLC, ≥99.9 %), ethyl acetate (anhydrous, 99.8 %), phenylmagnesium bromide (1.0 M in THF) and caffeine (99 %) were purchased from Sigma Aldrich. Petroleum ether 40-60 (anhydrous, ≥99.0 %) was purchased from Riedel-de-Haë n. Silica gel (for flash chromatography) was purchased from BDH. Ethylene glycol dimethacrylate, EGDMA (98.0 %), 2,2'-azobisisobutyronitrile, AIBN (98 %), chloroform (anhydrous, ≥99.0 % contains 0.5-1.0 % ethanol as stabilizer), methacrylic acid, MAA (99.0 %), acetonitrile (ReagentPlus®, 99.0 %), THF and acetone (anhydrous, 99.8 %) were purchased from Aldrich. Hydroxyethyl methacrylate, HEMA (≥ 99 %) was purchased from Aldrich and *N,N*-dimethyl formamide, DMF (anhydrous, 99.8 %) was purchased from Sigma-Aldrich.

EGDMA (98-100 °C/5 mmHg) and MAA (34 °C/5 mmHg) were dried over anhydrous sodium sulfate and distilled under vacuum prior to use. AIBN was recrystallised from methanol at low temperature. All other chemicals were used as received.

4.5.2 Synthesis of Cyanoisopropyl dithiobenzoate (CPDB)

CPDB **39** (Figure 4.10) was synthesised based on a literature procedure.[48],[127]

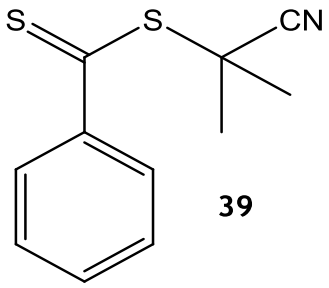

39

Figure 4.10 Chemical structure of CPDB **39**

a) Synthesis of bis(thiobenzoyl)disulfide

A two-necked, round-bottomed flask containing a magnetic stirring bar was oven-dried prior to use and fitted with a condenser. PhMgBr, 1.0 M in THF (32 mL, 32.0 mmol) was added *via* cannula to the flask containing dried THF (288 mL) and cooled to ~2 °C over an ice-bath. CS_2 (2.32 mL, 38.4 mmol) was added dropwise *via* an oven-dried syringe and the contents of the flask were brought slowly to 45 °C under stirring, and maintained at this temperature for four hours. The contents of the flask were poured onto an ice slurry to quench the reaction and give dithiobenzomagnesium bromide as a dark brown solution. The dark brown solution was washed three times with diethyl ether (3x50 mL). A final aliquot of ether (50 mL) was added to the solution, which was then acidified with 37 % aqueous HCl until the aqueous layer turned pale pink and the ethereal layer became very dark purple.

Extraction with ether was repeated a further two times to obtain dithiobenzoic acid. The combined organic layers were then washed twice with deionised water (120 mL), and 1.0 M NaOH (240 mL) used to extract sodium dithiobenzoate into the aqueous layer. The base extraction was repeated a further two times, affording sodium dithiobenzoate as a very dark purple solution.

Potassium ferricyanide (13.17 g, 40.0 mmol) was dissolved in deionised water (200 mL), and added dropwise over one hour to a vigorously stirred solution of sodium dithiobenzoate. The resultant purple/pink precipitate [bis(thiobenzoyl)disulfide] was filtered under reduced pressure and washed with deionised water. The solid product was dried overnight *in vacuo* at 40 °C and used directly without any further purification (2.341 g, 42 %). ^{1}H NMR, (500 MHz, δ ppm, $CDCl_3$): 8.10 (d, 4H,

J = 7.5 Hz, *o*-ArH), 7.60 (m, 2H, *J* = 7.5 Hz, *p*-ArH), 7.46 (dd, 4H, *J* = 7.5 Hz, *m*-ArH), see Appendix 1.

b) Synthesis of CPDB

Ethyl acetate (50 mL) was added to a mixture of 2,2'-azobisisobutyronitrile (1.574 g, 9.6 mmol) and bis(thiobenzoyl)disulfide (2.000 g, 6.3 mmol) and allowed to reflux for 18 hours under a nitrogen atmosphere. The volatiles were removed by rotary evaporation and the crude product purified by column chromatography, using silica gel as the stationary phase with petroleum ether 40-60/ethyl acetate (19/1, v/v) as the mobile phase. The red-coloured fractions with an R_f value of 0.29 were pooled and CPDB obtained as a dark purple coloured, viscous oil after drying under reduced pressure (2.508 g, 90 %). ^{1}H NMR (500 MHz, δ ppm, $CDCl_3$): 1.95 (s, 6H, 2xCH_3), 7.90 (d, 2H, *J* = 7.5 Hz, *o*-ArH), 7.50 (m, 1H, *J* = 7.5 Hz, *p*-ArH), 7.40 (t, 2H, *J* = 7.5 Hz, *m*-ArH). ^{13}C NMR (500 MHz, δ ppm, $CDCl_3$): 26.5 (CH_3), 41.7 [**C** (CN)], 120.0 (CN), 126.6, 128.5, 132.9, and 144.6 (ArC). The purity of CPDB was estimated by ^{1}H NMR spectroscopy to be > 90 %. The ^{1}H NMR and ^{13}C NMR spectra of CPDB (Appendix 2 and Appendix 3, respectively) were identical to those reported in the literature.[48],[127]

4.5.3 Preparation of caffeine-imprinted polymers *via* RAFT polymerisation

a) Monolithic polymers (P1 and P2)

The MIP for caffeine was prepared in a fashion similar to the general procedure described by Philip and Mathew[128] and Wang.[129] Caffeine (0.113 g, 0.5 mmol), MAA (0.199 g, 2.3 mmol), EGDMA (2.300 g, 11.6 mmol) and AIBN (0.042 g, 0.25 mmol) were dissolved in chloroform (4 mL) in a thick-walled glass Kimax culture tube together with CPDB (0.111 g, 0.5 mmol). The solution was deoxygenated by

sparging with oxygen-free nitrogen for 10 minutes while cooling in an ice-bath. The tube was sealed under nitrogen by means of a screw-cap and placed in an oil-bath for 48 hours with the temperature maintained at 60 ºC.

The caffeine-imprinted polymer, **P1,** was obtained as a monolith; the monolith was subsequently crushed, mechanically ground and wet-sieved using acetone. Particles of < 25 µm were collected after sedimentation (3x) from acetone. In order to remove traces of unreacted monomers and the template, the polymer was extracted overnight in a Soxhlet apparatus using methanol, and then dried at 40 ºC under vacuum. A non-imprinted control polymer, **P2,** was prepared in the same manner as **P1** but in the absence of caffeine (**P1**; 1.611 g, 64 % yield of particles of size < 25 µm, **P2**; 1.783 g, 71 % yield of particles of size < 25 µm).

b) Polymer Microspheres (P5 and P6)

Polymers were prepared by precipitation polymerisation *via* a Kugelrohr-based method. Caffeine (0.165 g, 0.85 mmol) was dissolved in a mixture of acetonitrile and toluene (3:1 v/v, 57/19 mL) in a 250 mL Kugelrohr flask. This was followed by the addition of MAA (0.292 g, 3.4 mmol), DVB-80 (2.208 g, 17.0 mmol) and AIBN (0.183 g, 1.12 mmol). Lastly CPDB (0.323 g, 1.46 mmol) was added.

The solution was deoxygenated by bubbling oxygen-free nitrogen gas through the solution for about 20 minutes at ice-bath temperature, and the reaction flask then sealed under nitrogen. Then the reaction flask was placed in a temperature-controlled Kugelrohr apparatus. The temperature was ramped from room temperature to 70 °C over a period of approximately 2 hours, and then kept constant at 70 °C for 48 hours thereafter.

After this time, the reaction flask was cooled to room temperature. A sample of the polymer was spotted onto a microscope slide and the bead size estimated under an optical microscope. The polymer was filtered off on a polyamide membrane (0.2 μm) filter, washed with acetonitrile (2 x 20 mL) and then methanol (20 mL).

The caffeine-imprinted polymer, **P5,** was transferred to a pre-weighed vial and dried to constant mass *in vacuo* at 40 °C for 24 hours. A non-imprinted control polymer, **P6,** was prepared in the same manner as **P5** but in the absence of caffeine (**P5**; 1.318 g, 53 %, **P6**; 1.730 g, 69 %).

4.5.4 Preparation of caffeine-imprinted polymers and non-imprinted polymers *via* conventional free radical polymerisation

a) Monolithic polymers (P3 and P4)

The caffeine-imprinted polymer synthesised *via* conventional free radical polymerisation, **P3,** was prepared in the same manner as **P1** but in the absence of CPDB (See Section 4.5.3a). A non-imprinted control polymer, **P4,** was prepared in the absence of both CPDB and caffeine (**P3**; 1.929 g, 77 % yield of particles of size < 25 μm, **P4**; 1.819 g, 73 % yield of particles of size < 25 μm).

b) Polymer Microspheres (P7 and P8)

The caffeine-imprinted polymer synthesised *via* conventional free radical polymerisation, **P7,** was prepared in the same manner as **P5** but in the absence of CPDB (See Section 4.5.3b). A non-imprinted control polymer, **P8,** was prepared in the absence of both CPDB and caffeine (**P7**; 2.189 g, 88 % and **P8**; 2.246 g, 90 %).

4.5.5 Post-Polymerisation Chemical Modifications of polymers

Polymer P2 was used in the post-polymerisation chemical modification experiments.[130],[131] Polymer P2 (50 mg), HEMA (500 mg) and AIBN (7 mg) were added to DMF (8 mL) in a Radleys Carousel reaction vessel equipped with magnetic stirrer.

The mixture was sparged with oxygen-free nitrogen at 0 °C for 5 min and then replaced into the Radleys Carousel reaction station. The polymerisation was carried out for 24 hours at 70 °C under a nitrogen atmosphere. After this time, the product was isolated by centrifugation and washed with methanol (2 x 10 mL), a centrifuge being used due to the low mass of product. Polymer **P2g** ("g" implies grafting) was transferred to a pre-weighed vial and dried to constant mass in *vacuo* at 40 °C for 24 hours. In a control experiment, Polymer **P4** was treated in the same manner as **P2** to give Polymer **P4g** (**P2g**; 0.078 g, **P4g**; 0.055 g).

4.5.6 Characterisation Techniques

^{1}H NMR spectra were recorded on a Bruker AV-500 NMR spectrometer at 500 MHz using $CDCl_3$ as solvent. ^{13}C NMR spectra were recorded on a Bruker AV-500 NMR spectrometer at 100 MHz with $CDCl_3$ as solvent.

Fourier Transform Infrared (FTIR) spectra of the polymers were acquired using a Spectrum One, FTIR Spectrometer from Perkin Elmer with Spectrum V3.02 as the software. The polymers were prepared as dispersions in KBr.

Nitrogen sorption porosimetry measurements were performed on an ASAP 2010 Accelerated Surface Area and Porosimetry Analyzer (Micromeritics Instrument

Corporation, Norcross, GA). Samples were dried at 40 ºC in *vacuo* overnight. Prior to measurement, 300 – 400 mg of the samples were placed in a dry BET tube and attached to the instrument, then degassed overnight at 100 ºC. Nitrogen gas was introduced to push the particles to the bottom of the tube. A slow vacuum to 500 mmHg and then fast vacuum to 100 mmHg pressure was applied in order to remove all gas molecules and remaining moisture from the sample. The sample was then reweighed and the saturation pressure, free space and quantity of gas adsorbed by the sample were measured. The quantity of gas adsorbed was calculated by measurement of the change in pressure of the system as the gas expands into the sample tube during adsorption.

The particle size and particle size distributions of the polymers were determined from scanning electron microscope images (Spectro Scan S90).

Elemental microanalyses of the polymers were carried out using a PerkinElmer 2400 Series II CHNS/O Elemental Analyzer, while halogen determination was carried out by a titration method.

4.5.7 Chromatographic Evaluation of Polymers

Column packing: An Alltech Model 1666 Slurry Packer was used to pack the polymers into empty stainless steel HPLC columns using procedures recommended by the manufacturer. The HPLC columns were 0.46 i.d x 15 cm in dimension and were fitted with 0.2 µm frits. Approximately 1.5 g of polymer was sufficient to pack each column. Acetone was used as the slurrying and packing solvent. The columns were packed at an air pressure of 15 psi and a solvent pressure of 500 psi (packing time per column ~ 10 minutes).

Column Washing: The columns were washed off-line using a Gilson Model 303 HPLC pump using a mixture of acetonitrile and acetic acid (95/5, v/v) at a flow rate of 0.3 mL/min and a pressure of 120 psi. Column P4 was washed first, followed by the P3 column. Thereafter, column P2 was washed followed by the P1 column. This washing arrangement (sequence) was to avoid the possibility of any cross-contamination with template and RAFT agent.

Analysis of the packed columns was carried out on a Waters HPLC system. The system comprised a Waters 1535 binary pump, a Waters 717 autosampler and a Waters 2487 Dual Wavelength absorbance detector. The software used for operation of the system and data handling was Waters Breeze.

The analyses were performed under isocratic conditions. All the procedures were carried out at ambient temperature. The UV detection wavelength was set at 274 nm. Acetone was used as the void marker and the flowrate was set at 0.5 mL/min with acetonitrile as mobile phase. 10 µL of a 10 mM standard solution of analyte in chloroform was injected onto each column and retention factors (*k'*) calculated according to standard chromatographic theory (Eq. 4.1).

$$k' = (t_r - t_o)/t_o \quad \text{---------- 4.1}$$

where t_0 and t_r are the retention times of the void marker and the analyte, respectively. The imprinting factor (IF) was calculated from the retention factors obtained for the analyte on the MIP and NIP columns (Eq. 4.2).

$$IF = k'_{MIP}/k'_{NIP} \quad \text{---------- 4.2}$$

The theoretical plate number, N, is a concept giving a quantitative measure of the efficiency of a column. The N value calculated for theoretical plates is an indirect measure of peak width for a peak at a specific retention time, as expressed by Equation 4.3.

$$N = 5.54 [t_r/W_{0.5}]^2 \quad \text{---------- 4.3}$$

where N is the number of theoretical plates, t_r is the retention time of the analyte and $W_{0.5}$ is the peak width at half height, calculated for each analyte using classical chromatographic theory assuming ideal peaks. Columns with high plate numbers are considered to be more efficient (*i.e.*, higher column efficiency) than columns with lower plate numbers. A column with a higher number of theoretical plates will have a narrower peak at a given retention time than a column with a lower number of theoretical plates.

4.6 Results and Discussion

As outlined in the Introduction, the main objective of the work presented in this chapter was to explore the potential benefits in applying controlled radical polymerisation techniques towards the synthesis of MIPs. The polymerisation method of choice in the present work was RAFT; caffeine **42** was selected as a model template for the purposes of the study and control polymers prepared using FRP.

4.6.1 Synthesis of RAFT agent, CPDB

The RAFT agent, CPDB **39**, was synthesised successfully according to the method of Liu *et al.*[127] CPDB **39** was selected as the RAFT agent because it has been used

successfully for many monomers such as methacrylates and styrene, and was expected to be compatible with the monomers used to imprint caffeine.[48],[127],[132]

This synthesis of CPDB **39** was partitioned into two stages (Figure 4.11). First of all, reaction of phenylmagnesium bromide **41** with carbon disulfide followed by a basic work-up and oxidation with potassium ferricyanide gave bis(thiobenzoyl) disulfide **40**.

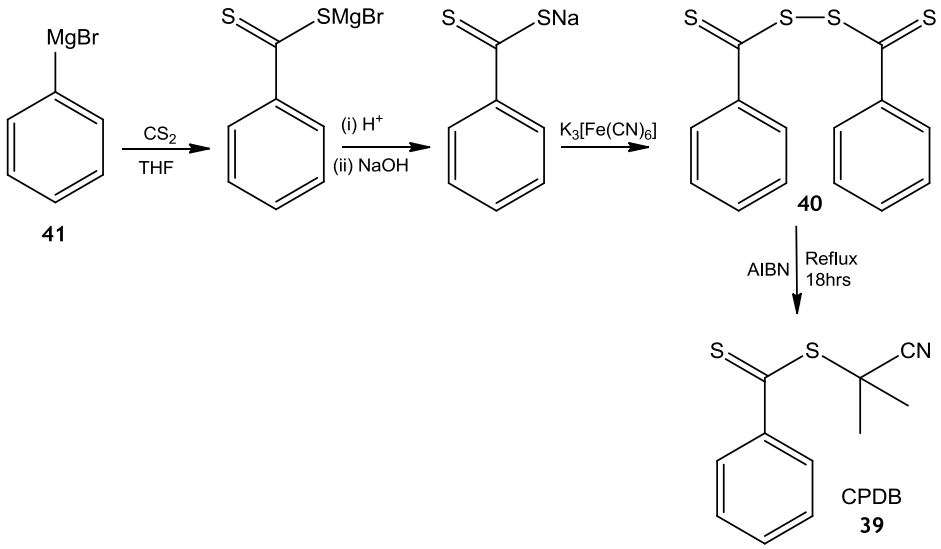

Figure 4.11 Synthesis route to the RAFT agent, CPDB

Bis(thiobenzoyl)disulfide **40** is a stable intermediate (stores well in the freezer) and is a useful precursor for the production of many different RAFT agents. Thermal treatment of bis(thiobenzoyl)disulfide **40** in the presence of AIBN gave CPDB **39** as a viscous, dark purple coloured oil. The ^{1}H NMR and ^{13}C NMR spectra (as shown in Appendix 2 and 3) were in agreement with the literature data.[48],[127]

4.6.2 Synthesis and characterisation of MIPs and NIPs

a) Monolithic Polymers

The MIPs (P1 and P3) and NIPs (P2 and P4) were synthesised successfully in the form of monoliths, using two different polymerisation approaches: RAFT polymerisation (P1 and P2) and conventional FRP (P3 and P4). The polymers were synthesised on a 2.5 g monomer scale. Polymers P1 and P2 were obtained as pink/purple coloured optically-transparent monoliths whereas P3 and P4 were obtained as white, opaque monoliths. In each case, the polymer monolith was ground, sieved and sedimented to deliver polymer particles suitable for packing into LC columns (particle size < 25 μm).

The size and shape of the various polymer particles were analysed by SEM. As expected for polymer particles produced through the mechanical grinding of monoliths, the particles obtained were irregularly shaped (Figure 4.12). The particle sizes were defined by the grinding, sieving and sedimentation processes. Only particles with sizes of <25 μm were collected and used in this study.

P1 and P2 had the typical appearance of a gel-type polymer when in the dry state in that they were optically transparent. In contrast, P3 and P4 scattered white light, suggestive of well-developed pore structures even when dry. These observations were confirmed by nitrogen sorption porosimetry experiments; the specific surface areas of P1 and P2 in the dry state were < 5 $m^2 g^{-1}$. For P3 and P4, the specific surface areas were 270 and 320 $m^2 g^{-1}$, respectively. Furthermore, the average pore diameters of P1, P3 and P4 (9.09, 7.46 and 7.56 nm, respectively), and the specific pore volumes of P1, P3 and P4 (0.01, 0.50 and 0.61 $cm^3 g^{-1}$, respectively) confirmed the fact that the presence of RAFT agent in the P1

polymerisation had a profound impact upon the morphology of the product. Unsurprisingly, due to the low specific surface area obtained for P2, the values of average pore diameter and specific pore volume could not be recorded for P2.

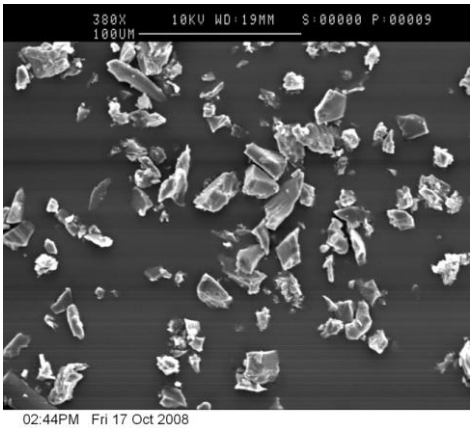

P1

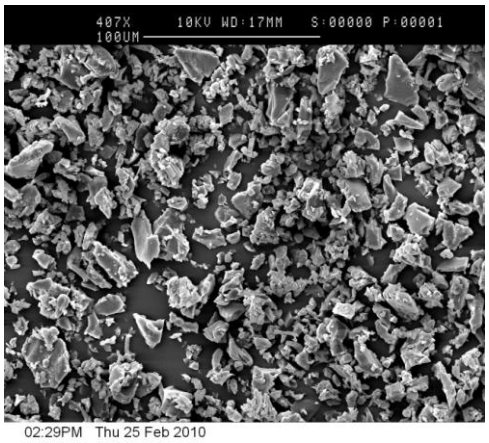

P2

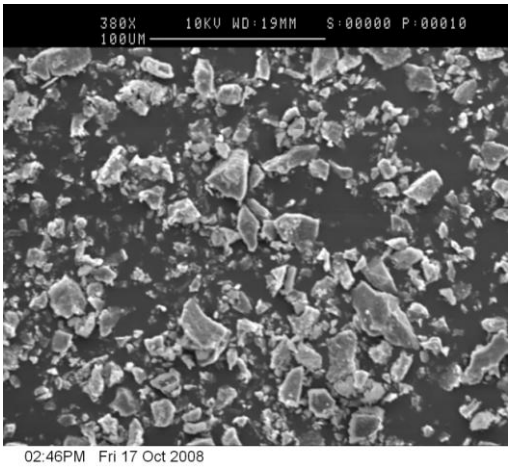

P3

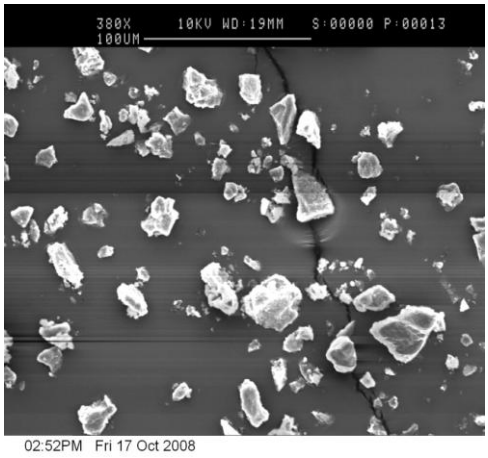

P4

Figure 4.12 Scanning electron microscopy (SEM) images of polymer particles which were prepared initially in monolithic form before being ground, sieved and sedimented to deliver polymer particles with size < 25 μm. (P1 and P2 were prepared *via* RAFT polymerisation; P3 and P4 were prepared *via* conventional FRP)

Elemental microanalysis of carbon, hydrogen, nitrogen and sulfur for the MIPs and NIPs were determined by using a PerkinElmer 2400 Series II CHNS/O Elemental Analyzer, while oxygen was calculated by difference. The results are summarised in Table 4.1

Table 4.1 Elemental Composition of Polymers prepared *via* CRP (P1 and P2) and FRP (P3 and P4) in monolithic form

Polymer Code	C (wt %)		H (wt %)		N (wt %)		S (wt %)		O (wt %) (by difference)	
	theory	#Exp.	theory	Exp.	theory	Exp.	theory	Exp.	theory	Exp.
P1 (MIP)	59.8	58.0	7.0	7.2	0.3	trace	1.2	1.9	31.7	32.9
P2 (NIP)	59.8	58.7	7.0	6.3	0.3	trace	1.2	0.9	31.7	34.1
P3 (MIP)	57.3	57.8	6.8	7.0	0	≠N.D	0	N.D	35.9	35.2
P4 (NIP)	57.3	57.5	6.8	7.2	0	N.D	0	N.D	35.9	35.3

Exp. – Results from experiment

≠ N.D – not determined

The results show that the compositions of polymers are corresponding well to the composition of the monomer feed. As expected, polymers prepared *via* RAFT polymerisation (P1 and P2) contained sulfur.

b) Polymer Microspheres

MIPs (P5 and P7) and NIPs (P6 and P8) in bead form were synthesised successfully *via* RAFT and conventional FRP, using precipitation polymerisation. The polymers were synthesised on the same scale as the monoliths *i.e.,* 2.5 g of monomer. P5 - P8 were obtained as beads with diameters around ~ 5 μm. The obvious visual difference between polymers P5 and P6 and polymers P7 and P8 was the pink/purple colouration of P5 and P6 arising from the RAFT agent.

SEM analyses were carried out; P5 – P8 were all beaded and the particles sizes were around 5 μm in each case. However, the polymers prepared *via* RAFT polymerisation had the appearance of a gel-type polymer when in the dry state; they also were optically transparent (Figure 4.13). Polymers P7 and P8 were white and opaque in the dry state. Results from the nitrogen sorption porosimetry experiments showed that the beaded polymers had similar specific surface areas to the monolithic polymers, especially the beads which had been prepared *via* RAFT polymerisation. The specific surface areas of P5 and P6 in dry state were < 5 m^2 g^{-1}. For P7 and P8, the specific surface areas were 570 and 590 m^2 g^{-1}, respectively, indicative of a well-developed pore structures. Moreover, the average pore diameters for P5, P7 and P8 were 6.07, 2.21 and 2.17 nm, respectively, and the specific pore volumes were 0.006, 0.32 and 0.31 cm^3 g^{-1}, respectively. The average pore diameter and specific pore volume for polymer P6 could not be computed, as one would expect for a non-porous polymer. The

results obtained support the fact that the presence of RAFT agent has a profound impact upon the morphology of the polymer product in the case of both monolithic materials and polymer microspheres.

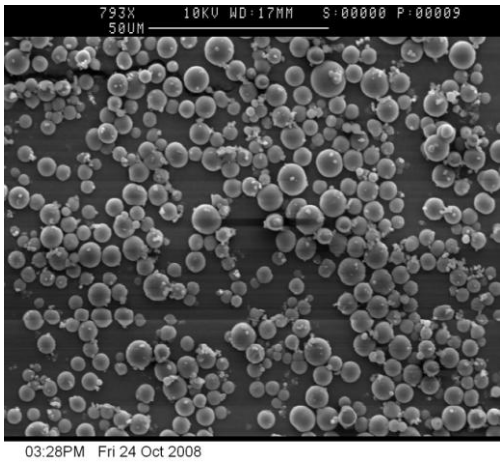

P5

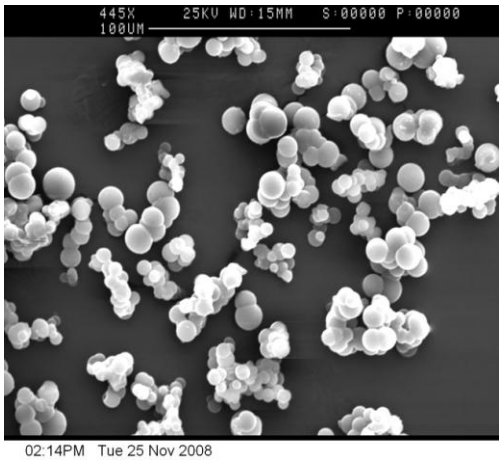

P6

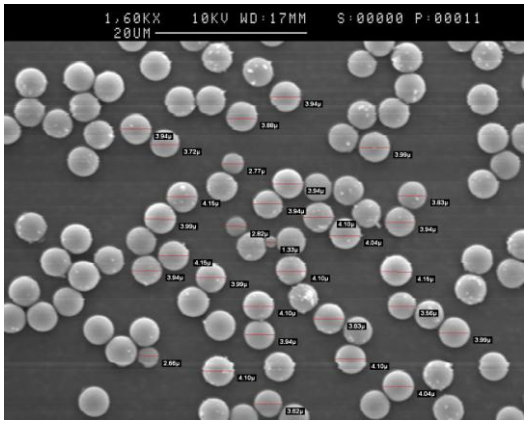

P7

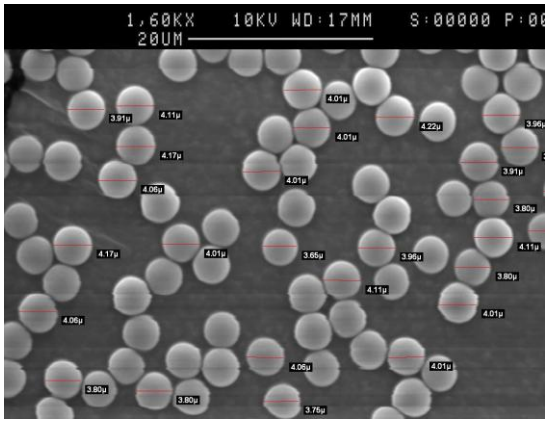

P8

Figure 4.13 Scanning electron microscopy (SEM) images of polymers prepared in bead form using precipitation polymerisation. P5 and P6 were prepared *via* RAFT polymerisation; P7 and P8 were prepared *via* conventional FRP

Elemental microanalysis is a valuable analytical method for obtaining information concerning the elemental composition of a sample. It not only determines what elements are present (qualitative analysis) but can be used to quantify the percentage of the different elements present (quantitative analysis). The elemental microanalysis data for the polymer beads is summarised in Table 4.2.

Table 4.2 Elemental Composition of Polymers prepared *via* CRP and FRP in bead form by precipitation polymerisation

Polymer Code	C (wt %)		H (wt %)		N (wt %)		S (wt %)		O (wt %) (by difference)	
	theory	#Exp.	theory	Exp.	theory	Exp.	theory	Exp.	theory	Exp.
P5 (MIP)	85.1	80.6	7.5	7.3	0.3	1.2	1.7	1.7	5.4	9.2
P6 (NIP)	85.1	81.9	7.5	7.4	0.3	1.3	1.7	0.8	5.4	8.6
P7 (MIP)	82.7	84.5	7.3	7.6	0	≠N.D	0	N.D	10.0	7.9
P8 (NIP)	82.7	85.4	7.3	7.7	0	N.D	0	N.D	10.0	6.9

Exp. – Results from experiment

≠ N.D – not determined

The results show that sulfur has been incorporated into those polymers prepared by RAFT polymerisation (P5 and P6). Furthermore, the composition of the polymers is rather similar to that predicted from the monomer feed composition.

4.6.3 Structural characterisation of the polymers

a) Monolithic Polymers

The monolithic polymers (P1 – P4) were characterised by FTIR spectroscopy. Unsurprisingly given the fact that the same comonomers were used in the production of P1 – P4, the results show that the MIPs prepared *via* RAFT polymerisation and conventional FRP have rather similar FTIR spectra (Figure 4.14-4.15). The presence of the three bands at 1731 cm^{-1} (C=O ester stretch), 1262 cm^{-1} and 1160 cm^{-1} (C-O ester stretching) support the presence of EGDMA residues in the MIPs. The signal at 1640 cm^{-1} is ascribed to a C=C stretch from pendant vinyl groups. It is very significant that this signal is more intense for those polymers synthesised in the presence of the RAFT agent (P1 and P2), as this suggests that P1 and P2 are of lower crosslink density than P3 and P4, which is in agreement with the visual appearances of the polymers and the nitrogen sorption porosimetry data.

The broad band at around 3430–3600 cm^{-1} can be ascribed to the CO_2H group from MAA residues (O-H stretch). The characteristic peaks corresponding to C=C stretching (1456-1480 cm^{-1}) were observed for P1, P2, P3 and P4. However, the signal ascribed to the thiocarbonyl group can only be seen for P1 and P2 (1050-1200 cm^{-1}); as expected, this is a very weak signal. Figures 4.14 and 4.15 show the FTIR spectra of the MIPs and NIPs, respectively, of polymers prepared *via* either RAFT polymerisation or conventional FRP.

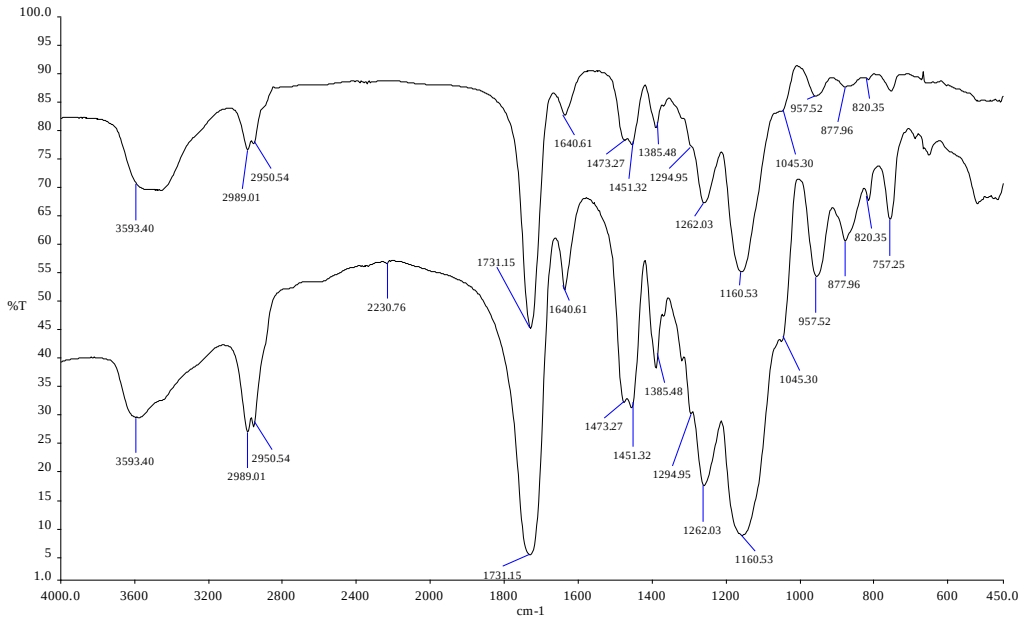

Figure 4.14 FTIR spectra of MIPs; P1 synthesised *via* RAFT polymerisation (lower) and P3 synthesised *via* conventional FRP (upper)

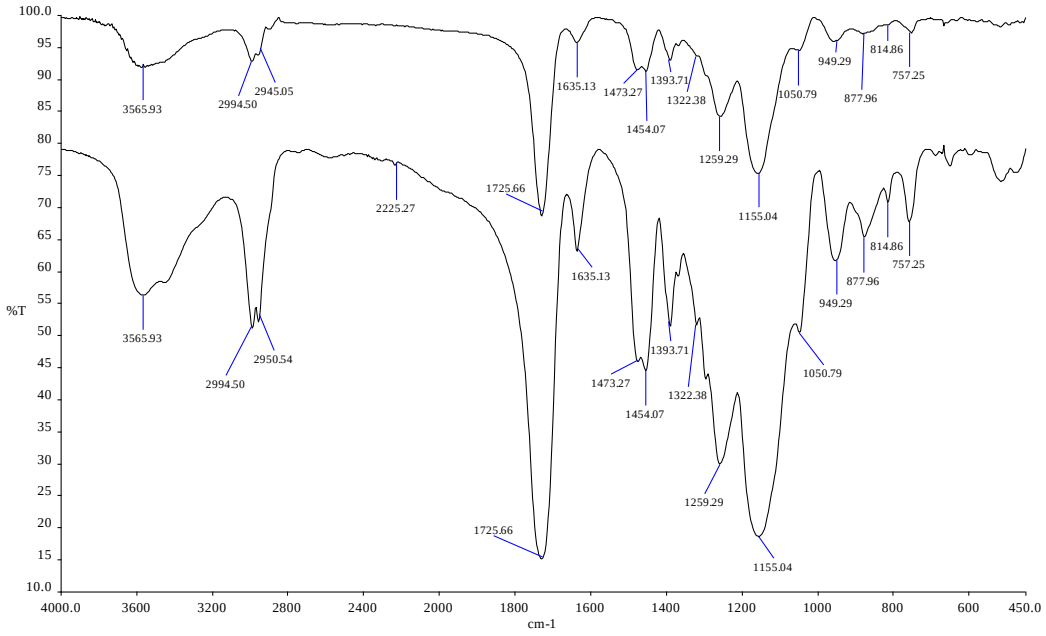

Figure 4.15 FTIR spectra of NIPs; P2 synthesised *via* RAFT polymerisation (lower) and P4 synthesised *via* conventional FRP (upper)

b) Polymer Microspheres

The polymer beads obtained (P5 - P8) were also characterised by FTIR spectroscopy (Figure 4.16-4.17). There were significant differences between the FTIR spectra of polymers prepared in monolithic and beaded form because DVB-80 rather than EGDMA is used as crosslinker in the production of polymer beads produced *via* precipitation polymerisation. However, the functional group derived from the RAFT agent (*i.e.,* the thiocarbonyl group) can still be seen clearly in the FTIR spectra of the polymers synthesised by RAFT polymerisation (P5 and P6) at wavelength 1050-1200 cm^{-1}.

The FTIR spectra of MIPs prepared *via* RAFT polymerisation (P5) and conventional FRP (P7) are similar. The presence of a small band at around 1630 cm^{-1} (C=C stretch from pendant vinyl groups) is more intense for polymers P5 and P6 than for P7 and P8, which suggests yet again that the crosslink density of polymer produced through RAFT polymerisation is lower than the crosslink density of polymer produced by FRP.

The broad band at around 3430-3600 cm^{-1} can be ascribed to the CO_2H group from MAA residues (O-H stretch), as seen previously for the monolithic polymers. The characteristic peaks corresponding to C=C stretching (1440-1500 cm^{-1}) and the C=O stretching vibration band of MAA (1695-1700 cm^{-1}) were observed for P5, P6, P7 and P8. The signal ascribed to the thiocarbonyl group can be seen clearly for P5 and P6 (1050-1200 cm^{-1}) but, as expected, not for P7 and P8. Figures 4.16 and 4.17 show the FTIR spectra of the MIPs and NIPs, respectively, of polymers prepared *via* either RAFT polymerisation or conventional FRP.

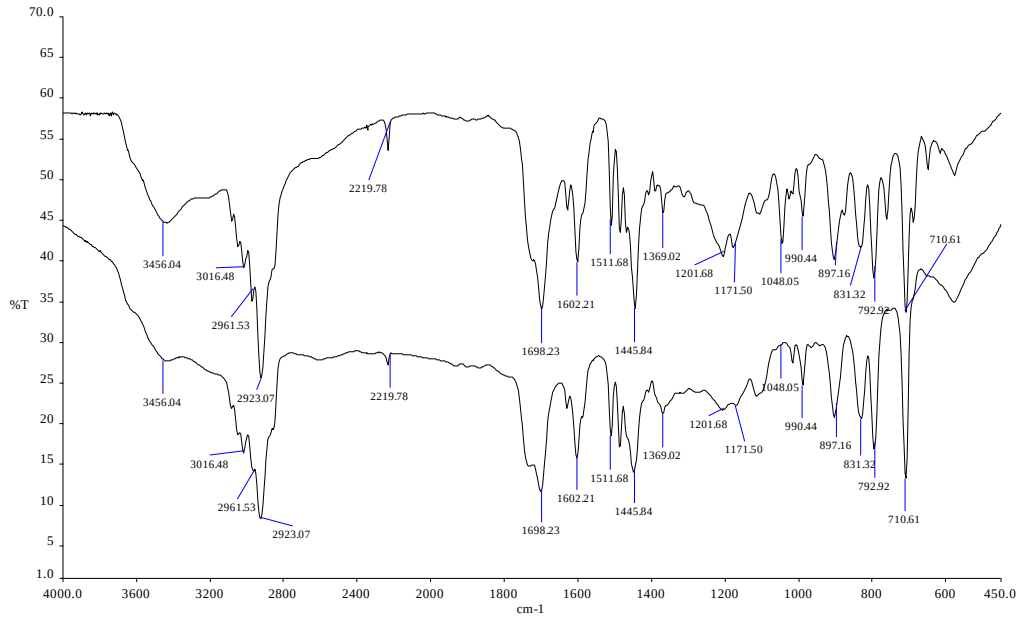

Figure 4.16 FTIR spectra of MIPs; P5 synthesised *via* RAFT polymerisation (upper) and P7 synthesised *via* conventional FRP (lower)

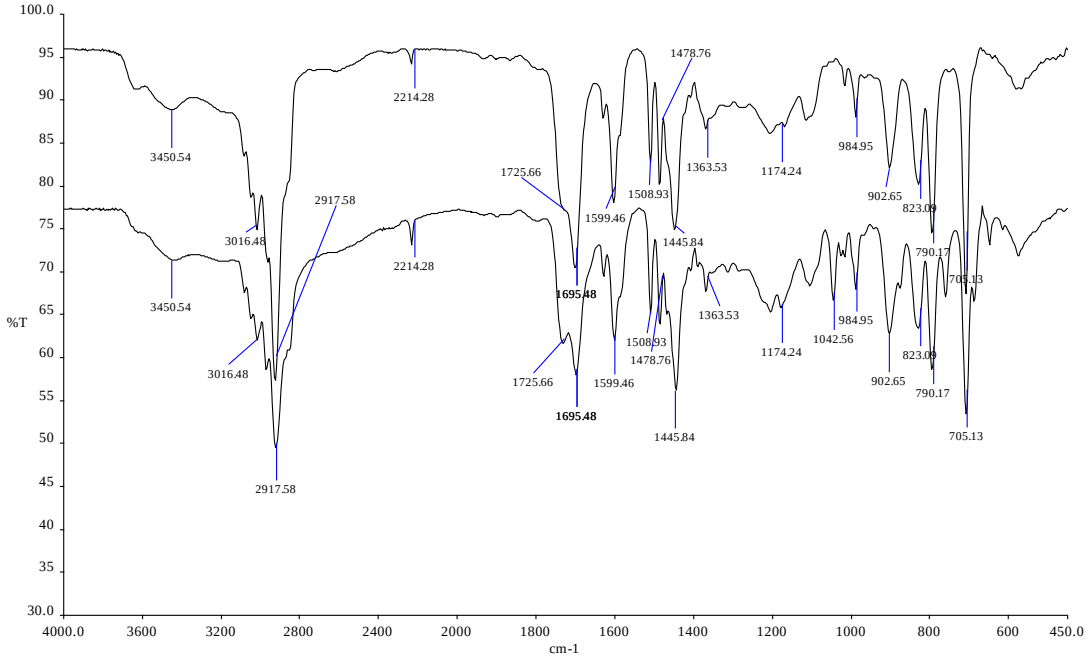

Figure 4.17 FTIR spectra of NIPs; P6 synthesised *via* RAFT polymerisation (lower) and P8 synthesised *via* conventional FRP (upper)

4.6.4 Retention factors (*k'*) and imprinting factors (IF) from HPLC studies

The molecular recognition properties of the polymers were evaluated in HPLC mode, as described in the Experimental section.

To evaluate the molecular recognition ability of the MIP columns prepared *via* RAFT polymerisation and conventional FRP, two xanthine derivatives, caffeine **42** and theophylline **43**, were injected in turn onto the columns. MAA has been used extensively for non-covalent molecular imprinting protocols and, significantly, has been shown to be useful for caffeine imprinting.[133],[134],[135] The structures of the two xanthines are shown in Figure 4.18.

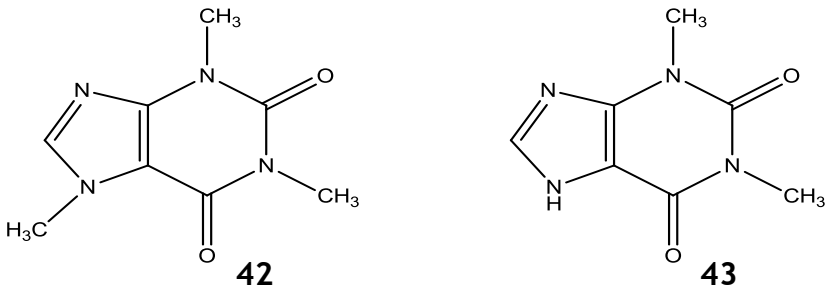

Figure 4.18 Molecular structures of caffeine **42** and theophylline **43**

Initially, after equilibrating the columns with acetonitrile, the elution of a 10 mM standard solution of caffeine **42** and theophylline **43** in chloroform[129] (injection volume= 10 μL) was investigated on each of the columns in turn, followed by an intimate mixture of caffeine **42** and theophylline **43**. Acetonitrile was used as the mobile phase under isocratic conditions. The retention factors on the imprinted (k'_{MIP}) and non-imprinted (k'_{NIP}) stationary phases and the imprinting factors (IF) were calculated according to standard chromatographic theory. Acetone was used as a void marker. Acetone is a neutral molecule with low affinity for the polymers;

therefore it can be used as a void marker. Furthermore, the acetone peak shape can be used to identify any problems within the column packing.

a) Monolithic Polymers

The elution profiles of caffeine **42** and theophylline **43** on HPLC columns packed with P1, P2, P3 and P4 were investigated. The injections of analytes on each column were repeated three times (n=3) and average retention times calculated. On the P1 and P3 imprinted columns, caffeine **42** was eluted with a retention factor of 0.53 and 0.45, respectively; while the retention factor of theophylline **43** on P1 and P3 was 1.12 and 1.02, respectively. Figure 4.19 and Figure 4.20 show a comparison of caffeine **42** and theophylline **43** on the P1 and P3 columns, respectively. The retention of theophylline **43** on the polymers was stronger than that of caffeine **42**, even although caffeine **42** was the template used during imprinting. A similar effect has been observed in previous work published by our group,[135] and can be rationalised on the basis that theophylline **43** is smaller than caffeine **42**, so fits into the caffeine **42** binding sites, and benefits from an additional hydrogen bond (Figure 4.21).

The retention factors of caffeine and theophylline **43** were somewhat higher on P1 than that of P3, which suggests that the use of CRP in the production of P1 has given rise to polymers with higher binding affinity. Injections of caffeine **42** and theophylline **43** on P1 and P3 give elution peaks with the peak-tailing characteristic of an imprinted HPLC stationary phase, indicating that both P1 and P3 had been imprinted.

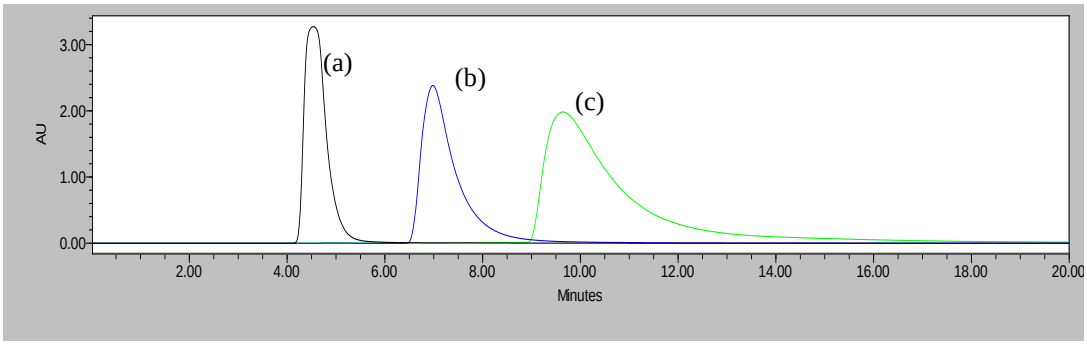

Figure 4.19 Comparison of acetone (a), caffeine **42** (b) and theophylline **43** (c) retention on P1 MIP column prepared *via* RAFT polymerisation

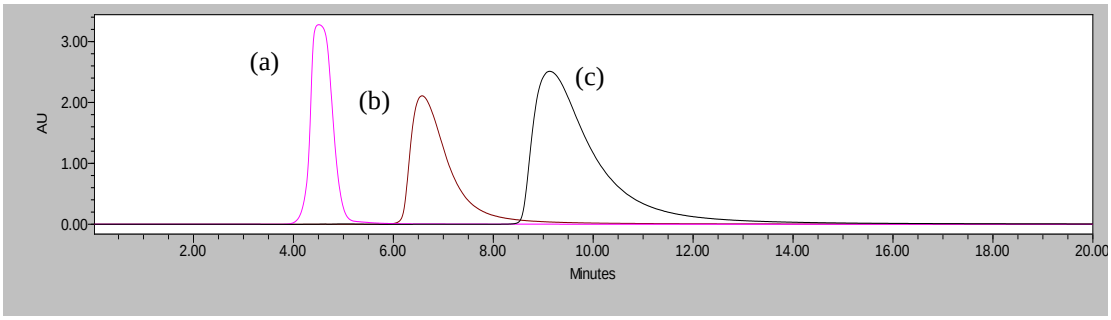

Figure 4.20 Comparison of acetone (a), caffeine **42** (b) and theophylline **43** (c) retention on P3 MIP column prepared *via* conventional FRP

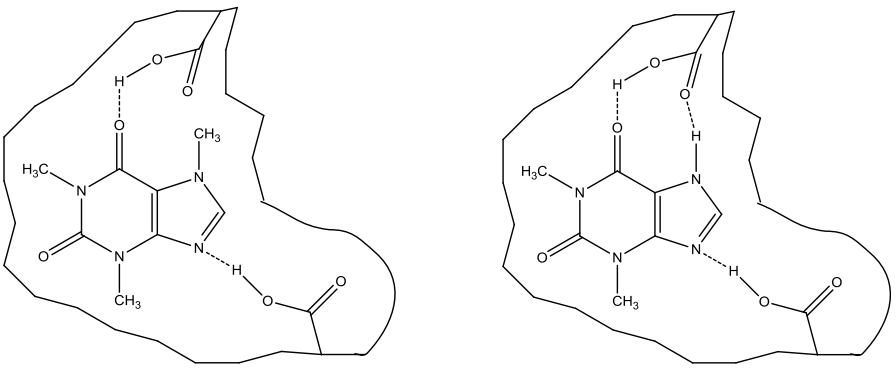

(a) (b)

Figure 4.21 Putative hydrogen bonds between caffeine **42** (a) or theophylline **43** (b) with the carboxylic acid groups in the caffeine-imprinted polymer, where MAA is the functional monomer

Investigations were also carried out where caffeine **42** and theophylline **43** were injected simultaneously onto the P1 and P3 columns to evaluate the cross-selectivity effect. Both columns showed rather similar chromatograms (Figure 4.22). It was clearly shown that the MIPs showed cross-selectivity for theophylline **43**. Furthermore, both columns allowed complete separation of caffeine **42** and theophylline **43** (base-line resolved peaks).

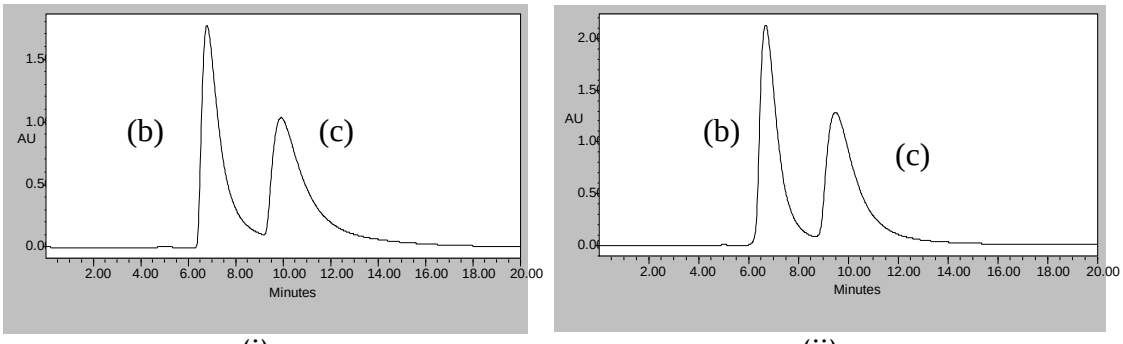

(i) (ii)

Figure 4.22 Chromatograms showing the separation of caffeine **42** (b) and theophylline **43** (c) on P1 (i) and P3 (ii) MIP columns

In contrast, and as expected, caffeine **42** and theophylline **43** were retained less-well on the non-imprinted P2 (Figure 4.23) and P4 (Figure 4.24) columns. The retention factors of caffeine **42** on P2 and P4 were 0.32 and 0.30, respectively, and 1.02 and 0.98 for theophylline **43**, respectively.

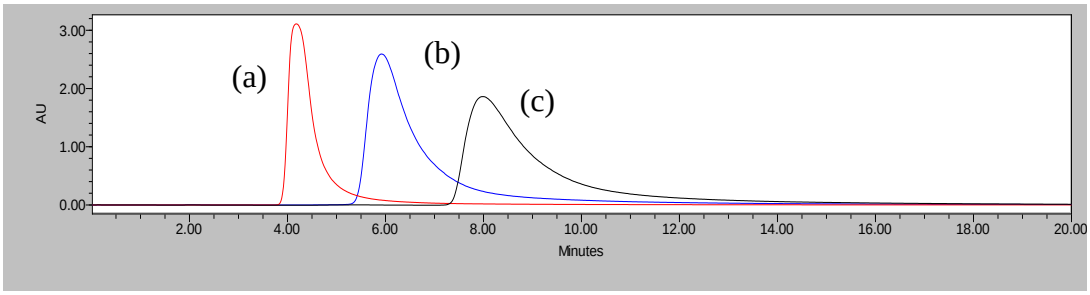

Figure 4.23 Comparison of acetone (a), caffeine **42** (b) and theophylline **43** (c) retention on P2 NIP column prepared *via* RAFT polymerisation

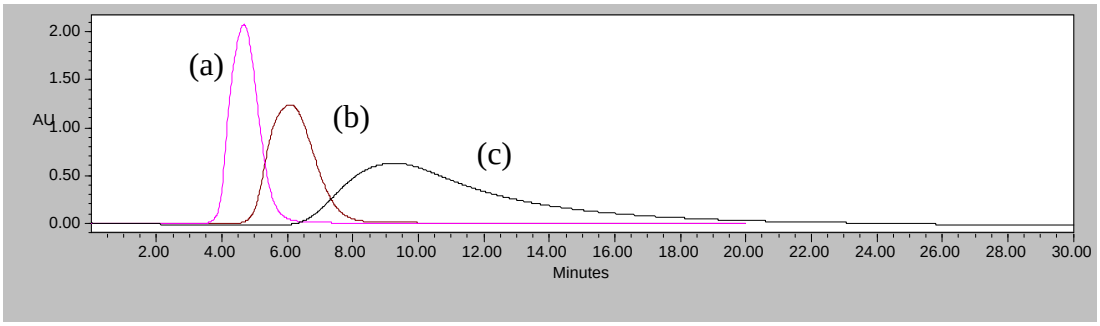

Figure 4.24 Comparison of acetone (a), caffeine **42** (b) and theophylline **43** (c) retention on P4 NIP column prepared *via* conventional FRP

The peaks were broad and there was a degree of peak-tailing, especially on the P4 column which was prepared *via* conventional FRP. Furthermore, injection of the mixture of analytes onto P2 and P4 showed that neither column was able to resolve completely the mixture of analytes (Figure 4.25). Yet again, the NIP

column prepared *via* RAFT polymerisation gave rise to better chromatographic performance than that of the column prepared by conventional FRP.

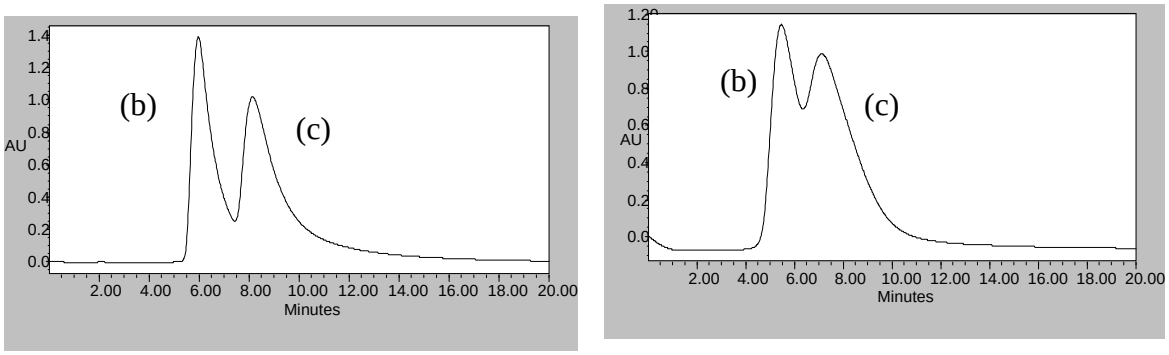

(i) (ii)

Figure 4.25 Chromatograms of the separation of caffeine **42** (b) and theophylline **43** (c) on P2 (i) and P4 (ii) columns

Imprinting factors (IF), calculated according to standard chromatographic theory, are a measure of the effectiveness of the molecular imprinting. The higher the IF value, the better the molecular recognition. The IF of caffeine **42** was found to be higher on P1 (1.7) than on P3 (1.5); analogous results were found for the IF of theophylline **43** (P1: 1.4 and P3: 1.0). Thus, even although the polymer prepared in the presence of the RAFT agent (P1) had a very low dry-state specific surface area, it performed surprisingly well as a chromatographic stationary phase, and out-performed a stationary phase produced by conventional synthesis methods. The results are summarised in Table 4.3.

Table 4.3 Retention factors, imprinting factors and theoretical plate numbers, *N*, of caffeine **42** and theophylline **43** on polymers synthesised *via* RAFT polymerisation (P1 and P2) and conventional FRP (P3 and P4)

Polymer Code	$N_{caffeine}$	$N_{theophylline}$	$k'_{caffeine}$	$k'_{theophylline}$	$IF_{caffeine}$	$IF_{theophylline}$
P1 (MIP)	306	285	0.53	1.12	1.7	1.4
P2 (NIP)	234	208	0.32	0.78	N/A	
P3 (MIP)	244	240	0.45	1.02	1.5	1.0
P4 (NIP)	184	173	0.30	0.98	N/A	

Furthermore, polymers synthesised *via* RAFT polymerisation (P1 and P2) were found to have higher numbers of theoretical plates, indicating higher column efficiency. Nevertheless, P4 has the lowest number of theoretical plates, indicating low efficiency of the column, and this was in agreement with the chromatogram (Figure 4.25) which shows incomplete separation of caffeine **42** and theophylline **43**.

b) Polymer Microspheres

To further explore the effect of implementing controlled radical polymerisation on the chromatographic performance of the polymeric products, precipitation polymerisation was carried out to deliver imprinted polymer microspheres. Caffeine-imprinted polymers (P5 and P7) and non-imprinted polymers (P6 and P8) were prepared by RAFT polymerisation (P5 and P6) and conventional FRP (P7 and P8). The particles produced were in the form of polymer microspheres with average bead diameters in the region of 5 μm.

The MIPs (P5 and P7) were packed into 4.6 I.D. x 150 mm HPLC columns and the retention behaviour of caffeine **42** and theophylline **43** were investigated. Injections of analytes were carried out in triplicate and average retention times of analytes calculated. On the P5 column (synthesised by RAFT polymerisation), caffeine **42** and theophylline **43** were eluted with a retention factor of 0.66 and 1.46, respectively (Figure 4.26). In contrast, caffeine **42** and theophylline **43** were retained relatively longer on the P7 column (retention factors 1.50 and 4.38, respectively). However, on P7 both caffeine **42** and theophylline **43** had extensive peak-tailing, as shown in Figure 4.27. The retention factors of caffeine **42** and theophylline **43** on P7 were higher than on P5, which suggested that P7 had stronger binding affinity for both analytes than P5.

Cross-selectivity is a property of MIPs wherein the MIP recognises not only the template used for the preparation of the polymer but also compounds that are structurally related to the template.[129] Therefore, a mixture of caffeine **42** and theophylline **43** was injected onto the P5 and P7 columns to evaluate the cross-selectivity effect. Good separation of caffeine **42** and theophylline **43** were

observed clearly on both columns (Figure 4.28). However, the most interesting feature that can be observed here is that the column prepared *via* RAFT polymerisation (P5) gave slightly faster separation than the column prepared *via* conventional FRP (P7) and showed good cross-selectivity, which are useful features in the field of separation science. In addition to this, peak-tailing is significantly less-pronounced on the P5 column.

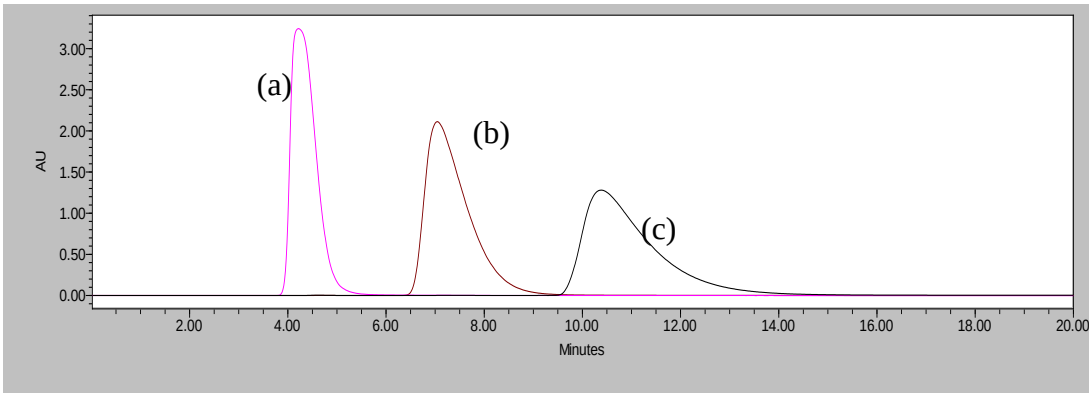

Figure 4.26 Comparison of acetone (a), caffeine **42** (b) and theophylline **43** (c) retention on P5 MIP column prepared *via* RAFT polymerisation

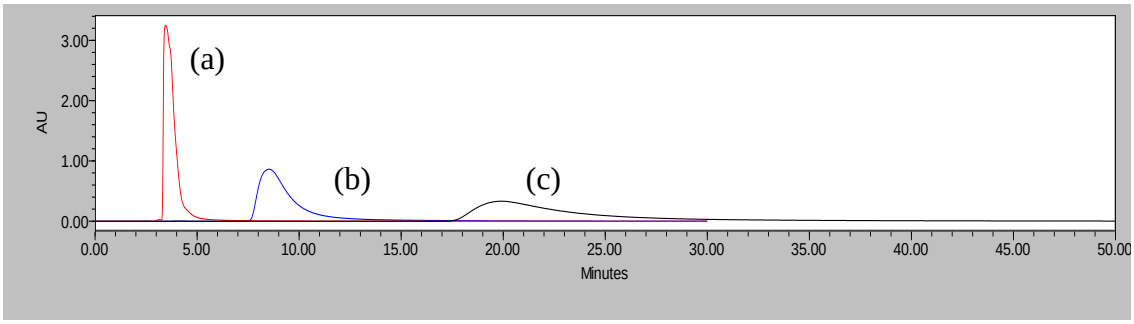

Figure 4.27 Comparison of acetone (a), caffeine **42** (b) and theophylline **43** (c) retention on P7 MIP column prepared *via* conventional FRP

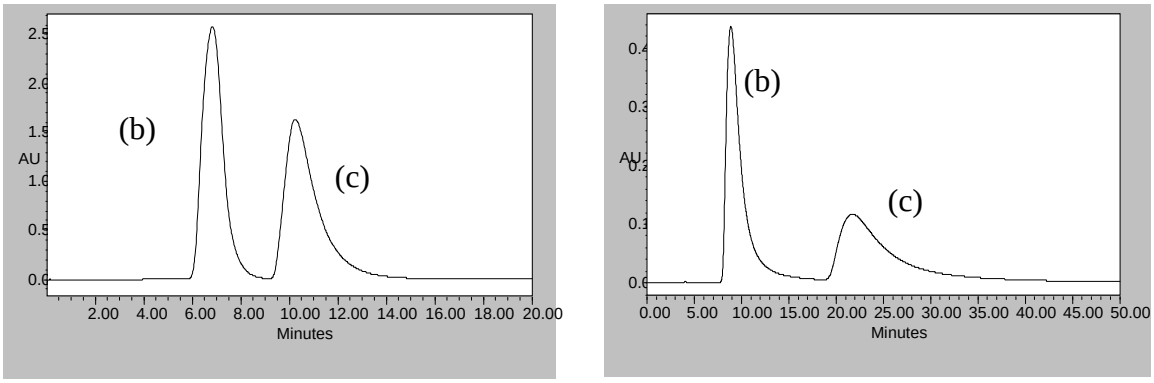

(i) (ii)

Figure 4.28 Chromatograms of the separation of caffeine **42** (b) and theophylline **43** (c) on P5 (i) and P7 (ii) columns

For caffeine **42** and theophylline **43** retention on the NIP columns, trends similar to those reported earlier for P2 and P4 were observed. As expected, caffeine **42** and theophylline **43** were retained relatively poor on the non-imprinted P6 (retention factors 0.44 and 1.12, respectively) and P8 (retention factors 1.27 and 3.62, respectively) polymers. The chromatograms are shown in Figure 4.29 and Figure 4.30 for P6 and P8, respectively.

When a mixture of analytes was injected, the column prepared *via* conventional FRP (P8) showed better separation of the analytes compared to the column prepared *via* RAFT polymerisation (P6), which gave incomplete separation. However, P6 gave a faster elution than P8 (Figure 4.31). Note, however, that both P6 and P8 are NIPs and so of less interest than the MIPs.

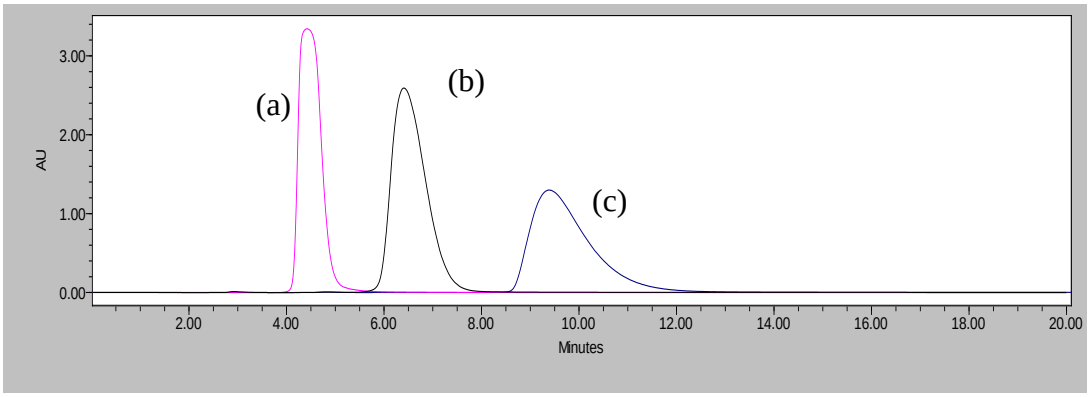

Figure 4.29 Comparison of acetone (a), caffeine **42** (b) and theophylline **43** (c) retention on P6 NIP column prepared *via* RAFT polymerisation

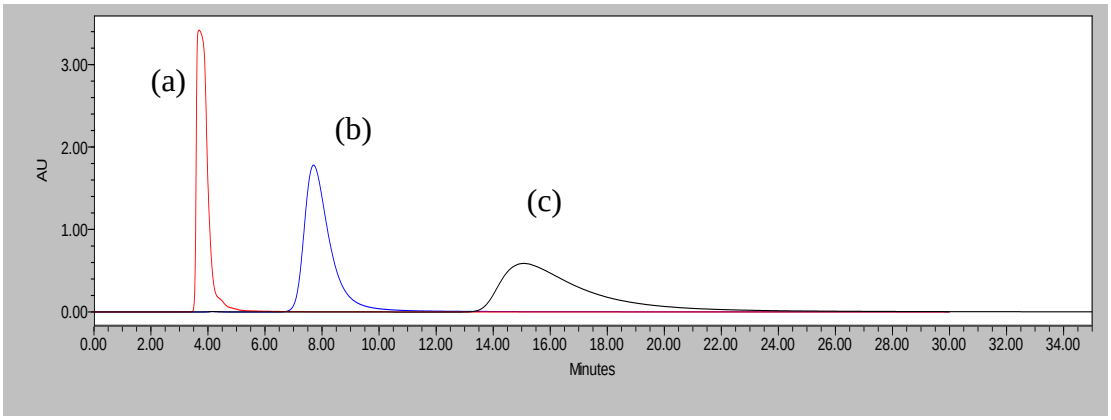

Figure 4.30 Comparison of acetone (a), caffeine **42** (b) and theophylline **43** (c) retention on P8 NIP column prepared *via* conventional FRP

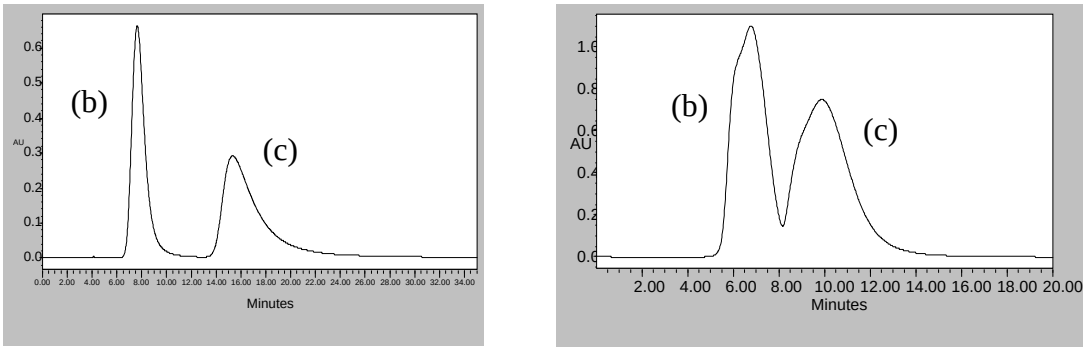

(i) (ii)

Figure 4.31 Chromatograms of the separation of caffeine **42** (b) and theophylline **43** (c) on P8 (i) and P6 (ii) columns

Again, the imprinting factors (IF) were calculated according to standard chromatographic theory. The IF values of caffeine **42** and theophylline **43** were found to be higher for P5 than for P7, indicative of the effectiveness of the column prepared *via* RAFT polymerisation (P5). Indeed, the number of theoretical plates was found to be higher for the columns prepared in the presence of RAFT agent (P5 and P6). Rather significantly, the columns packed with the polymer prepared *via* RAFT polymerisation had the highest efficiency of all. Table 4.4 summarises the chromatographic results of the four polymers prepared by precipitation polymerisation.

Table 4.4 Retention factors, imprinting factors and theoretical plate numbers, *N*, of caffeine **42** and theophylline **43** on polymers synthesised *via* RAFT polymerisation (P5 and P6) and conventional FRP (P7 and P8)

Polymer Code	$N_{caffeine}$	$N_{theophylline}$	$k'_{caffeine}$	$k'_{theophylline}$	$IF_{caffeine}$	$IF_{theophylline}$
P5 (MIP)	354	325	0.66	1.46	1.5	1.3
P6 (NIP)	327	304	0.44	1.12	N/A	
P7 (MIP)	298	252	1.50	4.38	1.2	1.2
P8 (NIP)	221	101	1.27	3.62	N/A	

Nevertheless, the IF value for P5 towards caffeine **42** and theophylline **43** was found to be lower than P1. This might be due to the different approach used to synthesise the polymer. P5 was synthesised *via* precipitation polymerisation which involved a low monomer concentration in solution, whereas P1 was synthesised in monolithic form with a high concentration of monomer.

4.6.5 Post-Polymerisation chemical modification; Poly(EGDMA-co-MAA)-*g*-HEMA

To exploit the 'livingness' of the polymers produced in this study, a simple post-polymerisation experiment was carried out as a proof of concept, *via* grafting using HEMA as monomer. Grafting techniques are an important way of changing the surface properties of a material. Techniques pertinent to the grafting of polymer particles are the 'grafting to', 'grafting from' and the 'grafting through' methods.

One of the most common ways of functionalising particulate materials for use in chromatography is the 'grafting to' approach. In this approach, a pre-formed polymer chain is used which carries an active terminal group that can be reacted with an active particle surface.[136] The 'grafting from' approach involves initiation at the particle surface and growth of the grafted polymer chain away from the particle surface.[137] This approach has been used successfully for NMRP,[21] ATRP[65] and RAFT[22] polymerisations. The 'grafting through' approach consists of the polymerisation of macromonomers or the polymerisation through vinyl groups which are bond covalently to the particle surface.[138],[139]

HEMA and its polymers are of great interest due to their hydrophilicity and biocompatibility (hydroxyl functional group); HEMA is readily polymerized or copolymerized and used in many applications. PolyHEMA is the most widely used hydrogel because the water content is similar to that of living tissues, it has bio- and blood-compatibility, and is resistant to degradation.[140]

Based on a method developed by Chen *et al.,*[131] reported the use of a combination of lauroyl peroxide (LPO) and AIBN, completely removes the thiocarbonylthio end groups of polystyrene and polyacrylate thus useful for post-polymerisation modification. In this study, HEMA was grafted successfully onto polymer P2 to give polymer P2g. An increase in mass was observed in going from P2 to P2g, which was already good evidence in support of a grafting outcome, however in order to give better confirmation of this result a simple polymer wettability test was carried out. Small quantities of P2g and a control polymer P4g were placed on a glass slide with a drop of water. P2g was found to sorb more water than P4g, suggesting that P2g was more hydrophilic as a result of grafting. In a control experiment (P2 and P4), no obvious effect was observed when water was in contact with the polymers, as they are not grafted with HEMA. Figure 4.32 shows a schematic representation of the grafting process.

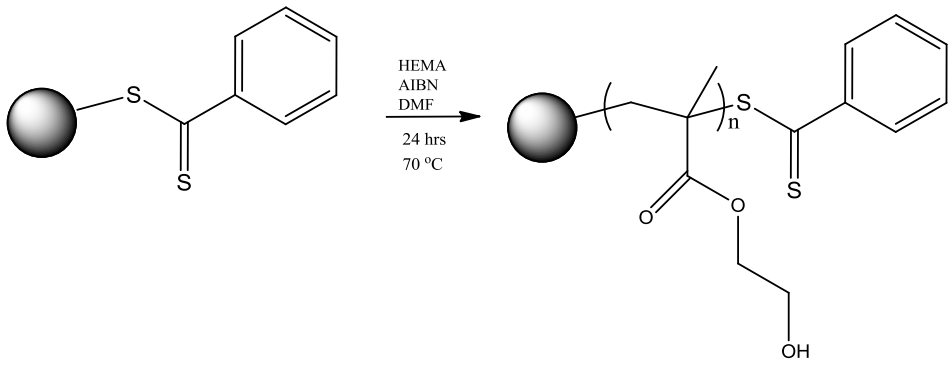

Figure 4.32 Schematic representation of grafting process

Results from elemental microanalysis confirmed the expected fall in the sulfur content of P2 upon grafting to give P2g. Additionally, the FTIR spectra, presented in Figure 4.33, suggests that HEMA has been grafted successfully from P2: broad hydroxyl band at 3300-3700 cm^{-1}, arising from the HEMA hydroxyl groups; thiocarbonyl group 1045 cm^{-1} still easily identifiable for P2g but less pronounced than for P2 suggesting a dilution effect; peak of C=O (1734 cm^{-1}) and peaks of CH_2 (1473-1454 cm^{-1}) retained in the spectrum of P2g. In a control experiment, no obvious grafting was observed when polymer P4 was exposed to HEMA grafting conditions (see Figure 4.34).

Although these are preliminary results, it would seem that P2 has been grafted with HEMA to give P2g. This is possible only because of the "living" character of polymers synthesised by RAFT polymerisation.

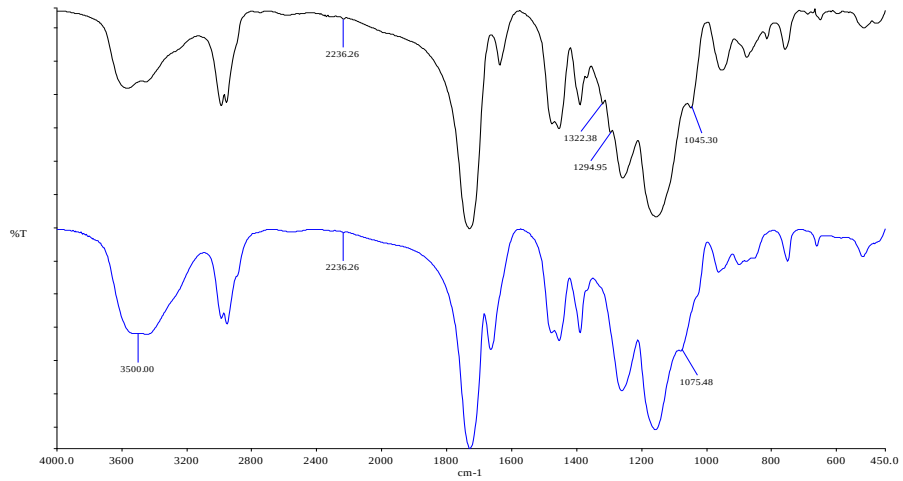

Figure 4.33 FTIR spectra of P2 (upper) and P2g (lower). P2 is expected to be amenable to grafting

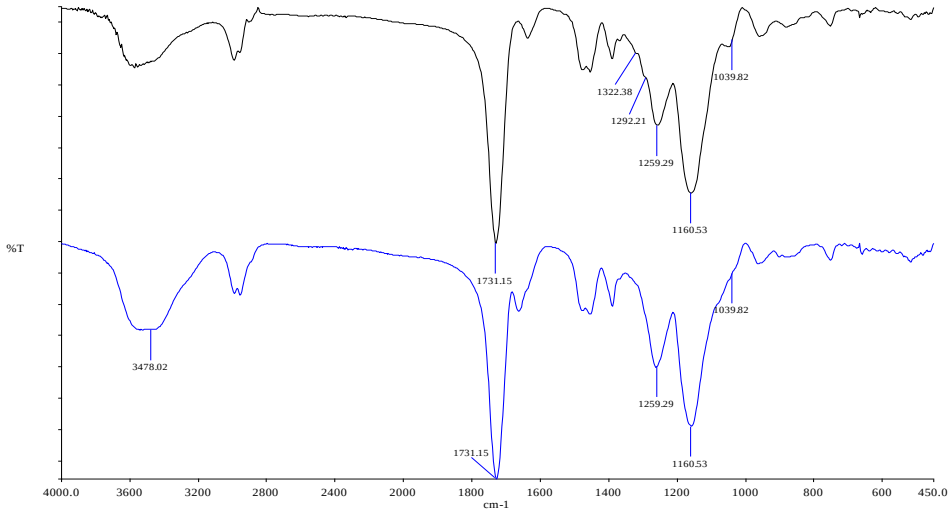

Figure 4.34 FTIR spectra of P4 (upper) and P4g (lower). P4 is not expected to be amendable to grafting

4.7 Conclusion

Caffeine-imprinted polymers in monolithic form and caffeine-imprinted polymer microspheres have been prepared successfully in good yields *via* both RAFT polymerisation and conventional FRP. The monoliths were ground to deliver imprinted particles, which were then applied as stationary phases in HPLC. The polymer microspheres were produced *via* a Kugelrohr based method, and were suitable for packing directly into columns prior to their use as stationary phases. The crosslinker is an important variable that affects the imprinting outcome.[129] DVB and EGDMA are two crosslinkers that have been most widely used in molecular imprinting. In this study, EGDMA was applied to the synthesis of the monolithic polymers, while DVB was used in the production of the polymer microspheres.

Polymers produced *via* RAFT polymerisation in monolithic form (P1 and P2) and microsphere form (P5 and P6) had the typical appearance of a gel-type polymer in the dry state, in that they were optically transparent. Perhaps unsurprisingly, therefore, the specific surface areas for these polymers were < 5 m^2g^{-1}. In contrast, all the polymers prepared *via* conventional FRP scattered white light, suggestive of well-developed pore structures even in the dry state.

The presence of sulfur in polymers P1, P2, P5 and P6 was confirmed by the elemental microanalysis results, and this indicated that the RAFT agent had been incorporated into the polymers. Similar conclusions could be drawn from the FTIR analyses.

It is interesting to compare the retention of the analytes on the different stationary phases having the same nominal compositions but which have been prepared *via* different polymerisation methods. The monolithic MIP prepared *via* RAFT polymerisation (P1) gave imprinting factor (IF) values for caffeine **42** (1.7) and theophylline **43** (1.4) which were higher than for the MIP prepared *via* conventional FRP [P3; caffeine **42** (1.5) and theophylline **43** (1.0)]; even although the polymer prepared in the presence of the RAFT agent had a very low dry-state specific surface area. A similar trend was observed for the microsphere-based materials. The IF values of caffeine **42** and theophylline **43** were found to be higher for the polymer prepared *via* RAFT polymerisation (P5); IF values of 1.5 and 1.3, respectively. In contrast, the IF values were rather low for those polymers synthesised *via* conventional FRP (P7); caffeine **42** (1.2) and theophylline **43** (1.2).

Polymers prepared by RAFT polymerisation gave rise to faster separation of caffeine **42** and theophylline **43** than polymers prepared by FRP. Peaks were narrower and more symmetrical on the former, indicating higher column efficiency compared to those polymers prepared by conventional FRP. Most importantly, the chemical separations are more efficient on polymers prepared by RAFT polymerisation than on the polymers prepared using FRP. Furthermore, the peak-tailing is significantly less-pronounced on the P1, P2, P5 and P6 polymers (RAFT).

Upon comparing the various IF values, it seems that the monolithic polymer produced *via* RAFT polymerisation (P2) performed particularly well as a chromatographic stationary phase, which is why this material was selected to demonstrate the grafting proof-of-concept, with HEMA as the monomer.

To conclude, this work clearly demonstrates that applying controlled radical polymerisation to MIP production can have a significant beneficial impact upon the properties of MIPs; improved homogeneity of binding sites and enhanced chromatographic performance. Furthermore, preliminary studies have suggested that additional benefits may arise from exploitation of the "living" character of CRP-produced MIPs vis-á-vis their post-polymerisation chemical modification.

4.8 References

[1] B. Zu, Y. Zhang, X. Guo and H. Zhang, *J. Polym. Sci. Pol. Chem.* **2010**, *48*, 532-541.

[2] M. Kempe and K. Mosbach, *J. Chromatogr. A.* **1995**, *694*, 3-13.

[3] O. Ramström and R. J. Ansell, *Chirality* **1998**, *10*, 195-209.

[4] N. A. O'Connor, D. A. Paisner, D. Huryn and K. J. Shea, *J. Am. Chem. Soc.* **2007**, *128*, 1680-1689.

[5] S. A. Piletsky, Y. P. Parhometz, N. V. Lavryk, T. L. Panasyuk and A. V. El'skaya, *Sensor. Actuat. B- Chem.* **1994**, *19*, 629-631.

[6] R. Thoelen, R. Vansweevelt, J. Duchateau, F. Horemans, J. D. Haen, L. Lutsen, D. Vanderzande, M. Ameloot, M. vandeVen, T. J. Cleij and P. Wagner, *Biosens. Bioelectron.* **2008**, *23*, 913-918.

[7] G. Theodoridis and P. Manesiotis, *J. Chromatogr. A.* **2002**, *948*, 163-169.

[8] C. J. Hawker, *Acc. Chem. Res.* **1997**, *30*, 373-382.

[9] A. Goto and T. Fukuda, *Prog. Polym. Sci.* **2004**, *29*, 329-385.

[10] A. R. Wang and S. Zhu, *J. Polym. Sci. Pol. Chem.* **2005**, *43*, 5710-5714.

[11] N. Ide and T. Fukuda, *Macromolecules* **1997**, *30*, 4268-4271.

[12] W. Huang, G. L. Baker and M. L. Bruening, *Angew. Chem. Int. Edit.* **2001**, *113*, 1558-1560.

[13] M. Achilleos, T. M. Legge, S. Perrier and C. S. Patrickios, *J. Polym. Sci. Pol. Chem.* **2008**, *46*, 7556-7565.

[14] R. T. A. Mayadunne, E. Rizzardo, J. Chiefari, Y. K. Chong, G. Moad and S. H. Thang, *Macromolecules* **1999**, *32*, 6977-6980.

[15] C. J. Hawker, G. G. Barclay, A. Orellana, J. Dao and W. Devonport, *Macromolecules* **1996**, *29*, 5245-5254.

[16] K. Matyaszewski and T. P. Davis, *Handbook of radical polymerization*, Wiley-Interscience, Hoboken, **2002**.

[17] K. Matyjaszewski and J. Xia, *Chem. Rev.* **2001**, *101*, 2921-2990.

[18] G. Moad, J. Chiefari, Y. K. Chong, J. Krstina, R. T. A. Mayadunne, A. Postma, E. Rizzardo and S. H. Thang, *Polym. Int.* **2000**, *49*, 993-1001.

[19] S. Perrier and P. Takolpuckdee, *J. Polym. Sci. Pol. Chem.* **2005**, *43*, 5347-5393.

[20] D. Greszta, Mardare, D., Matyjaszewski, K.,, *Macromolecules* **1994**, *27*, 638-644.

[21] M. K. Georges, R. P. N. Veregin, P. M. Kazmaier and G. K. Hamer, *Macromolecules* **1993**, *26*, 2987-2988.

[22] J. Chiefari, Y. K. Chong, F. Ercole, J. Krstina, J. Jeffery, T. P. T. Le, R. T. A. Mayadunne, G. F. Meijs, C. L. Moad, G. Moad, E. Rizzardo and S. H. Thang, *Macromolecules* **1998**, *31*, 5559-5562.

[23] K. A. Kun and R. Kunin, *J. Polym. Sci. A1.* **1968**, *6*, 2689-2701.

[24] W. L. Sederel and G. J. De Jong, *J. Appl. Polym. Sci.* **1973**, *17*, 2835-2846.

[25] B. A. Bolto, K. H. Eppinger and M. B. Jackson, *React. Polym. : Ion Exchangers, Sorbents.* **1983**, *1*, 139-143.

[26] V. Smigol, F. Svec and J. M. J. Fréchet, *Macromolecules* **1993**, *26*, 5615-5620.

[27] D. W. Lee, J. M. Piret, D. Gregory, D. J. Haddow and D. G. Kilburn, *Ann. NY. Acad. Sci.* **1992**, *665*, 137-145.

[28] W. Rolls, F. Svec and J. M. J. Fréchet, *Polymer* **1990**, *31*, 165-174.

[29] S. Emir, R. Say, H. Yavuz and A. Denizli, *Biotechnol. Progr.* **2004**, *20*, 223-228.

[30] Q. C. Wang, F. Svec and J. M. J. Fréchet, *Anal. Chem.* **1993**, *65*, 2243-2248.

[31] K. Lewandowski, F. Svec and J. M. J. Fréchet, *Chem. Mater.* **1998**, *10*, 385-391.

[32] R. D. Das, C. RoyChaudhuri, S. Maji, S. Das and H. Saha, *Biosens. Bioelectron.* **2009**, *24*, 3215-3222.

[33] F. Svec and J. M. J. Fréchet, *Anal. Chem.* **1992**, *64*, 820-822.

[34] C. J. Hawker, A. W. Bosman and E. Harth, *Chem. Rev.* **2001**, *101*, 3661-3688.

[35] E. C. Peters, F. Svec, J. M. J. Fréchet, C. Viklund and K. Irgum, *Macromolecules* **1999**, *32*, 6377-6379.

[36] C. Viklund, A. Nordström, K. Irgum, F. Svec and J. M. J. Fréchet, *Macromolecules* **2001**, *34*, 4361-4369.

[37] D. Benoit, V. Chaplinski, R. Braslau and C. J. Hawker, *J. Am. Chem. Soc.* **1999**, *121*, 3904-3920.

[38] K. Kanamori, K. Nakanishi and T. Hanada, *Adv. Mater.* **2006**, *18*, 2407-2411.

[39] N. Malic and R. A. Evans, *Aust. J. Chem.* **2006**, *59*, 763-771.

[40] M. J. Monteiro and H. de Brouwer, *Macromolecules* **2001**, *34*, 349-352.

[41] P. Vana, T. P. Davis and C. Barner-Kowollik, *Macromol. Theor. Simul.* **2002**, *11*, 823-835.

[42] G. Moad, E. Rizzardo and S. H. Thang, *Aust. J. Chem.* **2005**, *58*, 379-410.

[43] M. S. Donovan, A. B. Lowe, B. S. Sumerlin and C. L. McCormick, *Macromolecules* **2002**, *35*, 4123-4132.

[44] R. Severac, P. Lacroix-Desmazes and B. Boutevin, *Polym. Int.* **2002**, *51*, 1117-1122.

[45] C. J. Ferguson, R. J. Hughes, B. T. T. Pham, B. S. Hawkett, R. G. Gilbert, A. K. Serelis and C. H. Such, *Macromolecules* **2002**, *35*, 9243-9245.

[46] S. W. Prescott, M. J. Ballard, E. Rizzardo and R. G. Gilbert, *Macromolecules* **2002**, *35*, 5417-5425.

[47] H. de Brouwer, J. G. Tsavalas and F. J. Schork, *Macromolecules* **2000**, *33*, 9239-9246.

[48] G. Moad, Y. K. Chong, A. Postma, E. Rizzardo and S. H. Thang, *Polymer* **2005**, *46*, 8458-8468.

[49] H. Willcock and R. K. O'Reilly, *Polym. Chem.* **2010**, *1*, 149-157.

[50] L. Barner and S. Perrier, *Handbook of RAFT Polymerization*, Wiley-VCH, Weinheim, **2008**.

[51] C. H. Bamford, W. G. Barb, A. D. Jenkins and P. F. Onyon, *The Kinetics of Vinyl Polymerization by Radical Mechanisms*, Academic Press, New York, **1958**.

[52] G. Moad and D. H. Solomon, *The chemistry of radical polymerization, 2nd ed.*, Elsevier, Oxford, UK, **2006**.

[53] B. Dietrich, *Int. J. Polym. Sci.* **2009**, *2009*.

[54] M. Szwarc, *Nature* **1956**, *178*, 1168-1169.

[55] W. A. Braunecker and K. Matyjaszewski, *Prog. Polym. Sci.* **2007**, *32*, 93-146.

[56] K. Matyjaszewski, P. Kubisa and S. Penczek, *J. Polym. Sci. Pol. Chem.* **1974**, *12*, 1333-1336.

[57] K. Matyjaszewski, P. Kubisa and S. Penczek, *J. Polym. Sci. Pol. Chem.* **1975**, *13*, 763-784.

[58] S. Penczek, M. Cypryk, A. Duda, P. Kubisa and S. Slomkowski, *Prog. Polym. Sci.* **2007**, *32*, 247-282.

[59] S. Penczek, P. Kubisa and K. Matyjaszewski, *Adv. Polym. Sci.* **1985**, *68-69*, 1-298.

[60] S. Penczek, P. Kubisa and K. Matyjaszewski, *Adv. Polym. Sci.* **1980**, *37*, 1-144.

[61] M. Miyamoto, M. Sawamoto and T. Higashimura, *Macromolecules* **1984**, *17*, 265-268.

[62] R. Faust and J. P. Kennedy, *J. Polym. Sci. Pol. Chem.* **1987**, *25*, 1847-1869.

[63] T. Otsu and T. Tazaki, *Polym. Bull.* **1986**, *16*, 277-284.

[64] T. Otsu, M. Yoshida and T. Tazaki, *Makromol. Chem., Rapid Commun.* **1982**, *3*, 133-140.

[65] J.-S. Wang and K. Matyjaszewski, *J. Am. Chem. Soc.* **1995**, *117*, 5614-5615.

[66] G. Moad and D. H. Salomon, *The chemistry of free radical polymerization*, Pergamon, Oxford,UK, **1995**.

[67] G. Moad, E. Rizzardo and D. H. Solomon, *Macromolecules* **1982**, *15*, 909-914.

[68] E. Rizzardo and D. Solomon, *Polym. Bull.* **1979**, *1*, 529-534.

[69] D. H. Solomon, E. Rizzardo and P. Cacioli in *Polymerization process and polymers produced thereby*, *US4581429* **1986**.

[70] C. H. J. Johnson, G. Moad, D. H. Solomon, T. H. Spurling and D. J. Vearing, *Aust. J. Chem.* **1990**, *43*, 1215-1230.

[71] H. Fischer, *Chem. Rev.* **2001**, *101*, 3581-3610.

[72] G. Moad and E. Rizzardo, *Macromolecules* **1995**, *28*, 8722-8728.

[73] L. Boiteau, M. Moroni, A. Hilberer, M. Werts, B. de Boer and G. Hadziioannou, *Macromolecules* **2002**, *35*, 1543-1548.

[74] K. Matyjaszewski and S. G. Gaynor, *Applied Polymer Science*, Pergamon Press, Oxford, UK, **2000**.

[75] Y. Kotani, M. Kato, M. Kamigaito and M. Sawamoto, *Macromolecules* **1996**, *29*, 6979-6982.

[76] M. S. Kharasch, E. V. Jensen and W. H. Urry, *Science* **1944**, *102*, 128.

[77] F. Minisci, *Acc. Chem. Res.* **1975**, *8*, 165-171.

[78] M. Asscher and D. Vofsi, *J. Am. Chem. Soc.* 3921-3927.

[79] T. Pintauer and K. Matyjaszewski, *Chem. Soc. Rev.* **2008**, *37*, 1087-1097.

[80] M. Kato, M. Kamigaito, M. Sawamoto and T. Higashimura., *Polym. Prepr. Jpn.* **1994**, *43*, 1792-1793.

[81] M. Kato, M. Kamigaito, M. Sawamoto and T. Higashimura, *Macromolecules* **1995**, *28*, 1721-1723.

[82] V. Percec and B. Barboiu, *Macromolecules* **1995**, *28*, 7970-7972.

[83] W. Jakubowski, K. Min and K. Matyjaszewski, *Macromolecules* **2005**, *39*, 39-45.

[84] K. Matyjaszewski, W. Jakubowski, K. Min, W. Tang, J. Huang, W. A. Braunecker and N. V. Tsarevsky, *P. Natl. Acad. Sci. USA.* **2006**, *103*, 15309-15314.

[85] W. Jakubowski, B. Kirci-Denizli, R. R. Gil and K. Matyjaszewski, *Macromol. Chem. Physic.* **2008**, *209*, 32-39.

[86] W. Jakubowski and K. Matyjaszewski, *Angew. Chem. Int. Edit.* **2006**, *118*, 4594-4598.

[87] L. Mueller, W. Jakubowski, W. Tang and K. Matyjaszewski, *Macromolecules* **2007**, *40*, 6464-6472.

[88] H. Dong, W. Tang and K. Matyjaszewski, *Macromolecules* **2007**, *40*, 2974-2977.

[89] H. Chen, L. Yang, Y. Liang, Z. Hao and Z. Lu, *J. Polym. Sci. Pol. Chem.* **2009**, *47*, 3202-3207.

[90] M. Teodorescu and K. Matyjaszewski, *Macromolecules* **1999**, *32*, 4826-4831.

[91] M. Senoo, Y. Kotani, M. Kamigaito and M. Sawamoto, *Macromolecules* **1999**, *32*, 8005-8009.

[92] Y. Kotani, M. Kamigaito and M. Sawamoto, *Macromolecules* **1999**, *32*, 6877-6880.

[93] V. Percec, B. Barboiu, A. Neumann, J. C. Ronda and M. Zhao, *Macromolecules* **1996**, *29*, 3665-3668.

[94] a) C. Granel, P. Dubois, R. Jerome and P. Teyssie, *Macromolecules* **1996**, *29*, 8576-8582; b) P. Lecomte, I. Drapier, P. Dubois, P. Teyssie and R. Jerome, *Macromolecules* **1997**, *30*, 7631-7633.

[95] J. Xia and K. Matyjaszewski, *Macromolecules* **1997**, *30*, 7697-7700.

[96] D. M. Haddleton, C. B. Jasieczek, M. J. Hannon and A. J. Shooter, *Macromolecules* **1997**, *30*, 2190-2193.

[97] N. V. Tsarevsky and K. Matyjaszewski, *Chem. Rev.* **2007**, *107*, 2270-2299.

[98] J. K. Oh, C. Tang, H. Gao, N. V. Tsarevsky and K. Matyjaszewski, *J. Am. Chem. Soc.* **2006**, *128*, 5578-5584.

[99] J. Xia and K. Matyjaszewski, *Macromolecules* **1997**, *30*, 7692-7696.

[100] J. Gromada and K. Matyjaszewski, *Macromolecules* **2001**, *34*, 7664-7671.

[101] W. Jakubowski and K. Matyjaszewski, *Macromolecules* **2005**, *38*, 4139-4146.

[102] Y. K. Chong, T. P. T. Le, G. Moad, E. Rizzardo and S. H. Thang, *Macromolecules* **1999**, *32*, 2071-2074.

[103] P. Delduc, C. Tailhan and S. Z. Zard, *J. Chem. Soc., Chem. Commun.* **1988**, 308-310.

[104] D. Charmot, P. Corpart, H. Adam, S. Z. Zard, T. Biadatti and G. Bouhadir, *Macromol. Symp.* **2000**, *150*, 23-32.

[105] S. Z. Zard, *Angew. Chem. Int. Edit.* **1997**, *36*, 672-685.

[106] B. Quiclet-Sire and S. Z. Zard, *Pure Appl. Chem.* **1997**, *69*, 645-650.

[107] J. Chiefari and E. Rizzardo, *Handbook of Radical Polymerization* John Wiley & Sons, Hoboken, NY, **2002**.

[108] E. Rizzardo, Y. K. Chong, R. A. Evans, G. Moad and S. H. Thang, *Macromol. Symp.* **1996**, *111*, 1-12.

[109] D. Colombani, *Prog. Polym. Sci.* **1999**, *24*, 425-480.

[110] T. P. Le, G. Moad, E. Rizzardo and S. H. Thang in *Int. Pat. 9801478*, **1998**.

[111] T. P. Le, G. Moad, E. Rizzardo and S. H. Thang in *Int. Pat. 9801478* **1998**.

[112] Y. K. Chong, J. Krstina, T. P. T. Le, G. Moad, A. Postma, E. Rizzardo and S. H. Thang, *Macromolecules* **2003**, *36*, 2256-2272.

[113] J. Chiefari, R. T. A. Mayadunne, C. L. Moad, G. Moad, E. Rizzardo, A. Postma and S. H. Thang, *Macromolecules* **2003**, *36*, 2273-2283.

[114] A. Bruno, *Macromolecules* **2010**, *43*, 10163-10184.

[115] C. L. Duvall, A. J. Convertine, D. S. W. Benoit, A. S. Hoffman and P. S. Stayton, *Mol. Pharm.* **2009**, *7*, 468-476.

[116] C. N. Urbani and M. J. Monteiro, *Macromolecules* **2009**, *42*, 3884-3886.

[117] D. Taton, A. Z. Wilczewska and M. Destarac, *Macromol. Rapid Commun.* **2001**, *22*, 1497-1503.

[118] J. Loiseau, N. Doërr, J. M. Suau, J. B. Egraz, M. F. Llauro, C. Ladavière and J. Claverie, *Macromolecules* **2003**, *36*, 3066-3077.

[119] D. B. Thomas, B. S. Sumerlin, A. B. Lowe and C. L. McCormick, *Macromolecules* **2003**, *36*, 1436-1439.

[120] C. Barner-Kowollik, T. P. Davis, J. P. A. Heuts, M. H. Stenzel, P. Vana and M. Whittaker, *J. Polym. Sci. Pol. Chem.* **2003**, *41*, 365-375.

[121] M. H. Stenzel, T. P. Davis and A. G. Fane, *J. Mater. Chem.* **2003**, *13*, 2090-2097.

[122] M. M. Titirici and B. Sellergren, *Chem. Mater.* **2006**, *18*, 1773-1779.

[123] C. H. Lu, W. H. Zhou, B. Han, H. H. Yang, X. Chen and X. R. Wang, *Anal. Chem.* **2007**, *79*, 5457-5461.

[124] L. Barner, C. E. Li, X. Hao, M. H. Stenzel, C. Barner-Kowollik and T. P. Davis, *J. Polym. Sci. Pol. Chem.* **2004**, *42*, 5067-5076.

[125] R. Joso, M. H. Stenzel, T. P. Davis, C. Barner-Kowollik and L. Barner, *Aust. J. Chem.* **2005**, *58*, 468-471.

[126] L. Nebhani, S. Sinnwell, A. J. Inglis, M. H. Stenzel, C. Barner-Kowollik and L. Barner, *Macromol. Rapid Commun.* **2008**, *29*, 1431-1437.

[127] B. Liu, A. Kazlauciunas, J. T. Guthrie and S. Perrier, *Polymer* **2005**, *46*, 6293-6299.

[128] C. M. Philip and B. Mathew, *J. Macromol. Sci. A.* **2008**, *45*, 335-343.

[129] J. F. Wang, PhD Thesis, University of Strathclyde, Glasgow, **2004**.

[130] J. Xu, J. He, D. Fan, W. Tang and Y. Yang, *Macromolecules* **2006**, *39*, 3753-3759.

[131] M. Chen, G. Moad and E. Rizzardo, *J. Polym. Sci. Pol. Chem.* **2009**, *47*, 6704-6714.

[132] S. Perrier, T. P. Davis, A. J. Carmichael and D. M. Haddleton, *Eur. Pol. J.* **2003**, *39*, 417-422.

[133] K. Farrington, E. Magner and F. Regan, *Anal. Chim. Acta.* **2006**, *566*, 60-68.

[134] C. Baggiani, F. Trotta, G. Giraudi, G. Moraglio and A. V., *J. Chromatogr. A.* **1997**, *786*, 23-29.

[135] J. Wang, P. A. G. Cormack, D. C. Sherrington and E. Khoshdel, *Angew. Chem. Int. Ed.* **2003**, *42*, 5336-5338.

[136] M. Jiang, S. Wang and X. Jin, *J. Mater. Sci. Lett.* **1990**, *9*, 1239-1240.

[137] L. Flores-Santos, A. González-Montiel and E. Saldívar-Guerra in *Reactive Block Copolymers as Versatile Compatibilizers*, *944* American Chemical Society, **2006**, 342-357.

[138] H. G. Börner and K. Matyjaszewski, *Macromol. Symp.* **2002**, *177*, 1-16.

[139] S. Ohno and K. Matyjaszewski, *J. Polym. Sci. Pol. Chem.* **2006**, *44*, 5454-5467.

[140] D. G. Pedley, P. J. Skelly and B. J. Tighe, *Brit. Polym. J.* **1980**, *12*, 99-110.

CHAPTER 5

TOWARDS THE RATIONAL DESIGN OF MOLECULARLY IMPRINTED POLYMERS

5.1 Introduction

In the field of polymer chemistry, the imparting of properties of specific molecular recognition in polymers through molecular imprinting is undergoing a very rapid rise in popularity. Various reviews of this method have been published and it is beyond doubt that molecularly imprinted polymers (MIPs) can be produced reliably and can have very selective molecular recognition properties.[1],[2],[3],[4]

MIPs have been used increasingly in sensing of Volatile Organic Compounds (VOCs), especially for air quality control, explosive and warfare agent detection and other important applications.[5] Sensing applications of MIPs have been reviewed by Fu and Finklea,[6] Blanco *et al*.[7] and by McCluskey *et al*.[8] The uniqueness of MIP-based sensors comes from their ability to recognise the target molecule from other similar species. This functionality is not available in other relevant technologies, such as quartz crystal microbalances, Surface Acoustic Wave (SAW) devices or field effect transducers, where the sensitive coating usually adsorbs a broad variety of similar species and their actual identification requires more advanced, costly procedures. Recently, Bunte and coworkers[9] investigated the

application of acrylamide and methacrylic acid based MIPs for explosive compound sensing.

MIPs are normally designed using knowledge of the chemistry of the template molecule, together with the functional groups present and the types of molecular interactions that are possible. The types of monomers that are able to interact with the template molecule on the basis of the chemistry are then selected and the syntheses of a number of polymers are carried out. The success of this method, bearing in mind the complexity of the polymerisation process occurring, has been quite remarkable, with MIPs being produced that are able to recognise and bind the template molecule yet which do not have affinity, or have low affinity, for molecules with a similar structure. In passing, it is worthwhile noting that some MIPs do display "group selectivity", whereby they can recognise the template but also closely related structures (structural analogues).

Although the principles underpinning MIPs are intuitively simple, in practice the properties of the final structure are highly sensitive to the details of the synthetic protocol and to the final configuration/format of the material. At the same time, an enormous number of building components (monomers) are available and selection of these components can be tailored for a particular application.[10] These factors, when considered together, create an enormous optimisation landscape and it has been recognised that the rational design and fabrication of MIPs ideally requires some high-throughput strategies that can be used not only for the selection of the building components but also screening for an appropriate synthetic protocol.

The design and optimisation of MIPs is currently done mostly by rules of thumb and with trial and error processes. It is a relatively costly approach because of the sheer number of polymer formulations that are possible, as well as the possible influence of numerous and cumulative effects of different parameters relating to the synthesis and application of MIPs. More rational strategies in MIP design are required and the development of these strategies should start with a better understanding of adsorption and binding phenomena in MIPs on a molecular level since molecular recognition is a molecular scale phenomenon which is difficult to analyse in experiments. In this situation, molecular simulations present themselves as an expedient and flexible way to explore the problem from an in-depth fundamental perspective.

Therefore, our hypothesis was that atomistic molecular simulations can be used to enable the rational design and synthesis of MIPs, with methods akin to molecular modelling techniques.[11],[12] Such simulations can be designed to pre-determine requirements using the computational approach developed and as such may be an entirely new way to design MIPs. Techniques of this type are now becoming a very powerful tool in the production of new sets of 'smart' polymers that can be specifically designed to have the functionality required.[13] Finally, molecular simulation, if brought to a sufficient level of accuracy, can be used as a cost effective tool in material design optimisation by being able to efficiently scan through a number of building components with the desired molecular recognition characteristics.[14]

Recently, several computer simulation studies have focused on adsorption and binding phenomena in MIPs. In principle, computer simulation offers a detailed

description of adsorption and recognition phenomena in porous materials on a detailed molecular level, and allows the decoupling of the various factors which influence molecular recognition functionality and an assessment of their relative roles. In addition, by using computer simulations adsorption experiments can be mimicked and thus used to test/validate various structure characterisation models. In this way, it can link the information about the actual structure of the material and the binding site distributions extracted from the isotherms using appropriate methods. Depending on the property being studied, different models and simulation methods can be employed. This has originated a number of studies with a range of simulation strategies and levels of model detail and complexity. Figure 5.1 shows a general simulation strategy proposed by Zhang and Van Tassel.[15] This strategy requires essentially three simulation steps:

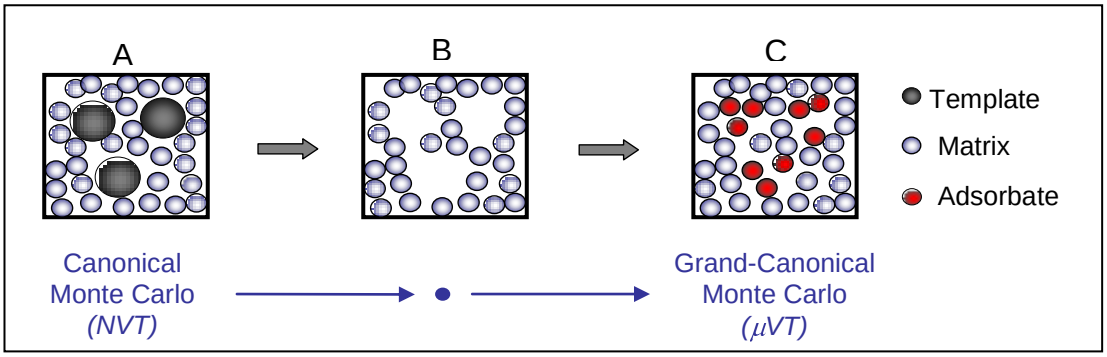

Figure 5.1 Schematic representation of the simulation steps performed for the synthesis and adsorption studies of the model MIP (in this study)[15]

A - In the first step, simulation of the equilibrium pre-polymerisation mixture is performed; in the most general case, this mixture includes template, functional monomer, crosslinkers and solvent.

B - In the second step, the equilibrium mixtures of pre-polymerisation components are frozen (quenched) in a specific configuration, followed by the removal of template and solvent.

C - The final structure obtained in the previous step serves as a model templated disordered porous structure in the subsequent adsorption studies.

A number of fundamental models of MIPs have been proposed.[15],[16],[17],[18],[19] For example, Yungerman and Srebnik[20] have considered a model of polymerising a Lennard-Jones fluid templated with rigid dimers, also made of two Lennard-Jones sites. This model allowed for the investigation of porosity and pore size distribution in the final structure as a function of the template concentration and degree of polymerisation. Recently, Wu *et al*. [21] proposed a simple 2D square lattice model of MIPs. This model is well suited to explore the binding site distributions in MIPs and how this characteristic depends on the relative concentration of the template and monomer species and on the strength of the template-functional monomer association.

More recently, detailed models have been developed to study MIPs. Computational design of MIPs has been proposed by Piletsky and coworkers,[22] based on energy minimisation methods to quantify interactions between various monomers and template molecules. Furthermore, Monti *et al*.[23] developed a computational approach based on a combination of molecular dynamic, molecular mechanic and binding protocols to investigate the formation of possible imprinted structures in the presence of theophylline **43**. Even although some interesting insights have been gained, most of these efforts suffer from two major drawbacks.[5] The first drawback is the focus on binding within a single cavity. This overlooks the heterogeneity of binding sites and binding phenomena issues over a range of concentration regimes. Furthermore, the accessibility of pore space remains beyond the scope of these models. The second drawback of these models is that the optimisation is reduced to a simplified scoring function approach based on the internal energy of complexation rather than on proper adsorption isotherms as measured in genuine laboratory experiments.

Thus, in this study a more general model of MIPs, with a specific emphasis on sensing applications, is developed. Specifically, it was based on accurate force fields validated against some experimental data. For example, the model must at least accurately describe vapour-liquid phase equilibria of individual components of the pre-polymerisation mixture, particularly the density of the liquid phase as this phase is the most relevant to the density of the final polymer. Furthermore, the model must capture the essential characteristics of real MIPs and feature complex three dimensional porous spaces. The model should focus on generating complete binding adsorption isotherm data, which is the data that can be compared directly to the experiments. Finally, it must be able to reproduce and/or predict experimental data.

The system developed was focused on a specific MIP based on MAA as functional monomer, EGDMA as crosslinker and chloroform as solvent/porogen. The template used was pyridine. From the point of view of the present work, pyridine was an attractive template because structurally it is relatively simple (which facilitates the molecular modelling work) and it can be volatilised into the gaseous state (which facilitates the acquisition of binding isotherms). Furthermore, the synthesis of pyridine imprinted polymers, and related polymers have already been reported in the literature.[24],[25] The Gibbs Ensemble Monte Carlo (GEMC) method has been employed to study the Vapour-Liquid Equilibrium (VLE) of organic components of imprinted polymers in order to validate the model. The adsorption characteristics of pyridine-imprinted and non-imprinted polymers were investigated.

5.2 Aim of Study

This body of work was a collaborative venture with the research group of Dr Lev Sarkisov at the University of Edinburgh. The aim of the study was to develop a computational model for MIPs which will predict the qualitative binding isotherm of a MIP synthesised *in silico* (Edinburgh). However, in order to test the predictive power of the model, the data generated must be compared to binding isotherm data generated for real imprinted polymers. Thus, the role of Strathclyde in the collaboration was to supply appropriately characterised molecularly imprinted polymers which were fit for purpose. More specifically, the real binding isotherm data must be generated from gas phase sorption experiments, at least in the first instance, so that the effects of solvent can be ignored and the predictive model simplified accordingly. In this regard, pyridine imprinted polymers were identified as a useful starting point for the collaborative venture.

5.3 Experimental Section

5.3.1 Chemicals, Materials and Purification

Pyridine (anhydrous, 99.8 %), acetone (CHROMASOLV®Plus for HPLC, ≥99.9 %), chloroform (anhydrous, ≥99.0 % contains 0.5-1.0 % ethanol as stabilizer), ethylene glycol dimethacrylate, EGDMA (98.0 %), methacrylic acid, MAA (99.0 %), AIBN (98.0 %) and calcium hydride (powder, reagent grade, 90-95 %) were purchased from Aldrich. Methanol (ACS reagent, ≥99.8 %), sodium sulfate (ACS reagent, anhydrous powder, ≥99.0 %), phosphorus pentoxide (ACS reagent, powder, ≥98.0%) and molecular sieves (beads, 4 Å) were purchased from Sigma-Aldrich. Potassium carbonate (anhydrous, ≥99.0 %) was purchased from Fluka. Pyridine was dried by refluxing and distilling over calcium hydride at 120 °C. Then, it was stored over molecular sieves (4 Å). EGDMA (98-100 °C/5 mmHg) and MAA (34 °C/5 mmHg)

were dried over anhydrous sodium sulfate and distilled under vacuum prior to use. AIBN was recrystallised from methanol at low temperature.

Chloroform was purified as ethanol-free chloroform by washing HPLC grade chloroform twice with an equal volume of water in a separating funnel. The chloroform layer was collected and dried over anhydrous potassium carbonate. It was then filtered and dried by refluxing over phosphorus pentoxide for 1 hour. Finally, it was distilled and stored in a dark bottle over molecular sieves (4 Å).

5.3.2 Synthesis of Pyridine MIPs and NIP

In this study, three polymers were prepared in the form of polymer monoliths. These polymers were synthesised in the presence of ethanol-free chloroform as porogen with AIBN as initiator and EGDMA as crosslinker. Pyridine was used as template and MAA as the functional monomer. The polymerisations were carried out on 5 g monomer scale. The three polymers synthesised were namely FS1 (NIP), FS2 (MIP) and FS3 (MIP); Table 5.1 shows the details of the polymerisation conditions.

In general, the template was dissolved in ethanol-free chloroform within a 50 mL Kimax© culture tube fitted with a screw cap. This was followed by addition of the functional monomer, MAA, and the crosslinker, EGDMA. The AIBN was added at a level of 1 mol % relative to the total number of polymerisable double bonds. The solution was then deoxygenated by bubbling oxygen-free nitrogen gas through the solution for about 30 minutes at ice-bath temperature. The Kimax© tube was then sealed under nitrogen and placed in an oil bath set at 60 °C for a period of 48 hours.

Table 5.1 Synthesis conditions used in the production of FS1, FS2 and FS3

Polymer Code	Mole Ratio T:M:X	Pyridine/ mL (mmol)	MAA/ mL (mmol)	EGDMA/ mL (mmol)	Chloroform/ mL	AIBN/ g (mmol)
FS1	0:4:20	-	0.40 (4.6)	4.53 (23.2)	6.67	0.08 (0.5)
FS2	1:4:20	0.09 (1.2)	0.40 (4.6)	4.53 (23.2)	6.67	0.08 (0.5)
FS3	4:4:20	0.37 (4.6)	0.40 (4.6)	4.53 (23.2)	6.67	0.08 (0.5)

Notes : T= template, M= functional monomer and X= crosslinker. The ratios quoted are the mole ratios of the three components in the feed.

After this time, the polymer monoliths obtained were ground mechanically using a Fritsch Pulverisette ball mill then wet-sieved with acetone. Particles in the size range 25-38 microns were isolated, and then Soxhlet extracted with methanol to remove the template, residual monomers and initiator. The polymer was collected and dried to constant mass *in vacuo* at 40 °C for 24 hours. The mass of polymer in the size range 25-38 μm was recorded. (**FS1**: 28 %; **FS2**: 22 %; **FS3**: 30 %).

5.3.3 Brunauer, Emmett and Teller (BET) nitrogen sorption porosimetry analysis

BET was used to determine the specific surface areas of the polymers from gas (nitrogen) sorption data in the lower range of the sorption isotherm. This method derives accurate and reliable data both theoretically and practically. The technique operated as a single point BET measurement (one adsorption pressure).

The porosimeter used was a Micromeritics ASAP 2010 BET ANALYZER. Prior to use, the samples were heated overnight in a vacuum oven at ~ 40 °C to ensure that all the gas molecules, moisture and residual solvent had been removed from the samples. The mass of polymer used in each analysis was approximately 0.3 g – 0.4 g. After the degassing process at 100 °C overnight, the polymers were analysed with computer control Module ASAP 2010 Version 2.00 to give the specific surface areas.

5.3.4 Molecular Models

Molecular species involved in this study were MAA, EGDMA, chloroform and pyridine. The Transferable Potential for Phase Equilibria (TraPPe) was adopted to describe the interaction among these species. The force-field parameters in this study were taken from the TraPPe force-field of Siepmann and coworkers (Martin and Siepmann 1998;[26] Chen and Siepmann 1999;[27] Martin and Siepmann 1999;[28] Wick *et al*. 2000;[29] Chen *et al*. 2001;[30] Stubb *et al*. 2004;[31] Kamath *et al*. 2005;[32] Rai and Siepmann 2007.[33]) TraPPe parameters for benzene, pyridine, chloroform and toluene were taken directly from the references, whereas the MAA parameters were taken from those proposed by Clifford and coworkers[34] for saturated carboxylic acids. Then was validated by Herdes and Sarkisov[5] by the

simulation of MAA vapour-liquid equilibrium data. In the same work, EGDMA was modelled by Herdes and Sarkisov as two MAA molecules and a bridging ethylene glycol. Parameters for ethylene glycol were taken from TraPPe directly. Gibbs Ensemble Monte Carlo (GEMC) has been used to validate the model.

The basic details of the GEMC simulation are as follows; the systems consist of two simulation boxes which are allowed to exchange molecules and change their size. The system was then equilibrated *via* molecular dynamic simulation in the Number-Volume-Temperature (NVT) ensemble. As the simulation progresses, one box evolved towards the liquid phase while the other box evolved towards the co-existing vapour phase. Hence, the properties of the phases in coexistence were calculated directly in a single simulation. The calculated interactions include Lennard-Jones interactions with the standard Lorentz-Berthelot mixing rules applied to the interactions between united atoms of different types and long-range electrostatic contributions, calculated using the Ewald summation.

The dynamic mixtures of MAA, pyridine and chloroform were performed at ρ = 1 atm and T = 298 K and the number of hydrogen bonds formed between the carboxylic acid group of MAA and the ring nitrogen of pyridine was monitored. The association constant estimated from calculation was in the range between 1.5 and 3 M^{-1}. Figure 5.2 shows a TraPPe presentation of species involved in MIP formation where the sizes of the interaction sites do not correspond to the actual collision diameter.

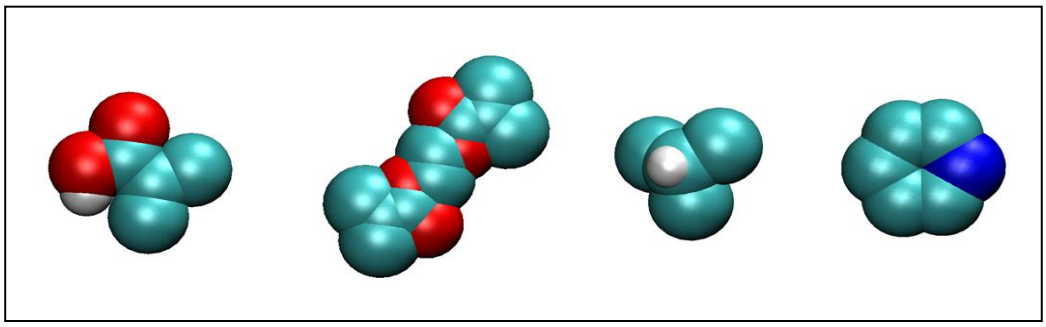

Figure 5.2 Molecular visualisation of the components involved in the model. From left to right; molecules of MAA, EGDMA, chloroform and pyridine.
(Atoms coloured as; C-cyan, O-red, N-dark blue and H-grey. Figure serves only as an illustration)[5]

5.3.5 Simulation Study

The initial configurations of the systems were prepared by placing all the molecules in a simulation box using a simple Monte Carlo code. The system was then equilibrated *via* molecular dynamic simulations in the NPT ensemble. In this simulation, the temperature was set to T = 298 K and pressure was set at ρ = 1 atm, to reflect typical laboratory conditions. All molecularly dynamic simulations were performed using the Gromacs simulations package.[35] Equilibration was done with the time step of 0.002 ps and at least 15 x 10^6 time steps for each run, while the simulation sample was at least 30 ns. Periodic boundary conditions were used for the simulation box. The Linear Constraint Solver (LINCS) algorithm was employed to constrain the molecular bonds. The Berendsen coupling scheme was adopted for isotropic baro- and thermostat.[36] The Particle Mesh Ewald (PME) method was used for electrostatic calculations. To visualise and analyse the results of the simulations, the Visual Molecular Dynamic

(VMD) software was used. Figure 5.3 shows a visual snapshot of the various stages of material formation and function in the system.

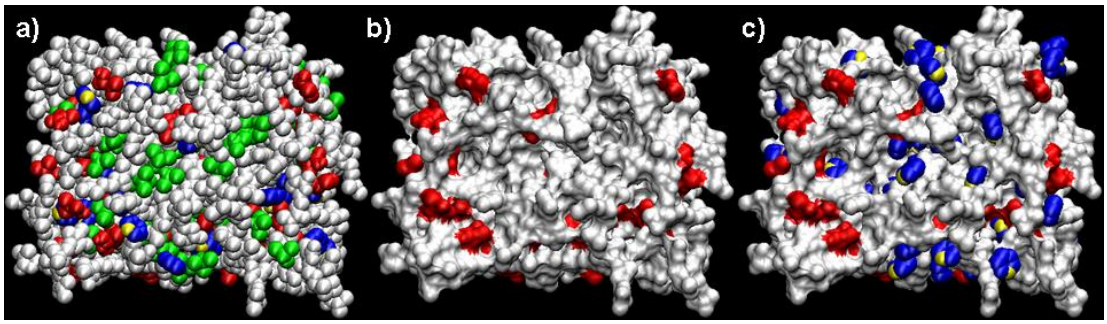

Figure 5.3 Computer graphics of the various stages of MIP4:4_d material formation and function. **(a)** Typical equilibrated mixture of 40 pyridine (blue with amino groups shown in yellow), 40 MAA (red), 200 EGDMA (grey) and 50 chloroform (green) molecules; **(b)** The visualisation of chloroform and pyridine molecules were removed; **(c)** Typical configuration of pyridine adsorbed in a model MIP matrix.

5.4 Results and Discussion

5.4.1 Synthesis of the polymers and BET studies

Pyridine MIPs and a NIP were synthesised successfully in the form of polymer monoliths. The MIPs were synthesised using two different template to functional monomer ratios; the T: M: X ratios used in this study were 1: 4: 20 and 4: 4: 20. The different T: M: X ratios used were designed to capture the effect of specificity enhancement as one goes from the 4: 4: 20 system to the 1: 4: 20 system in a computer simulation. This is considered to be a good test for the predictive model. The mass of the products obtained in the desired particle size range (25-38 μm) were considered to be perfectly adequate.

Specific surface area is a critical factor influencing the operation and behaviour of many materials. The measurement of the specific surface areas and specific pore volumes of the polymers from BET analysis showed that the three polymers had well-defined pore structures and rather similar specific surface areas and specific pore volumes (Table 5.2). As can be seen in Table 5.2, increasing the amount of template in the system decreased the porosity and pore volumes of the polymers, although this effect is modest.

Table 5.2 Specific surface areas and specific pore volumes from BET analysis for FS1, FS2 and FS3.

Polymer Code	Specific Surface Areas (m^2/g)	Specific pore volumes (cm^3/g)
FS1	440	0.569
FS2	410	0.556
FS3	390	0.511

The polymers were then supplied to our collaborators for more extensive gas sorption studies involving the sorption of pyridine from the gaseous phase.

5.4.2 Simulation Results

Twelve materials were prepared and characterised in silico as shown in Table 5.3. The MIP 1:4:20 group consist of 10 pyridine, 40 MAA and 200 EGDMA molecules,

while the MIP 4:4:20 group consists of 40 pyridine molecules and the NIP group 0:4:20 has no template (pyridine) present.

Table 5.3 Summary of the compositions and characteristics of the system (S-surface areas and V-pore volumes)

Materials		Pyridine (no. of molecules)	MAA (no. of molecules)	EGDMA (no. of molecules)	$CHCl_3$ (no. of molecules)	S (m^2/g)	V (cm^3/g)
NIP	a	0	40	200	760	2836	1.648
	b				380	2144	0.872
	c				190	1235	0.467
	d				50	217	0.142
MIP 1:4	a	10	40	200	760	2511	1.685
	b				380	1870	0.899
	c				190	1053	0.483
	d				50	279	0.175
MIP 4:4	a	40	40	200	760	2729	1.744
	b				380	2205	0.982
	c				190	1410	0.564
	d				50	592	0.251

The formation of transient complexes between MAA and pyridine was observed during the equilibration process. However, it was disturbed by the propensity of MAA to form dimers. In addition to that, pyridine has only one functional group which can interact with an MAA molecule. The functional monomer-template complex was relatively weak as suggested in previous studies.[25] In this model, the porosity of the materials was controlled by the amount of solvent present in the

system. However, they do not have an explicit mechanism of the polymerisation in this model. The intention was to optimise the amount of chloroform so that the resulting model structure can produce the experimental nitrogen sorption isotherm in the low pressure region. Unfortunately, due to lack of data in that region, the fitting was impossible. Therefore, the study was focused on a range of plausible structures.

As can be seen in Table 5.3, variations in the amount of chloroform have a dramatic effect on the structural characteristics of the materials. At the highest concentration of solvent, these materials exhibit specific surface areas up to 2836 m^2/g and specific pore volumes of about 1.7 cm^3/g. As the amount of chloroform decreased, the specific surface areas and specific pore volumes decreased substantially.

Furthermore, as the amount of solvent was decreased, a growing impact of the presence of template can be observed. At the lowest concentration of the solvent (series d), the imprinted materials have significantly enhanced specific surface areas and specific pore volumes when compared to the non-imprinted materials. This effect was particularly strong for the MIP4:4_d system. However, more interestingly, all these materials can be considered to be microporous.

It is worthwhile to compare the pore sizes distributions calculated for MIP4:4_a and MIP4:4_d as Table 5.3 indicates that MIP4:4_a has the higher specific surface area. The largest pore size present in the MIP4:4_a was about 14 Å with the majority of pores being around 10 Å in size (Figure 5.4). This was believed to be derived from the template presence in the system. Moreover, Figure 5.5 shows a

comparison of pore sizes distributions between the NIP_d material and MIP4:4_d. Even although the porosity of MIP4:4_d was significantly higher than that of NIP_d, the effect of imprinting was less evident from the pore size distributions.

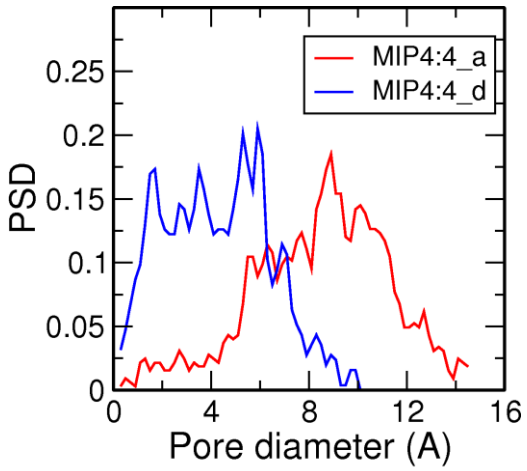

Figure 5.4 The effect of polymer density (solvent concentration) as compared between MIP4:4_a (red line) and MIP4:4_d (blue line).

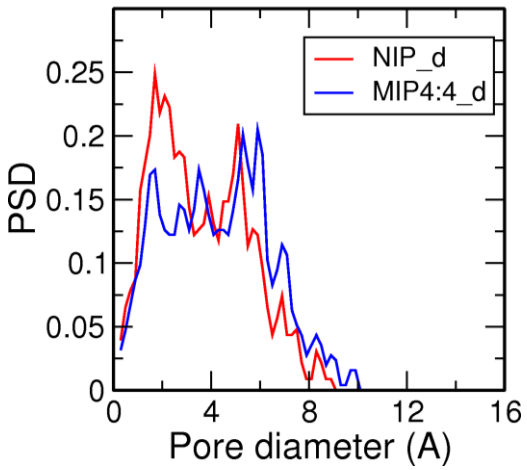

Figure 5.5 The effect of template as compared between NIP_d (red line) and MIP4:4_d (blue line)

5.5 Conclusion

The model developed in this study was based on the force-field and validated using vapour-liquid phase equilibria of individual components. Assembly of the model imitates the process of MIP synthesis. The model was able to capture the adsorption of pyridine and the templating effect was in agreement with experiment data. Interestingly, the model can visualise the realistic microstructure of MIPs and linked the features to adsorption and molecular recognition properties for the model materials.

At its current stage, the model is lacking as an explicit description of a polymerisation process, although in its present form it does allow for a qualitative prediction of the binding isotherm of a MIP and its corresponding NIP. A more accurate depiction of the polymerisation process could be developed from the kinetic by using the Monte Carlo approach. Additionally, the model can be further fine-tuned to produce the nitrogen sorption in the microporous region, accurately. This calibration required the experimental adsorption data of MIPs below 0.01 ρ/ρ_o. Unfortunately, the experimental data could not been achieved below that value. To conclude, in the context of molecularly imprinted polymers, it seems natural to incorporate both more details of polymerisation protocols and accessibility analysis in a framework of a single model, and this will be pursued in future studies.

5.6 References

[1] B. Sellergren, *TrAC*. **1997**, *16*, 310-320.

[2] K. Haupt and K. Mosbach, *Chem. Rev.* **2000**, *100*, 2495-2504.

[3] B. Tóth, T. Pap, V. Horvath and G. Horvai, *Anal. Chim. Acta.* **2007**, *591*, 17-21.

[4] L. I. Andersson, *J. Chromatogr. B.* **2000**, *739*, 163-173.

[5] C. Herdes and L. Sarkisov, *Langmuir* **2009**, *25*, 5352-5359.

[6] Y. Fu and H. O. Finklea, *Anal. Chem.* **2003**, *75*, 5387-5393.

[7] M. C. Blanco-López, M. J. Lobo-Castañón, A. J. Miranda-Ordieres and P. Tuñón-Blanco, *TrAC*. **2004**, *23*, 36-48.

[8] A. McCluskey, C. I. Holdsworth and M. C. Bowyer, *Org. Biomol. Chem.* **2007**, *5*, 3233-3244.

[9] G. Bunte, J. Hürttlen, H. Pontius, K. Hartlieb and H. Krause, *Anal. Chim. Acta.* **2007**, *591*, 49-56.

[10] K. Karim, F. Breton, R. Rouillon, E. V. Piletska, A. Guerreiro, I. Chianella and S. A. Piletsky, *Adv. Drug Deliver. Rev.* **2005**, *57*, 1795-1808.

[11] I. A. Nicholls, K. Adbo, H. S. Andersson, P. O. Andersson, J. Ankarloo, J. H. Dahlstrom, P. Jokela, J. G. Karlsson, L. Olofsson, J. Rosengren, S. Shoravi, J. Svenson and S. Wikman, *Anal. Chim. Acta.* **2001**, *435*, 9-18.

[12] Y. Liu, F. Wang, T. Tan and M. Lei, *Anal. Chim. Acta.* **2007**, *581*, 137-146.

[13] W. B. Liechty, D. R. Kryscio, B. V. Slaughter and N. A. Peppas, *Annu. Rev. Chem. Biomol. Eng.* **2010**, *1*, 149-173.

[14] M.-X. Zheng, S.-J. Li and X. Luo, *J. Macromol. Sci. Pure.* **2007**, *44*, 1187 - 1194.

[15] L. H. Zhang and P. R. Van Tassel, *J. Chem. Phys.* **2000**, *112*, 3006-3013.

[16] S. Cheng and P. R. Van Tassel, *J. Chem. Phys.* **2001**, *114*, 4974-4981.

[17] S. Srebnik and O. Lev, *J. Chem. Phys.* **2002**, *116*, 10967-10972.

[18] S. L. Zhao, W. Dong and Q. H. Liu, *J. Mol. Liq.* **2007**, *136*, 241-248.

[19] L. Sarkisov and P. R. Van Tassel, *J. Phys. Chem. C.* **2007**, *111*, 15726-15735.

[20] I. Yungerman and S. Srebnik, *Chem. Mater.* **2006**, *18*, 657-663.

[21] X. Y. Wu, W. R. Carroll and K. D. Shimizu, *Chem. Mater.* **2008**, *20*, 4335-4346.

[22] S. A. Piletsky, K. Karim, E. V. Piletska, C. J. Day, K. W. Freebairn, C. Legge and A. P. F. Turner, *Analyst* **2001**, *126*, 1826-1830.

[23] S. Monti, C. Cappelli, S. Bronco, P. Giusti and G. Ciardelli, *Biosens. Bioelectron.* **2006**, *22*, 153-163.

[24] D. L. Rathbone and Y. Ge, *Anal. Chim. Acta.* **2001**, *435*, 129-136.

[25] H. S. Andersson, A. C. Koch-Schmidt, S. Ohlson and K. Mosbach, *J. Mol. Recogn.* **1996**, *9*, 675-682.

[26] M. G. Martin and J. I. Siepmann, *J. Phys. Chem. B.* **1998**, *102*, 2569-2577.

[27] B. Chen and J. I. Siepmann, *J. Phys. Chem. B.* **1999**, *103*, 5370-5379.

[28] M. G. Martin and J. I. Siepmann, *J. Phys. Chem. B.* **1999**, *103*, 4508-4517.

[29] C. D. Wick, M. G. Martin and J. I. Siepmann, *J. Phys. Chem. B.* **2000**, *104*, 8008-8016.

[30] B. Chen, J. J. Potoff and J. I. Siepmann, *J. Phys. Chem. B.* **2001**, *105*, 3093-3104.

[31] J. M. Stubbs, J. J. Potoff and J. I. Siepmann, *J. Phys. Chem. B.* **2004**, *108*, 17596-17605.

[32] N. Lubna, G. Kamath, J. J. Potoff, N. Rai and J. I. Siepmann, *J. Phys. Chem. B.* **2005**, *109*, 24100-24107.

[33] N. Rai and J. I. Siepmann, *J. Phys. Chem. B.* **2007**, *111*, 10790-10799.

[34] S. Clifford, K. Bolton and D. Ramjugernath, *J. Phys. Chem. B* **2006**, *110*, 21938-21943.

[35] E. Lindahl, B. Hess and D. van der Spoel, *J. Mol. Model.* **2001**, *7*, 306-317.

[36] H. J. C. Berendsen, J. P. M. Postma, W. F. van Gunsteren, A. DiNola and J. R. Haak, *J. Chem. Phys.* **1984**, *81*, 3684-3690.

CHAPTER 6

GENERAL CONCLUSIONS AND FUTURE WORKS

The overarching goal of the research works presented in this thesis was to enhance the usefulness of MIPs, through either optimising the physical format of a MIP within a specific application, bringing polymer forming processes under tighter control or, most radically of all, to evolve computational methods capable of informing and directing MIP synthetic campaigns at their outset. Substantial progress has been achieved in all three areas.

Chapter 3 describes a study in which MIPs have been used as stationary phases for the separation and quantification of ketamine in hair samples. In the course of the study, in which the stationary phases were connected directly to a mass spectrometer, it was found that ketamine could be detected easily by the method; the method is known as MILC-MS/MS. An obvious advantage of this on-line method is that crude hair extracts can be injected directly onto the MIP columns without any need for a prior clean-up step. Furthermore, even although the current generation of MIPs cannot be considered to be ideal chromatographic stationary phases, they nevertheless perform satisfactorily and we believe that the MILC-MS/MS set-up which has been developed for ketamine can be easily extended to include different analytes as well as other types of sample.

Controlled radical polymerisation has been exploited in the production of MIPs in an effort to exert tighter control over the polymer growth processes (Chapter 4). More specifically, RAFT polymerisation was used in an effort to produced MIPs with improved homogeneity of binding sites and enhanced chromatographic performance. This was successful; the polymers synthesised *via* RAFT polymerisation allowed chemical separations which were more efficient compared to polymers prepared *via* conventional approaches. Although the polymers prepared by RAFT polymerisation have had very low dry-state specific surface areas, they performed very effectively indeed as chromatographic stationary phases (used in wet-state). However, a more in-depth study of polymer growth and morphology may be of interest to develop this area, for example by extending the study to include other RAFT agents or other controlled radical polymerisation methods.

Chapter 5 describes a computer simulation method which was developed to aid in the rational design of MIPs. This type of approach is cost effective, produced no chemical waste from failed experiments and offers potential time-savings in MIP development. It was discovered that the simulation model developed through collaboration was able to predict, in a qualitative manner, the binding isotherms of MIPs. It also shed some light on pore forming processes and gave us confidence that such an approach is likely to become of increasing value in the future as the MIP field matures further.

APPENDIX 1

^{1}H NMR SPECTRUM OF BIS(THIOBENZOYL)DISULFIDE (in $CDCl_3$)

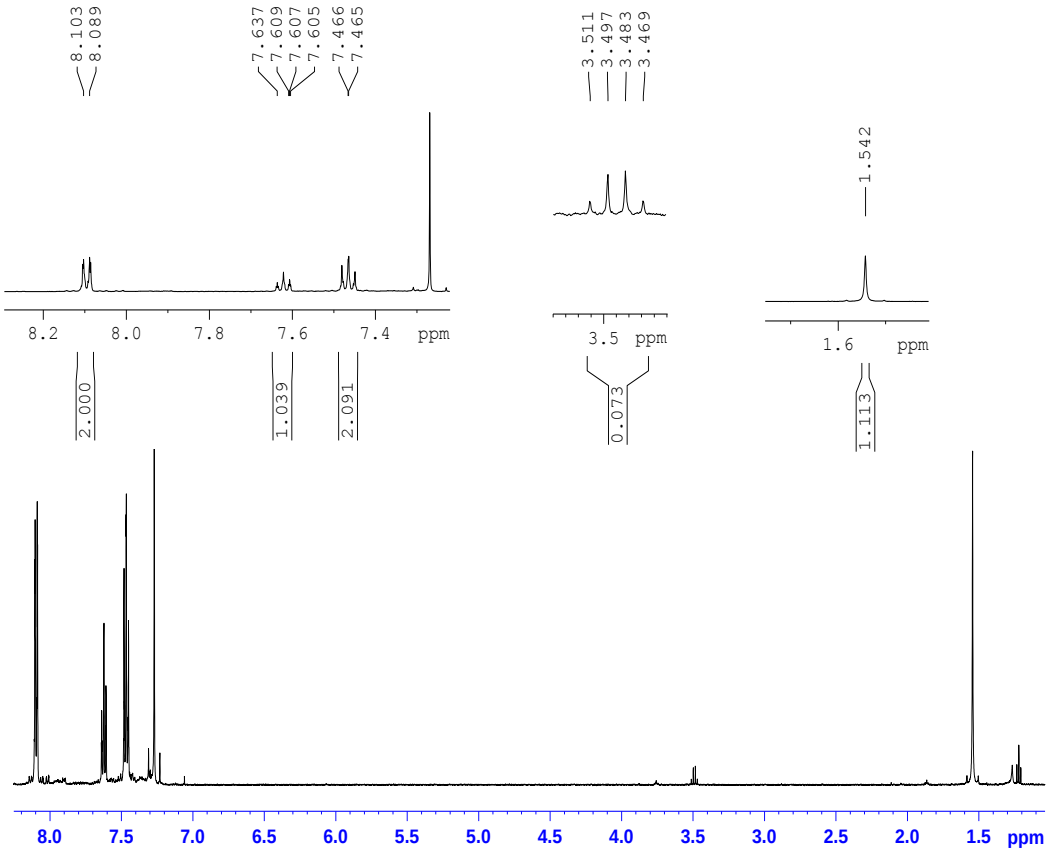

APPENDIX 2

^{1}H NMR SPECTRUM OF CPDB ($CDCl_3$)

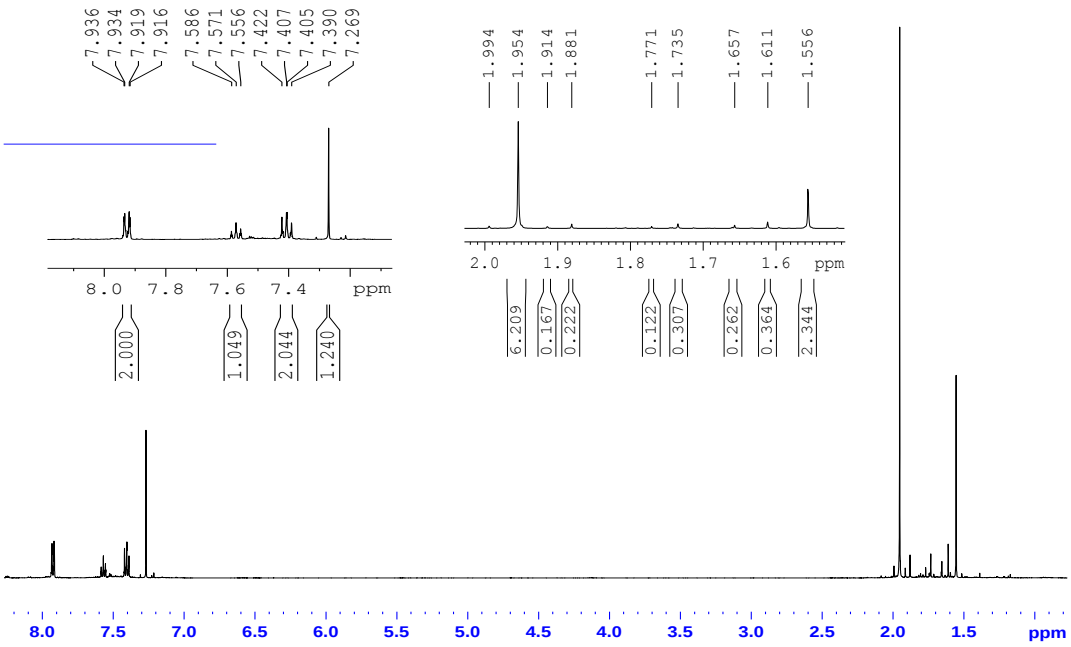

APPENDIX 3

^{13}C NMR SPECTRUM OF CPDB ($CDCl_3$)